臺灣二 OO 三年國際科學展覽會

科　　別：地球與太空科學科

作品名稱：臭氧事件日-氣象與地形對臭氧於近地大氣層之生成與傳輸影響

得獎獎項：地球與太空科學科第三名

美國第五十四屆國際科技展覽會

學　　校：國立臺中第二高級中學

作　　者：梁辰睿

040011-08 梁辰睿

作者簡介

梁辰睿，1985 年 2 月生於台中市，今年十八歲，目前就讀於國立臺中第二高級中學三年級。父親任教於逢甲大學環境工程與科學系，母親任職於自來水公司第四區處，弟弟就讀於國立西苑中學國中部二年級。由於曾學過多年的長笛，因此平常喜歡聽音樂，也喜愛打籃球和桌球。二年多來，隨美籍之個人英文教師勤學英文，已具備相當的英文說寫能力，期盼未來能任職於美國 NASA，探索宇宙新知。

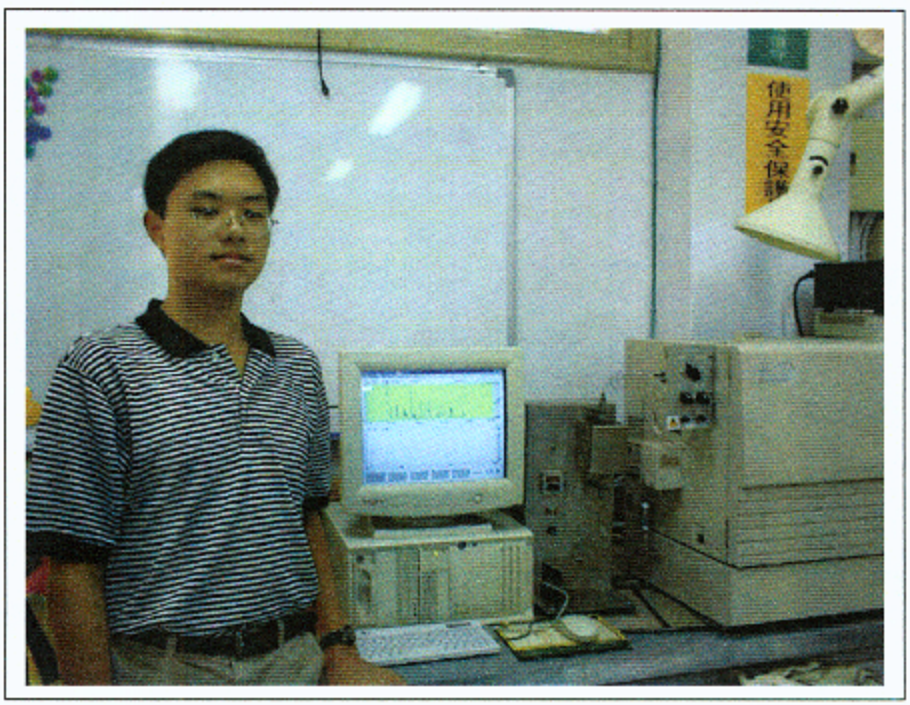

臭氧事件日–
氣象與地形對臭氧於近地大氣層之生成與傳輸影響

Ozone Event Days–
The Effect of Meteorology and Topography on Formation and Transformation of Ozone in the Lower Atmosphere

摘 要

2001、2002 年監測資料被用以探討風場、時間、地形對臭氧傳輸影響。完成沿海地區與盆地內各二次採樣分析，探討各污染物與風場之垂直變化，及地面臭氧分布與風場變化。結果顯示各月份與全年之日間，其相對濕度與 O_3 相關度最高，日照次之。提高濕度，最能抑制[O_3]。夜間 NO 與 O_3 的相關度最高，濕度次之。臭氧事件日時：(1).11:00 即可產生高臭氧，(2).沿海地區在臭氧事件日仍保持低[O_3]，(3).盆地效應改變風場，使近山地區[O_3]居高不下，(4).因處 O_3 不斷被吹入，沿海地區傍晚時之[O_3]下降速度減緩。臭氧事件日之 O_3 生成速率 *R* 與消失速率常數 *L* 被求出，其中 14:00 後之 *R* 與 *L* 值均由正值轉負值，顯示大氣反應型式明顯轉變。*R* 與 *L* 值在 14:00~15:00 間最小，係因 O_3 反應生成光化學煙霧所致。16:00 後另一低 *R* 與 *L* 值，則可能導因 O_3 與微粒或水份反應。分析結果顯示：(1).污染物會隨高程而略增，最高濃度在 300~500 m 處，(2).各高程大氣均可分析出 73 種主要 HC，其隨高度之分布被繪出與探討，(3).低層大氣會有較多低分子量 HC，而高層大氣則有較多高分子量 HC。結果亦顯示：(1).盆地內[O_3]、[NO]與[NO_2]不僅較沿海地區高，且於各高程之變動亦較大，(2).沿海地區 THC、烷、烯類均較高，且隨高程增加而增高，但在盆地內則相反，(3).二地區各高程之鹵化物、芳香族、氧化物與其他有機物之平均濃度相近，但沿海地區之濃度變動較大。探討 O_3 之二傳輸現象獲知：(1).風吹向盆地內時，[O_3]隨風向遞增，*R* 與 *L* 會由 12:00 之正值，轉爲 14:00 之負值；(2).風由盆地內外吹時，[O_3]隨風向遞減，*R* 與 *L* 值提前於 12:00 即爲–202.561 與–1.621，但 14:00 時 *R* 與 *L* 值增大爲–76.411 與 0.244，(3).風向並非決定[O_3]的主要因素，地形與環境因素才是。實驗結果證實：(1).不同 HC 會影響 O_3 之生成與消失，(2).改變[NO]。對[O_3]影響不大，但高[NO]會使得[O_3]下降略緩，(3).降低 HC 與[NOx]雖可使[O_3]略降，但提高濕度最能抑制[O_3]，(4).在 O_3 的衰減量上，[O_3]隨濕度增加而快速降低，但衰減率則隨[O_3]。的增加而降低。一個臭氧之統計模式被建立，臭氧與水反應速率常數與速率式也被求出。

關鍵字：臭氧、氣象、地形、生成、傳輸

Abstract

The monitoring data were used to investigate the effect of surface wind, time, and terrain on the transformation of ozone. The sampling and the analysis in the coastal and in Taichung basin were completed. The vertical distribution of O_3, NO_X and HC and the different altitude wind were investigated. The contour of O_3 and surface wind with 3D map were plotted. The results show that the correlation behaves relativity of relative humidity with ozone is the best, and solar radiation is the next. Enhancing environmental moisture can efficiently decrease ozone concentration. In each ozone event day are: (1) the high [O_3] always starts from 11:00, (2) the ozone concentration on the coastal is always low due to the high humidity, (3) the high [O_3] in the east of the basin is due to the basin effect which causes changes the surface wind, and (4) in the evening, the descend rate of [O_3] in the coastal area is lower because ozone blows into the coastal area. The formation rate (*R*) and disappear rate constant (*L*) of the ozone event day were obtained. The values of *R* and *L* change from plus to minus before 14:00. The values of *R* and *L* are lower at 14:00~15:00 due to the photochemical smog formation. And another lower *R* and *L* value before 16:00 may be due to ozone react with particle or water. The results of analysis indicate that: (1) the concentration increases with increasing altitude, and the maximum is at 300~500 m height, (2) 73 kinds of hydrocarbons were identified, and the concentration variation with altitude was also investigated, and (3) most of low molecular weight HC are at lower altitude, otherwise high molecular weight HC are at higher altitude. The results also show that: (1) [O_3], [NO], and [NO_2] on the basin are not only lower than on the coastal, but also their variability of concentration are big, (2) THC, paraffins, and olefins on the coastal are higher than on the basin, and the concentrations increase with increasing altitude on the coastal, but on the basin is decreasing, (3) the average concentrations of halides, aromatics, oxides, and others are similar on both area, but concentration variability on the coastal is obvious. Two types of O_3 transformation was investigated, the phenomenon indicts that: (1) when wind blew into the basin, [O_3] increased with wind direction. The value of *R* and *L* change from positive (12:00) to negative (14:00); (2) when wind blew out of the basin, [O_3] decreased with wind direction. The more small value of *R* (–202.561) and *L* (–1.621) appeared at 12:00 earlier. But the value of *R* and *L* will become bigger to –76.411 and 0.244; (3) ozone concentration does not just dependent on wind direction., topography and surrounding conditionsa are more important effect. The experimental results show that: (1) ozone formation or disappearance depends on different HC, (2) the effect

of $[NO]_o$ is small for ozone photochemical reaction, but $[O_3]$ decreases with increasing [NO], (3) the descend rate of O_3 depends on high humidity more than different kinds of HC or [NO], and (4) the descend amount of ozone increases with increasing humidity strongly, and the descend rate of ozone decreases with enhancing $[O_3]_o$. A statistical model was developed. The reaction rate and rate constant of ozone reaction with water were also obtained.

Keyword: Ozone, Meteorology, Topography, Formation, Transformation

壹、研究動機與目的

國內臭氧(O_3)濃度逐年升高，常是造成空氣品質不良的首要污染物，對健康與環境的危害，已不容忽視。台灣地區屬高濕度的海島型氣候，大氣中高水份的存在，以及多山地形，明顯影響臭氧之生成與傳輸，但此影響結果卻少見於國內外文獻。台中地區不僅臨海，且過半面積爲盆地，空氣污染物易因盆地效應而累積，造成局部高濃度，深深影響當地居民的健康。此種現象，尤其以台中地區高臭氧濃度最爲嚴重。O_3 生成受氮氧化物(NO_X)、碳氫化合物(HC)與氣候等因素影響，其傳輸更與當地之風場及地形有關。國內外不乏 O_3 有關之研究報告，其中以探討區域間 O_3 之現象最多，區域包含某城市與郊區[1~5]、工業區或全球[6~9]；其次探討氣象或季節對 O_3 之影響[4,5,9~13,18]；鑽研 O_3 之光化模式，包含 ANNS[6,7]、CIT[5]、UAM[12,13]、PBM[3]、PAQSM[14]、AQSMs[17]等模式；以及探討 O_3 之生成或控制[15~20]與 O_3-NO_X-HC 之比值或作用[1,2,9,18]。一般探討 O_3 的生成，大都僅考慮 NO_X、HC 與日照，欠缺含蓋完整的氣象與地形影響評估，且往往忽略高空之 HC 質與量分佈，以及風場變化，使研究成果仍存有一些不確定因素。基於此，本研究嘗試更深入探討氣象與地形的影響，期能使 O_3 的各種機制更爲闡明。

貳、研究架構與流程

詳細工作流程，如圖 1 所示，依序爲：1.監測資料蒐集與分析、2.環境實測與 3.基礎實驗。在監測資料處理上，蒐集 2001、2002 年氣象與空氣品質資料，詳加分析整理，以瞭解 O_3 生成與傳輸之關係。尤其台中地區擁有 22 個空氣品質監測站與 2 個氣象站，足供本研究相當完整之歷年資料。另外也配合實測工作，蒐集當日氣象與空氣品質資料，一併深入探討。實測工作包含污染物之垂直濃度與高空風場偵測，以瞭解其垂直濃度分布，及隨地形之變化。基礎實驗是在可控制反應參數下，於方形玻璃反應器中，進行一些特定實驗，以補足文獻中欠缺資料，以及用以佐證監測資料解析與實測工作所提出之結論，使研究工作更爲完善。

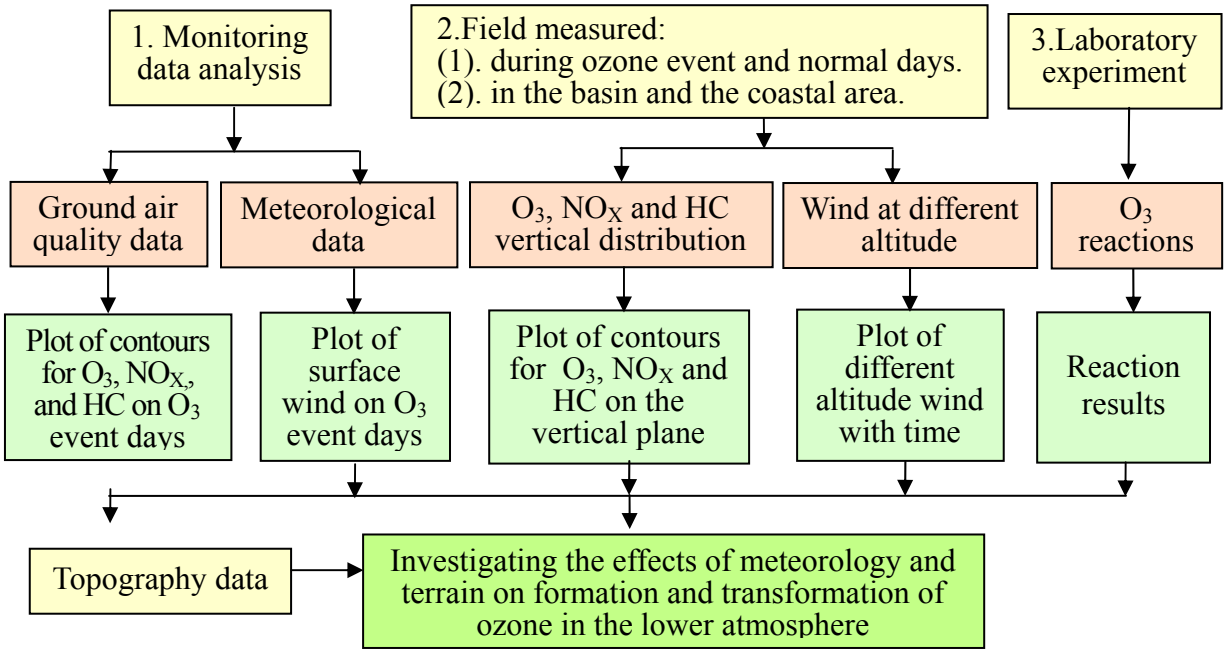

Figure 1 Steps in the study process

參、建立大台中地區之數位化地圖

建立大台中地區之數位化地圖，對本研究有其確切的必要性。因此，在研究之初，即先行完成這項工作。所建立之大台中地區數位化地圖有二種，並均採用 UTM 座標，其中一爲 3D 圖(圖 2(a))，具備可改變不同之視角；另一爲平面色差圖(圖 2(b))，分別滿足後續配合各種研究結果之展示所需。

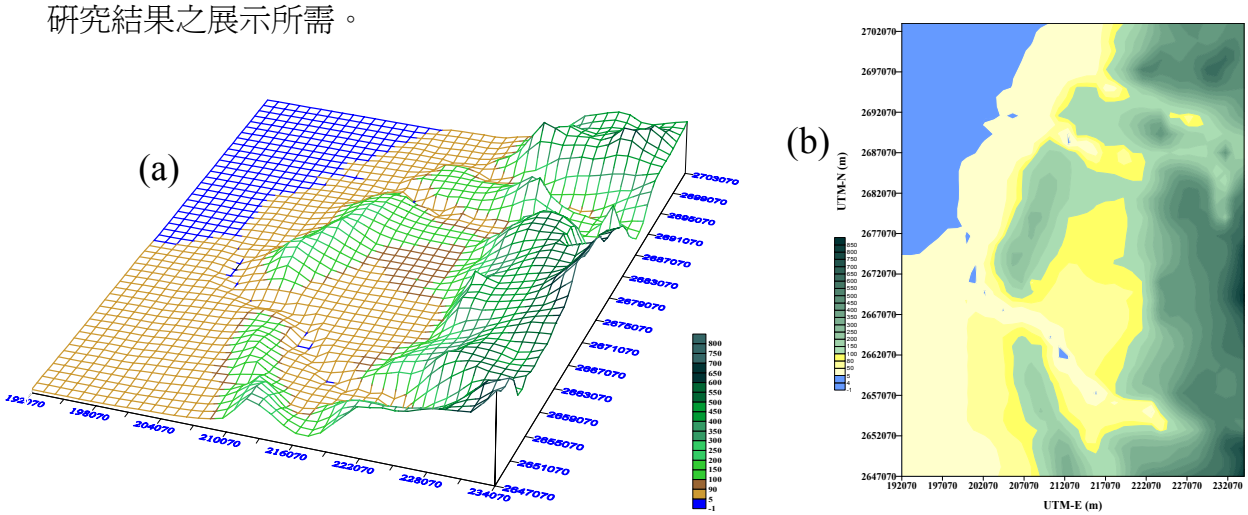

Figure 2　Plot of two 3D topographic maps of the Taichung Area

肆、各項監測之歷史資料分析

大台中地區擁有高達 22 個空氣品質監測站，與 2 個氣象站，可提供本研究相當完整之歷年地面資料。研究中，蒐集區域內 2001、2002 年之監測數據，來詳細整理與分析，從中瞭解各氣象因素與污染物濃度對臭氧生成與傳輸間的關係。圖 3 爲大台中地區各類測站之位置、本研究採樣地點與其 UTM 座標，其中 Line-1 ~3 分別爲三條可構成一直線之具有 O_3 監測項目測站組合，其在後面研究中被用以輔助說明臭氧之傳輸變化。

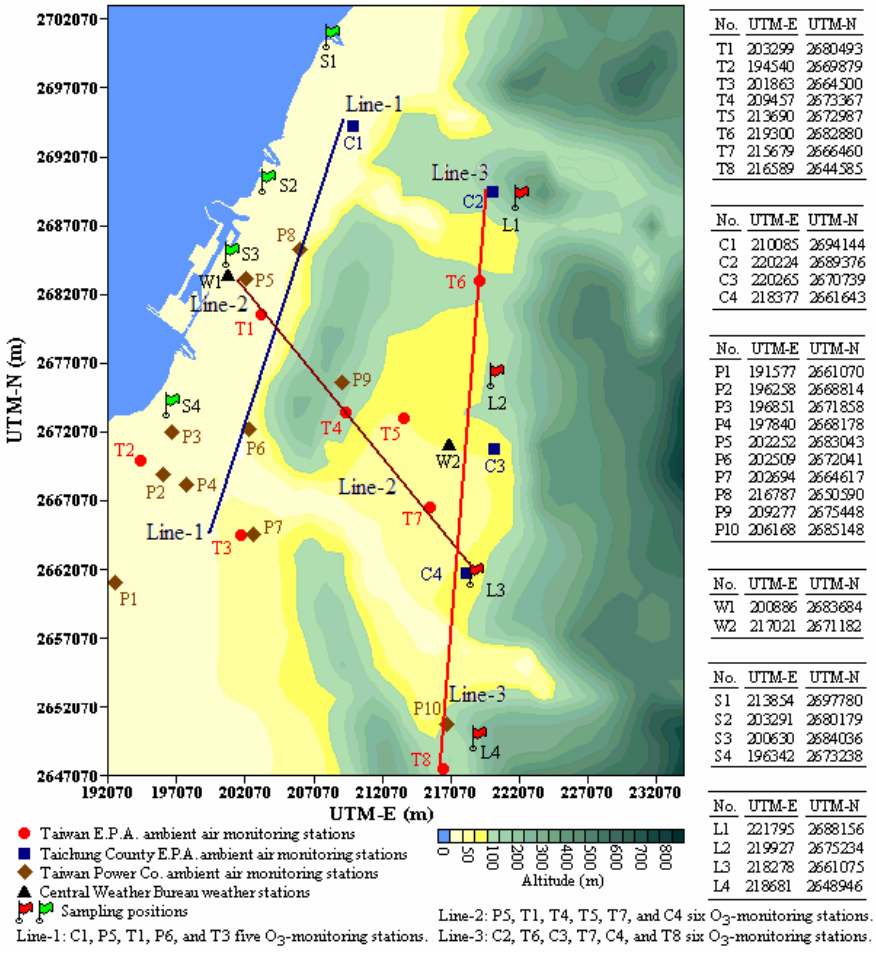

No.	UTM-E	UTM-N
T1	203299	2680493
T2	194540	2669879
T3	201863	2664500
T4	209457	2673367
T5	213690	2672987
T6	219300	2682880
T7	215679	2666460
T8	216589	2644585

No.	UTM-E	UTM-N
C1	210085	2694144
C2	220224	2689376
C3	220265	2670739
C4	218377	2661643

No.	UTM-E	UTM-N
P1	191577	2661070
P2	196258	2668814
P3	196851	2671858
P4	197840	2668178
P5	202252	2683043
P6	202509	2672041
P7	202694	2664617
P8	216787	2650590
P9	209277	2675448
P10	206168	2685148

No.	UTM-E	UTM-N
W1	200886	2683684
W2	217021	2671182

No.	UTM-E	UTM-N
S1	213854	2697780
S2	203291	2680179
S3	200630	2684036
S4	196342	2673238

No.	UTM-E	UTM-N
L1	221795	2688156
L2	219927	2675234
L3	218278	2661075
L4	218681	2648946

Figure 3　Plot of the positions of monitoring stations on Taichung Area

一、臭氧與各參數之相關係數

運用相關係數式來逐一求出一些氣象參數與空氣污染物濃度分別與臭氧濃度的相關係數值，評估各參數在臭氧生成與傳輸上的重要性。相關係數計算式爲：

$$r_{xy} = \frac{\sum_{i=1}^{n}(x_i - \bar{x})(y_i - \bar{y})}{\sqrt{\sum_{i=1}^{n}(x_i - \bar{x})^2}\sqrt{\sum_{i=1}^{n}(y_i - \bar{y})^2}} \quad (1)$$

其中 r_{xy} 爲相關係數，其值越趨近於 1 或–1，兩者之關係度越高，而正值表示二者爲正比相關性，反之負值爲反比相關性；$\bar{x}, \bar{y}$ 分別爲 x, y 數列平均值；n 爲數據組總數。

本研究選擇以具備最完整監測項目之 C2 空氣品質監測站的數據，來進行本項工作，求得逐月與全年日、夜間之日照度、濕度、氣溫、CH_4、NMHC、SO_2、CO、NO、NO_2 分別與臭氧濃度的相關係數值，各參數相關係數列於表 1 中。

Table 1　Results of the relative coefficients between some parameters and ozone.

Parameters	Jan.	Feb.	Mar.	Apr.	May	June	July	Aug.	Sep.	Oct.	Nov.	Dec.	Annual
Solar radiation													
daytime	0.546	0.596	0.693	0.672	0.564	0.409	0.654	0.520	0.719	0.628	0.484	0.445	0.578
Relative humidity													
daytime	-0.683	-0.737	-0.752	-0.633	-0.615	-0.410	-0.542	-0.455	-0.785	-0.665	-0.527	-0.416	-0.602
nighttime	-0.576	-0.532	-0.551	-0.333	-0.334	-0.135	-0.185	-0.110	-0.226	-0.177	-0.410	-0.295	-0.322
Ambient temperature													
daytime	0.333	0.452	0.479	0.496	0.679	0.631	0.604	0.638	0.674	0.753	0.431	0.314	0.540
nighttime	-0.404	-0.387	-0.297	0.032	0.268	0.148	0.235	0.247	-0.044	-0.077	-0.315	-0.345	-0.078
Methane, CH_4													
daytime	-0.314	-0.046	-0.097	-0.400	-0.052	-0.132	-0.144	-0.010	0.012	-0.181	0.081	-0.044	-0.111
nighttime	-0.295	-0.488	-0.528	-0.447	-0.162	-0.248	-0.159	-0.149	-0.200	-0.188	-0.373	-0.066	-0.275
Non-methane hydrocarbon, NMHC													
daytime	-0.034	-0.167	-0.032	0.202	-0.017	-0.242	-0.375	-0.342	-0.256	-0.033	-0.138	-0.078	-0.126
nighttime	-0.228	-0.342	-0.230	-0.201	-0.160	-0.133	0.021	-0.069	-0.106	-0.106	-0.253	-0.096	-0.159
Sulfur dioxide, SO_2													
daytime	0.161	0.233	0.250	0.082	0.222	-0.024	-0.107	-0.097	0.340	0.269	0.329	0.181	0.153
nighttime	-0.130	-0.270	0.184	0.011	0.173	0.083	0.188	-0.178	0.312	-0.060	-0.163	-0.104	0.004
Carbon monoxide, CO													
daytime	-0.183	0.081	-0.117	-0.078	0.009	-0.076	0.013	-0.072	0.048	-0.026	0.111	0.041	-0.021
nighttime	-0.355	-0.316	-0.213	-0.162	-0.093	-0.252	0.126	-0.052	0.015	-0.247	-0.287	-0.311	-0.179
Nitric oxide, NO													
daytime	-0.348	-0.151	-0.482	-0.336	-0.186	-0.329	-0.470	-0.350	-0.445	-0.447	-0.444	-0.389	-0.365
nighttime	-0.395	-0.474	-0.492	-0.254	-0.171	-0.288	-0.227	-0.309	-0.410	-0.417	-0.364	-0.511	-0.359
Nitrogen dioxide, NO_2													
daytime	-0.076	-0.060	-0.188	-0.247	0.027	-0.066	0.101	0.053	0.301	0.092	0.080	-0.048	-0.003
nighttime	-0.547	-0.534	-0.318	-0.148	-0.056	-0.253	-0.030	-0.198	-0.129	-0.397	-0.547	-0.388	-0.295

Note: Daytime and nighttime are at 06:00-18:00 and 18:00-06:00 next day.

由表 1 獲知在各月份與全年之日間(06:00-18:00)中，日照、相對濕度與氣溫三個氣象參數與臭氧濃度間之相關度，均高於六個空氣污染物與臭氧間的相關度，尤其是相對濕度在各月份與全年的相關係數值均爲最高或次高，而且均爲負關係度，顯示臭氧濃度明顯隨相對濕度的增加而降低。另外，高日照下通常其氣溫亦較高，而由表 1 亦得知二者與臭氧臭氧濃度間均爲正關係度，且其相關係數值非常相近，是除相對濕度外明顯影響臭氧濃度之參數。由此結果獲知提高環境中水份，最能抑制臭氧濃度。六個空氣污染物與臭氧間的相關度明顯低於三個氣象參數，尤其值得一提的是 CH_4、NMHC 在日間的濃度變化，對臭氧濃度並未產生明顯之影響。六個空氣污染物中，以 NO 與臭氧間的相關度稍高(全年值約–0.36)，但由於其爲負相關度，顯現 NO 會反應而濃度降低，但也促使臭氧濃度增加。

表 1 亦顯示夜間雖無光化學反應進行，但臭氧仍會與水份、CH_4、NO、NO_2 作用(四者之相關係數值均約–0.3)，其中又以 NO 與臭氧間的相關度最高，相對濕度次之。

二、運用監測資料分析風場、時間、地形對臭氧傳輸之影響

欲由各項監測之歷史資料來獲知地形對臭氧傳輸之影響，則需繪製地面風場以及臭氧隨位置、地形與時間之關係圖，從中判讀風場與地形對臭氧傳輸之影響。本研究將 2001 與 2002 年上、下半年中，出現臭氧事件日最嚴重之 2001 年 4 月 27 日、10 月 7 日與 2002 年 5 月 25 日、8 月 2 日四天之地面風場以及臭氧逐時等濃度曲線置、地形與時間之變化，繪製成圖 4~6。各圖中，再細分成由沿海地區 C1、P5、T1、P6 與 T3 五測站所構成之 Line-1 臭氧之變化圖(圖 4(a), 5(a)與 6(a))，跨越盆地與沿海地區 P5、T1、T4、T5、T7 與 C4 六測站所構成之 Line-2 臭氧隨位置與時間之變化圖(圖 4(b), 5(b)與 6(b))，以及由盆地內 C2、T6、C3、T7、C4 與 T8 六測站所構成之 Line-3 臭氧之變化圖(圖 4(c), 5(c)與 6(c))。

圖 4 顯示 2001 年 4 月 27 日臭氧事件日時，盆地東側由 11: 00 之吹西南風，逐漸轉成南風、東南風至東風；盆地中心之風向變化相同，但提早 1~2 小時。大台中地區西測北半部一值吹著東風，南半部風速較小，但風向改變較大，由吹西風逐漸轉成吹南風、東南風與東風。各地在 09: 00 時之臭氧濃度均不高(< 45 ppb)，但 11: 00 時除沿海地區 C1、P5、T1 測站外，各地臭氧均開始明顯增高，其中 T3、T7 與 C3 三測站已超過 100 ppb。Line-1 諸測站位於下風處(T3 除外)，其來自上風處之臭氧一直傳輸至此，使得濃度隨時間而增高，尤其因傳輸之時間延遲使最高濃度出現在 15: 00，而非上風處(盆地內)之最高濃度出現在 13: 00 左右。Line-2 與 Line-3 諸測站均以 T7 之濃度隨時間變化最大，而大部分時間之濃度也最高。值得注意的是在此臭氧事件日之地面風速均不大(< 4 m/sec)，臭氧的水平傳輸並不強烈，所以各地臭氧濃度的差異也不小。另外，各地臭氧濃度在 11: 00 時開始迅速升高，但在 17: 00 後也顯示臭氧濃度快速下降，遊其以 C4 測站處下降最快。盆地內各地在 21: 00 時之臭氧濃度已< 20 ppb。但位於下風處之沿海地區，臭氧濃度下降較緩慢，21: 00 時臭氧仍在 30 ppb 左右。

2001 年 10 月 7 日臭氧事件日時，盆地內東測風場北半部一直吹東風(見圖 5)，南半部由 11: 00 之吹南風，逐漸轉成西南風至東風；盆地中心處風向變化較小，由南風逐漸轉成東風。大台中地區西測則一直維持吹東風。但值得一提的是各地風速隨時間有增高之趨勢，地面最

大風速高答 6 m/sec。在 09: 00 時之各地臭氧濃度大都< 30 ppb，11: 00 時沿海地區臭氧濃度升高至 30~50 ppb，而盆地內則升格至 65~80 ppb 間。大部分地區之臭氧濃度以 15: 00 時最高，13: 00 時略低些。Line-1 之 C1、P5 與 T1 三測站位於下風處， 所以 17: 00 以後之變化較小。P6 與 T3 二站之濃度快速降低。圖 5(a)與(b) 之濃度隨時間變化相近，臭氧濃度隨時間等比例增高。15: 00 時 Line-3 除 C2 測站外，其餘各站臭氧濃度均> 100 ppb。另外，17: 00 以後風速增至 4.5 m/sec 以上，污染物之傳輸速度加速，使下風處之 P5 與 T1 於 19: 00、21:00 之臭氧濃度與 T4、T5 之濃度相近。T7 之逐時濃度均最高，顯示該地區有利於臭氧的產生，其原因應與 2001 年 4 月 27 日臭氧事件日時相同，即當地存有高 HC 排放源。

2002 年 5 月 25 日臭氧事件日時，11: 00~19: 00 地面風速均在 3 m/sec 左右，但各地之風向隨時間的變化大，且相當不同，大部分地區之每小時風向均明顯改變(見圖 6)。09: 00 各地臭氧濃度均已相當高，C4 與 T3 二測站測值>75 ppb。11: 00 時 T3 測站臭氧濃度已>110 ppb，且由於有較強之風由 T3 測站南方往北吹，使位處正下風處的 P5 與 C1 的濃度在 90 ppb 左右。圖 6(a)顯示臭氧濃度在各小時中，濃度對位置之關係曲線非常相似，以 13: 00 時之濃度最高，之後各站測值以近似等遞減量方式下降。而有趣的是一直保持最高濃度的 T3 測站，在 21: 00 時之臭氧濃度卻最低，小於 10 ppb。

圖 7 爲 2002 年 8 月 2 日臭氧事件日時，11: 00~19: 00 地面風速均在 2.5~4.5 m/sec 之間，盆地內之風向隨時間增加，顯現出明顯之盆地效應，依地形由吹西南風轉成吹東北風。09: 00 各地臭氧濃度均不高，僅 C4 測站測值約 60 ppb。11: 00 時盆地內各測站臭氧濃度已明顯升高，此時 C4 測站測值已接近 120 ppb，由此盆地效應使位處正下風處的 T5、T7 、C4 與 T8 的濃度均高於 90 ppb。圖 6(c)顯示臭氧濃度在各小時中，濃度對位置之關係曲線非常相似，僅在 15: 00 時 C2 之濃度反升高至 120 ppb，之後各站測值以近似等遞減量方式下降。值得一注意的是 T7 測站濃度一直未明顯增高，以及沿海測站濃度均爲最低。

所有測站在 13: 00 時之臭氧濃度均> 100 ppb。在 15: 00 時除 T8 測站外，所有盆地內測站之臭氧濃度均大於 120 ppb，此時之 C4 測站之測值更達 185 ppb。同時，與前二臭氧事件日不同的是，本日各小時之最高濃度是出現在 C4 測站位置，而非位在 T7 測站。由於本日可謂二年來最嚴重之臭氧事件日，日間之臭氧濃度異常的高，使台中盆地內得入夜後(19: 00 與 21: 00)的臭氧濃度也在 40~60 ppb 間，高於平常日子同時間的臭氧濃度。綜合圖 4~6 之結果分析，顯示一年半以來三個最嚴重之臭氧事件日具有下列特徵：

(1).最嚴重之臭氧事件日大都發生在地面風速不大(3 m/sec 左右)時，風向在大台中地區南半部爲吹東南風→南風→東南風→東風，而北半部則爲吹東風或東南風。

(2).位於盆地內東測之 T7 與 C4 二測站位置，是臭氧事件日中最高濃度之處。由於 T7 測站之高濃度常突出其四周其他測站，顯現顯示該地區有利於臭氧的產生，其原因應與該處之交通繁忙與工廠較密集所致。

(3).會有臭氧或其前軀物由外西南端或東南端傳輸進入大台中地區，造成下風處臭氧濃度升高，其中以 2002 年 5 月 25 日臭氧事件日時最此現象爲明顯。

(4).沿海地區的風場與盆地內不同，因此盆地內的高臭氧濃度對沿海地區的影響不大。

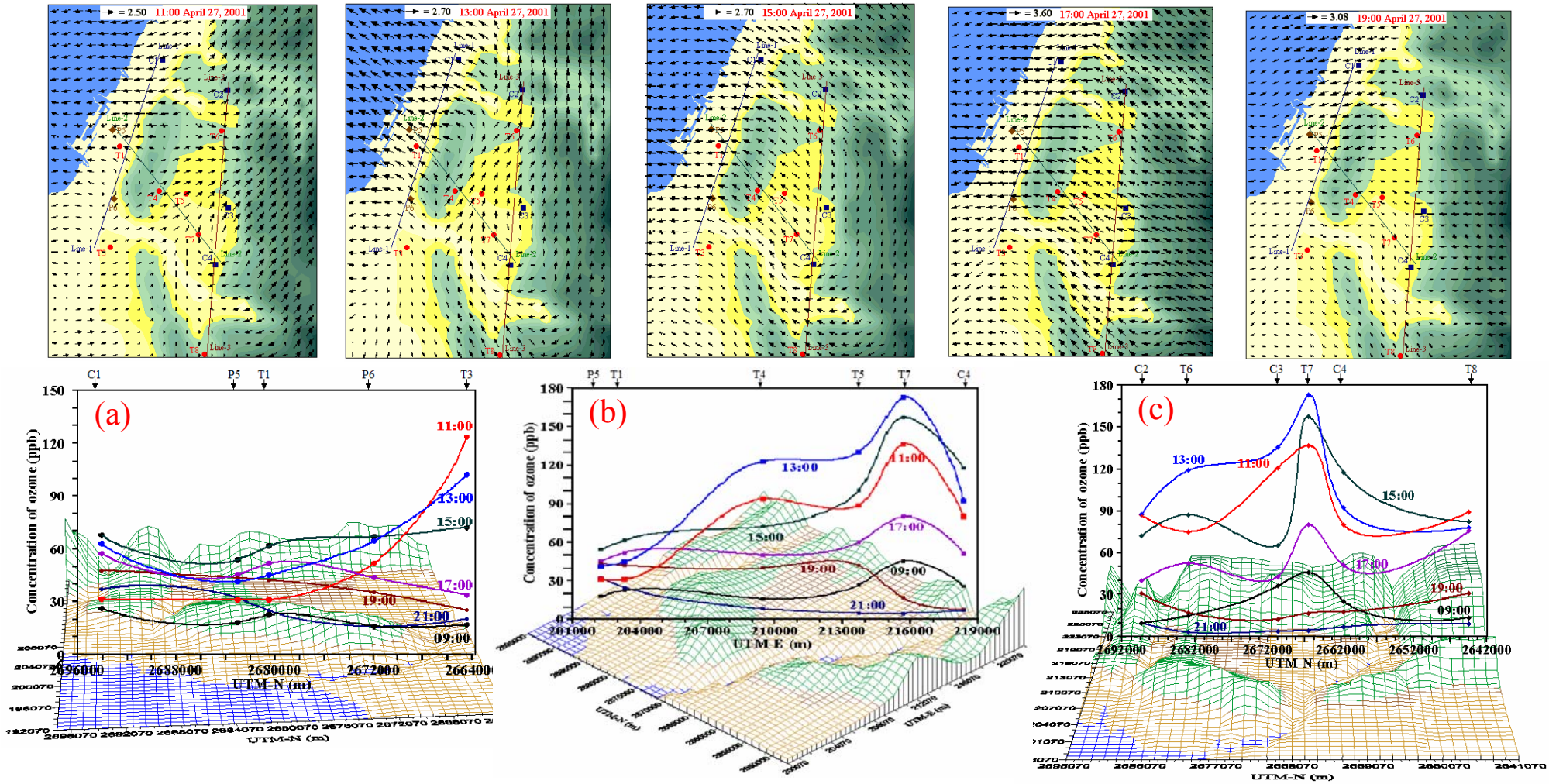

Figure 4 Measurements of ozone and surface wind from air-monitoring stations of the Taichung Area on April 27, 2001. (a) five air-monitoring stations in the coastal area. (b) six air-monitoring stations from sea side to the east of basin. (c) six air-monitoring stations in the Taichung Basin.

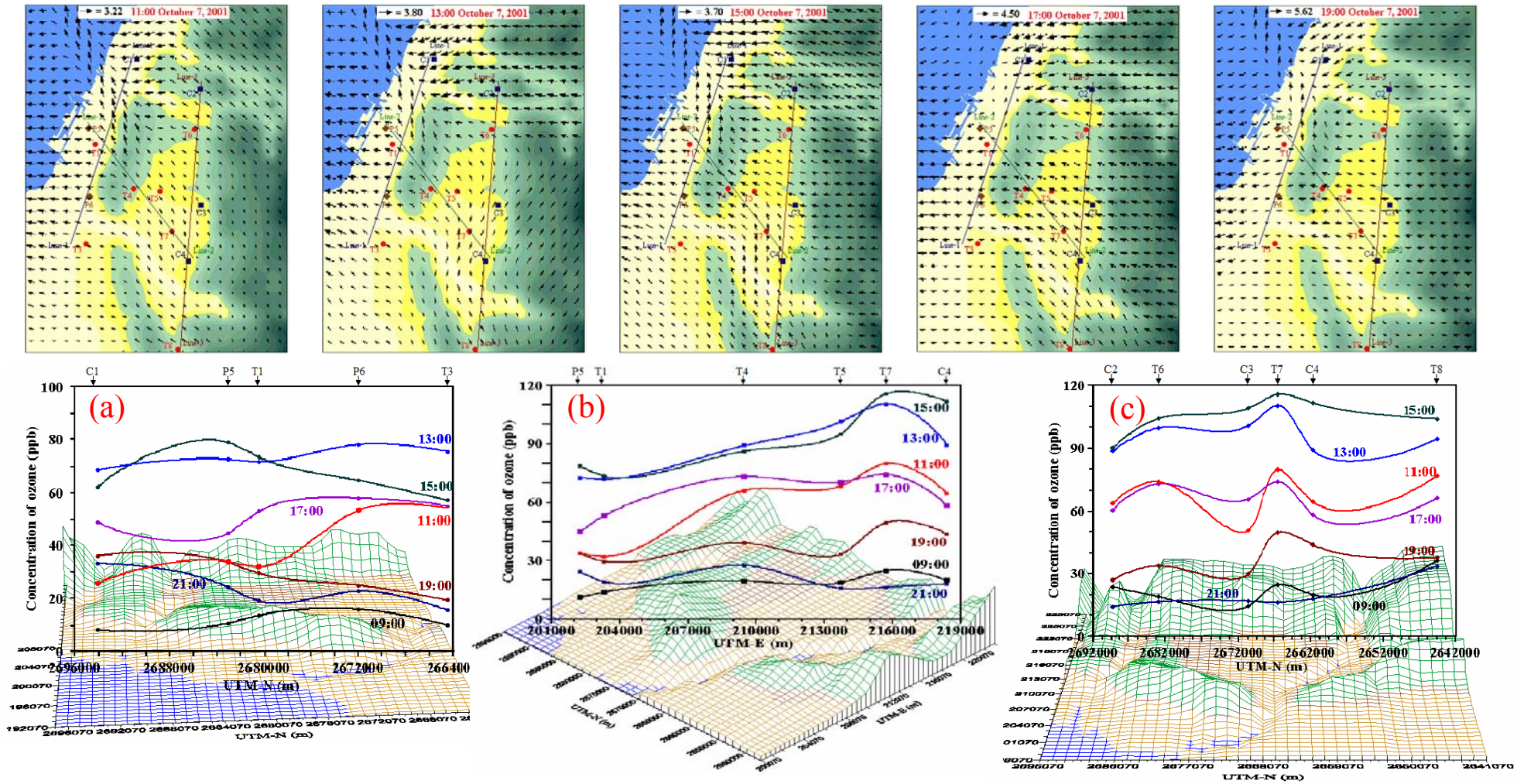

Figure 5 Measurements of ozone and surface wind from air-monitoring stations of the Taichung Area on October 7, 2001. (a) five air-monitoring stations in the coastal area. (b) six air-monitoring stations from sea side to the east ofbasin. (c) six air-monitoring stations in the Taichung Basin.

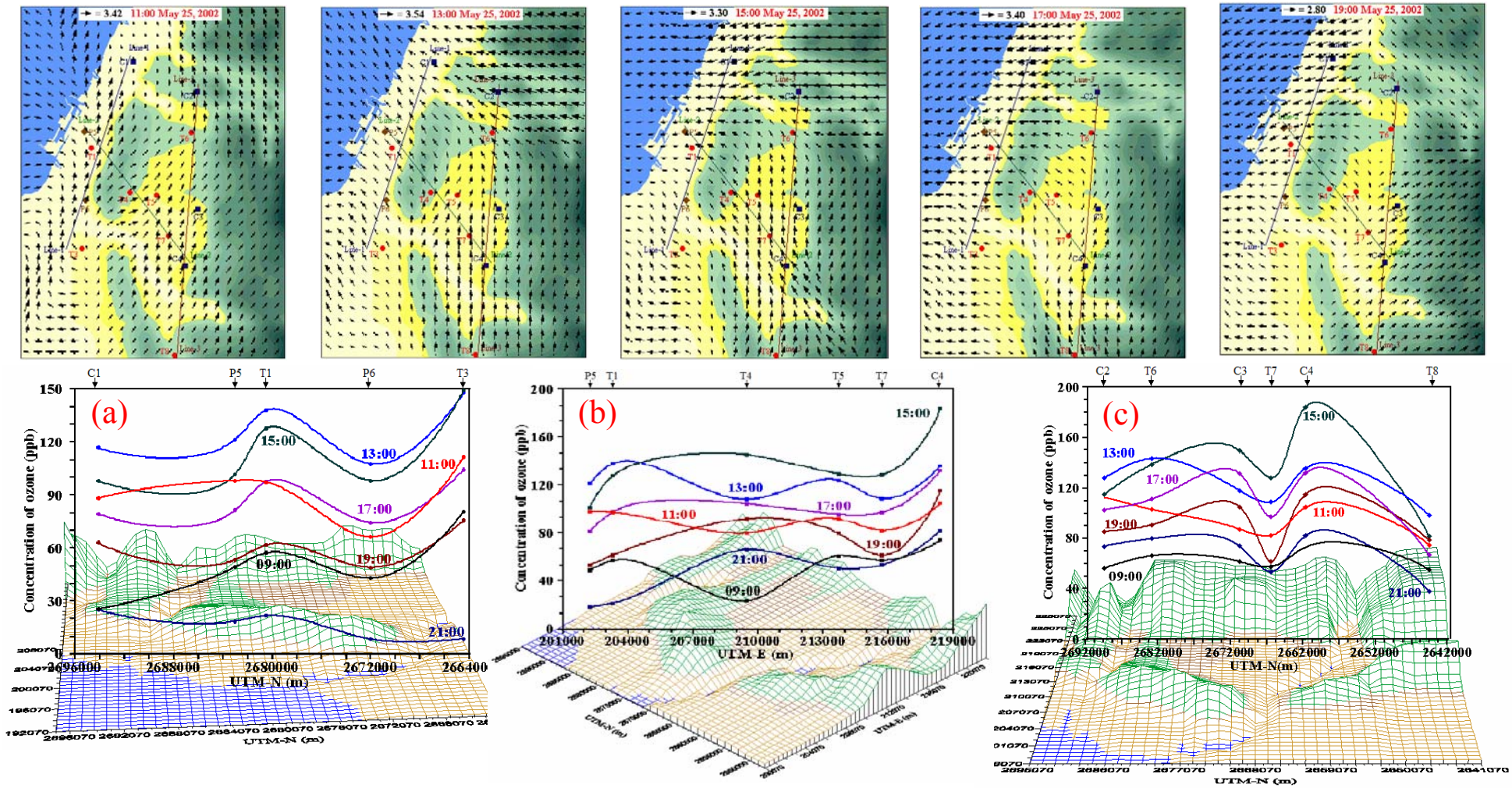

Figure 6 Measurements of ozone and surface wind from air-monitoring stations of the Taichung Area on May 25, 2002. (a) five air-monitoring stations in the coastal area. (b) six air-monitoring stations from sea side to the east of basin. (c) six air-monitoring stations in the Taichung Basin.

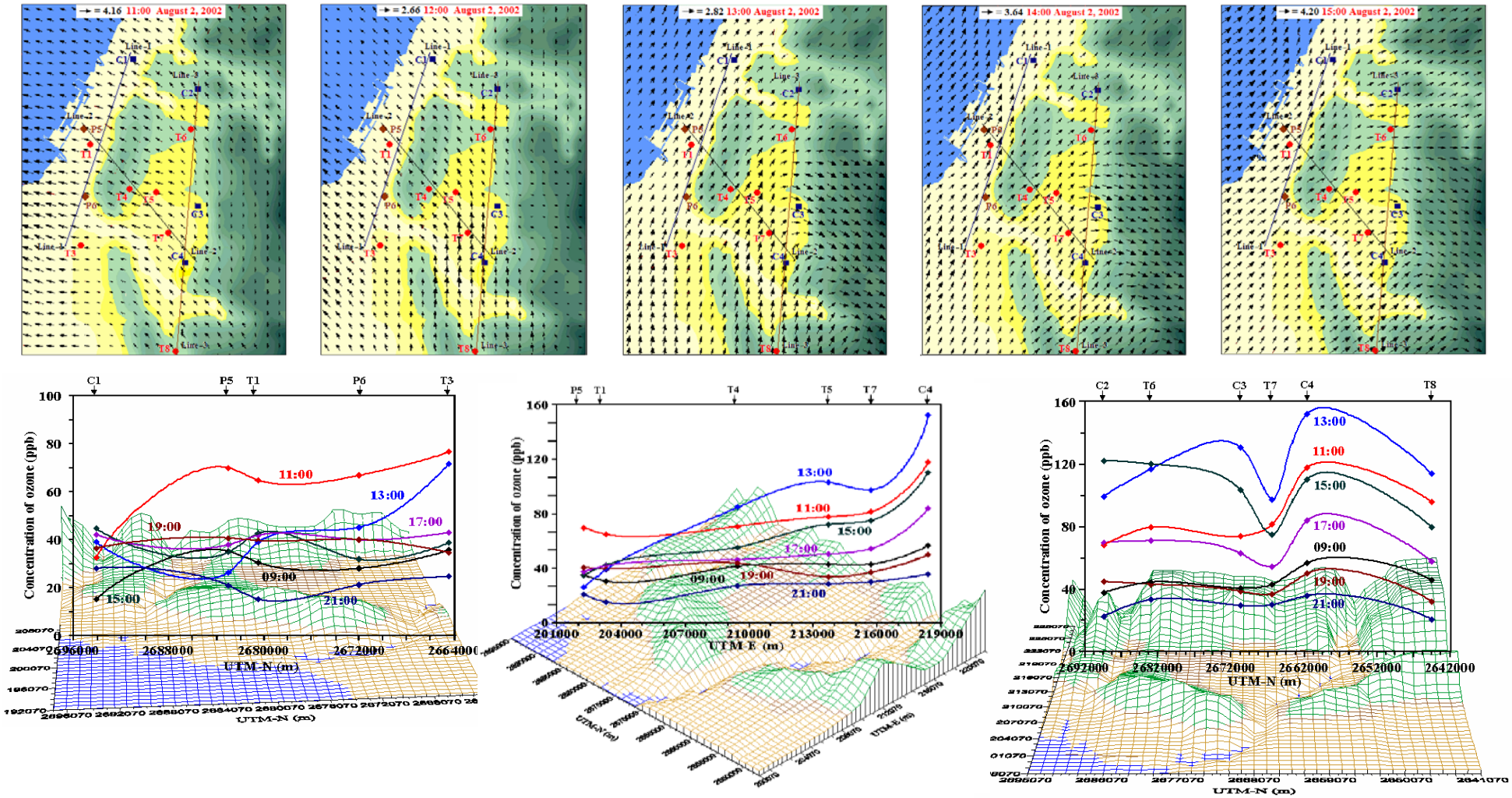

Figure7 Measurements of ozone and surface wind from air-monitoring stations of the Taichung Area on August 2, 2002. (a) five air-monitoring stations in the coastal area. (b) six air-monitoring stations from sea side to the east of basin. (c) six air-monitoring stations in the Taichung Basin.

考慮臭氧在大氣中之非穩定狀態與一維的傳輸與反應作用，可獲得(2)式[21]

$$\frac{\partial[\mathrm{O_3}]}{\partial t}+\frac{\partial(u[\mathrm{O_3}])}{\partial x}=R-L[\mathrm{O_3}] \tag{2}$$

其中 u、R 與 $L[\mathrm{O_3}]$分別爲風速、臭氧產生速率與消失速率，而 L 爲消失速率常數。將(2)式改寫成差分式(3)式，其中$[\mathrm{O_3}]_i^n$爲於位置 i 與時間 t_n 之臭氧濃度。

$$\frac{[\mathrm{O_3}]_i^{n+1}-[\mathrm{O_3}]_i^n}{\Delta t}+\frac{u_i^n[\mathrm{O_3}]_i^n-u_{i-1}^n[\mathrm{O_3}]_{i-1}^n}{\Delta x_{i\leftrightarrow i-1}}=R^n-L^n[O_3]_i^n \tag{3}$$

由圖 5 獲知當日 11:00~17:00 之風向保持與 Line-2 之各測站位置平行，顯示各測站該時段所測得數據滿足(2)式之非穩定狀態與一維的傳輸條件。將該時段之數據整理並列於表 2 中，運用表 2 數據配合(3)式以 $\left(\frac{[\mathrm{O_3}]_i^{n+1}-[\mathrm{O_3}]_i^n}{\Delta t}+\frac{u_i^n[\mathrm{O_3}]_i^n-u_{i-1}^n[\mathrm{O_3}]_{i-1}^n}{\Delta x_{i\leftrightarrow i-1}}\right)$ 對 $[\mathrm{O_3}]_i^n$ 做圖，可得斜率$-L^n$與截距 R^n 值，所得結果亦列於表 2 中。

Table 2 Observed ozone concentrations and surface wind speeds and calculated R and L values in T7, T4, T1, and P5 on October 7, 2001.

i	1 (T7)		2 (T4)		3 (T1)		4 (P5)		R	L
t_n	$[\mathrm{O_3}]$ (μg/m^3)	u (m/hr)	$[\mathrm{O_3}]$ (μg/m^3)	u (m/hr)	$[\mathrm{O_3}]$ (μg/m^3)	u (m/hr)	$[\mathrm{O_3}]$ (μg/m^3)	u (m/hr)	(μg/m^3-hr)	(1/hr)
11:00	154.6	4680	127.9	3600	62.1	6840	65.6	5760		
12:00	200.1	6480	152.5	4320	105.5	7200	107.8	6840	80.27	0.657
13:00	213.9	6120	172.5	6840	139.0	7920	140.5	7920	238.26	1.883
14:00	228.6	5760	180.0	8640	143.2	7200	145.5	6480	30.98	0.215
15:00	223.9	8280	166.8	9000	142.3	7200	152.5	6120	–213.05	–1.262
16:00	184.3	11160	149.2	12600	124.6	7920	116.3	7920	–128.87	–0.468
17:00	143.6	9360	141.7	11880	102.8	11160	86.9	7920	–201.03	–1.082

$\Delta x_{1\leftrightarrow 2}$=9296 m, $\Delta x_{2\leftrightarrow 3}$=9418 m, $\Delta x_{3\leftrightarrow 4}$=2757 m.

由表 2 獲知 R 與 L 值在 14:00 後，均由正轉爲負值，顯示大氣主要反應有明顯的轉變。8 爲當日四測站之$[\mathrm{O_3}]$與 R、 L 逐時變化。圖顯示$[\mathrm{O_3}]$ 在 14:00 左右最高，R 與 L 值在 12:~13:00 間最大，在 14:00~15:00 間最小。14:00 係因 NOx 與 HC 反應使臭氧濃度增高 14:00~15:00 間，因光化學煙霧(photochemic smog)產量最大，消耗臭氧使 R 與 L 由正轉爲值[22]。然而 16:00 以後又出現另一低的 R 與 L 值，顯現另一種臭氧之消耗反應在進行，此反的形勢與種類未知，是否是臭氧與大氣中之微或水份反應，則有待更進一步的深入探討。

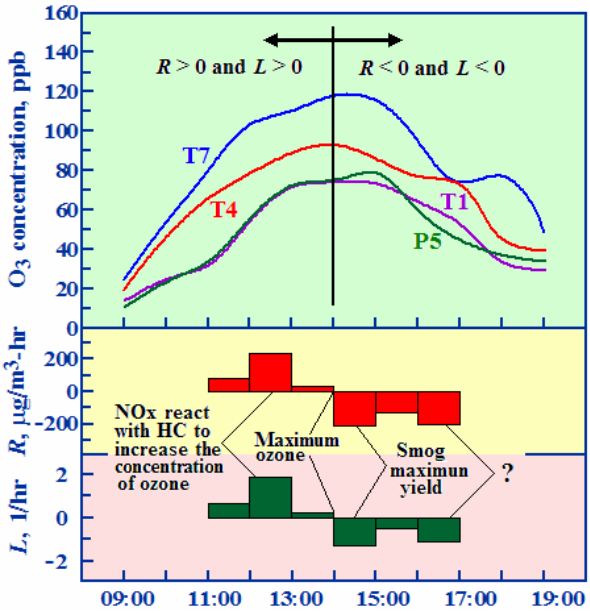

Figure 8 O_3 concentrations, R and L values of the Taichung Area on October 7, 2001.

伍、垂直縱深之大氣樣品採集與分析

垂直縱深採樣工作係藉助一套附有絞盤、絞繩與大型氣球之裝置(見圖 9)，大型氣球升空同時將數個小型定時採氣設備一併拉上不同高程位置，而小型定時採氣設備包含定時器、採氣泵與 10 公升之 Tedler 採氣袋。由於受限於國內航線空域關係，大型氣球無法升空過高，

因此垂直採樣高程爲 ground、100、200、300、400、500 m 等六個不同高度。採集樣品於現場分別進行 HC 濃縮，及直接進行 NO、NO_2 與 O_3 分析。採樣時並使用衛星定位儀(GPS)與雷射測距儀(Bushnell, Laser Rang-finder 1000)來標定座標與高程。

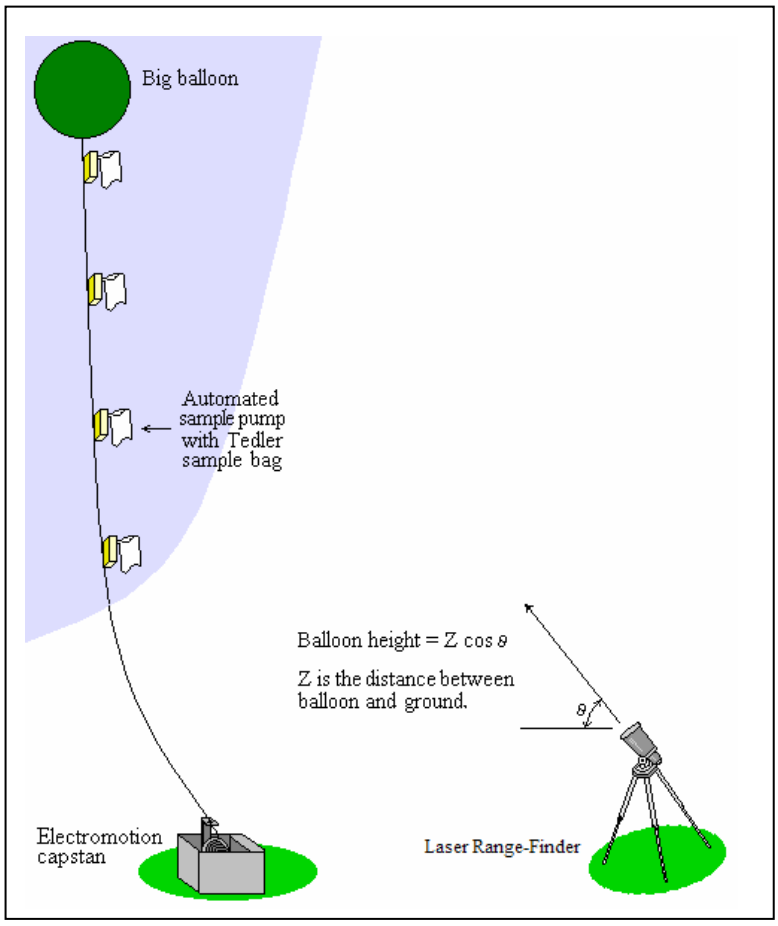

Figure 9 Schematic of the sampling apparatus for air pollutant at different altitude.

一、HC 之濃縮採樣

由於大氣中 HC 濃度通常甚低，使濃縮採樣與分析不可或缺。研究中，濃縮採樣係依 U.S. EPA TO-10A 與 TO-14A 方法，使用固體吸附劑 Tenax TA 做爲捕集材料，於液態氮冷卻下，進行濃縮採集工作，濃縮倍率訂爲 15,000 倍，如此可分析出 低於 ppb 範圍之 HC 的質與量。濃縮採樣之設備如圖 10 所示。

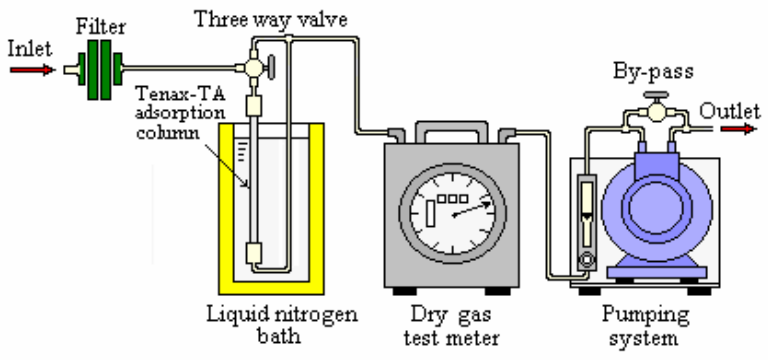

Figure 10 Primary concentration of air samples (VOCs) on Tenax-TA at liquid nitrogen temperature.

二、O_3、NO_X 與 HC 之分析

採用分析儀分別爲 API Model-200A NO_X Analyzer 與 DASIBI Model-1008-PC O_3 Analyzer，所依據方法分別爲 NIEA A417.10T 與 NIEA A420.10T。其中以 10 公升 Tedler 袋來採集大氣樣品，足夠 NO_X 與 O_3 分析儀於現場直接抽引分析與 HC 濃縮所需。

濃縮後試樣以液氮冷凍帶回實驗室，再以熱脫附系統配合氣相層析質譜儀(Shimadzu QP-5050A GC/MS)來進行 HC 之定性與定量分析。分析時將採樣後之 Tenax-TA 吸附管裝於熱脫附系統上，於 150 °C 脫附，再經液氮驟冷低溫凝聚後，引入 GC/MS 中分析。採用毛細分離管爲長 60 m 內徑 0.25 mm 之 Chrompack DB-1。GC 操作條件爲：(1).oven 初溫: −20 °C(由 GC/MS 自動控制通入液態 CO_2 來控溫)，(2).以 8 °C/min 升溫至 200 °C 後保持於此溫度，(3).載氣流率: 3 ml/min，(4).split rate: 1/10。MS 操作條件爲：(1).Range: 33~300 mass，(2).Detector volts: 1.1 kV，(3).Scan interval: 0.5 sec，(4).Scan speed: 500。

三、高空風場測定

掌握當地風場變化，尤其 1000 公尺以下低高空之風向、風速，更是瞭解 O_3 擴散不可或缺的資料。量測方法係採用施放氣球式，所施放氣象氣球浮力通常小於 100 克以控制上升速度，氣球下並無繫掛任何感應器，故必須配合經緯儀來量測之。氣球施放後由已定位之數位式經緯儀(World Z105−8)開始讀取仰角和方位角，每隔 20 秒讀一次，直到看不見爲止。所得數據依單經緯儀法(Single−theodolite meyhod)之風向與風速關係式(見圖 11)，來求取不同高度之風向及風速。

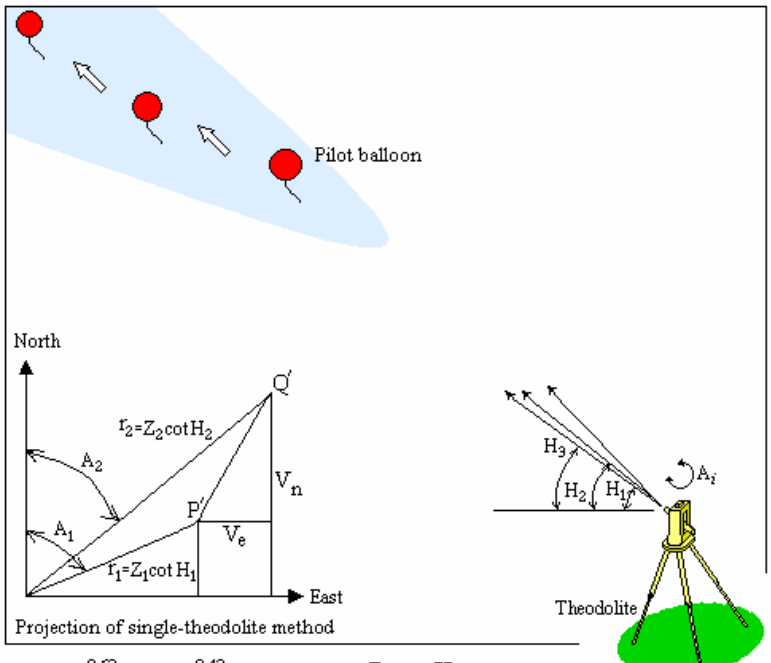

$U=72L^{0.63}/(L+W)^{0.42}$ $\quad r_1=Z_1\cot H_1$

$V_e=Z_2\cot H_2\sin A_2-Z_1\cot H_1\sin A_1$

$V_n=Z_2\cot H_2\cos A_2-Z_1\cot H_1\cos A_1$

$\phi=\tan^{-1}(V_e/V_n)$ $\quad P'Q'=V_e/\sin\phi$ $\quad V=P'Q'/t$

where U, W, L, and Z_1 are uprise speed, weight, buoyance, and height of balloon, r_1 is the projection on the ground of balloon at point P, V_e and V_n are the projection of wind speed on east and north, ϕ is the degree between V_e and V_n, $P'Q'$ is the projection of PQ on the ground, and V is mean wind speed.

Figure 11　Schematic of the wind field measure apparatus at different altitude.

四、採樣分析結果

順利完成二次沿海區域採樣工作(6 月 27、28 日與 8 月 1、2 日)，二次內陸區域採樣工作(7 月 1、2 日與 9 月 14、15 日)，以及採樣後之分析工作。值得特別一提，由於高空採樣工作相當費時費力，而本研究無論於沿海地區或盆地內均分別選定四個採樣點，二者之採樣點南北最大距離均超過 30 km，若於一天內完成四個採樣點的採樣工作，則含路程之花費時間會超過 5 小時，無法於每個採樣點採得臭氧於每日 11:00~14:00 間的高峰濃度試樣。所得結果恐難以用於闡釋該地區之風場、時間、地形對臭氧傳輸之影響。因此，本研究選定每天僅於 11:00~14:00 間進行二個採樣點之高空採樣工作，且連續二天來完成四個採樣點的採樣方法，同時每次採樣所選定的連續二天，均必須具有非常相近的氣候狀況，如此以減少因非同日與同時多點採樣所造成之誤差。

圖 12 爲以 GC/MS 分析所得之 TIC 圖與 VOCs 名稱與出現位置代表圖。其中化合物定性工作之 SI 值(吻合度)，僅 21 個化合物介於 70~80 間，其餘化合物之 SI 值均高過 80，而亦有不少化合物的 SI 值更高於 90，足見本研究採用高濃度倍率(15000 倍)、超低溫(液態氮冷卻)濃縮採樣，以及運用線上熱脫附操作與毛細分離管柱低啓始溫度(液態二氧化碳冷卻) 之分析操作等程序，相當的成功，爲後續研究工作提供高可信度之數據。

分析所得結果之詳細分類如后，其中紅色數字爲該化合物在右圖中之編號。定量分析上，本研究採用 RESTEK 公司符合 U.S. EPA Method TO-14A Calibration Mix (cat.#34400)與 Method TO-15 Ozone Precursor Mixtures (cat.#34420)之標準氣體，如同採樣工作操作方式，取三個適量的標準氣體，分別濃縮於三根 Tenax TA 濃縮管中。經由 GC/MS 之定性與定量分析，求出各碳氫化合物之平均相對感度係數(Relative response factor, RRF)，其中選定甲苯之感度係數爲 1，所得結果如圖 12 所繪。因感度係數之製造過程與採樣完全相當，如此可以避開兩者因操作程序不同所造成之誤差。

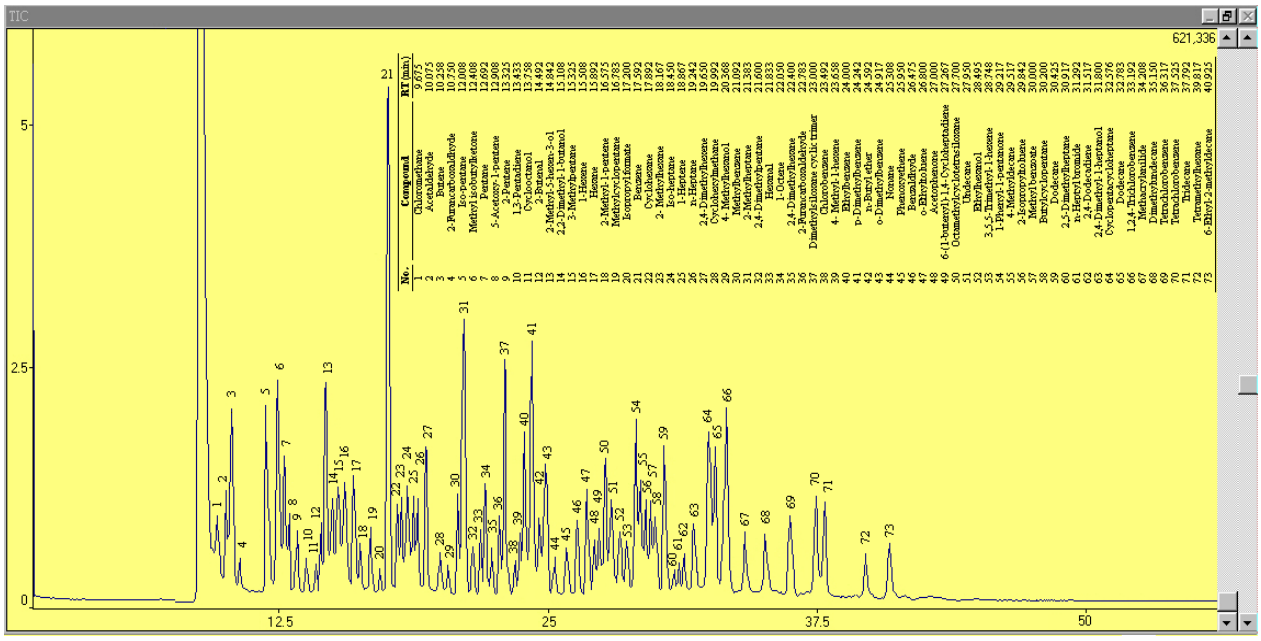

Figure 12　Chromatogram of air pollutant (VOCs) separation obtained after collecting VOCs in a concentrator with Tenax-TA.

Table 3 Summary of the qualitative analysis

烷類：(21 個化合物)
- [5] Iso-pentane
- [7] Pentane
- [15] 3-Methyl pentane
- [17] Hexane
- [23] 2- Methyl hexane
- [24] Iso-heptane
- [26] n-Heptane
- [27] 2,4-Dimethyl hexene
- [31] 2-Methyl heptane
- [32] 2,4-Dimethyl pentane
- [35] 2,4-Dimethyl hexane
- [44] Nonane
- [51] Undecane
- [55] 4-Methyldecane
- [59] iso-Dodecane
- [60] 2,5-Dimethyl heptane
- [65] Dodecane
- [68] Dimethyl undecane
- [71] Tridecane
- [72] Tetramethyl hexane
- [73] 6-Ethyl-2-methyl decane

多官能基類：(5 個化合物)
- [12] 2-Butenal
- [13] 2-Methyl-5-hexen-3-ol
- [20] Isopropyl formate
- [45] Phenoxy ethane
- [67] Methacryl anilide

烯類、二烯類：(12 個化合物)
- [3] Butene
- [8] 5-Acetoxy-1-pentene
- [9] 2-Pentene
- [10] 1,3-Pentadiene
- [16] 1-Hexene
- [18] 2-Methyl-1-pentene
- [25] 1-Heptene
- [34] 1-Octene
- [39] 4-Methyl-1-hexene
- [49] 6-(1-butenyl)-1,4-Cycloheptadiene
- [53] 3,5,5-Trimethyl-1-hexene
- [62] 2,4-Dodecadiene

芳香族類：(7 個化合物)
- [21] Benzene
- [30] Toluene
- [40] Ethyl benzene
- [41] p-Xylene
- [43] o- and m-Xylene
- [47] o-Ethyl toluene
- [56] Isopropyl toluene

醇類：(5 個化合物)
- [11] Cyclooctanol
- [14] 2,2-Dimethyl-1-butanol
- [29] 4- Methyl hexanol
- [52] Ethylhexanol
- [63] 2,4-Dimethyl-1-heptanol

醛、酮類：(8 個化合物)
- [2] Acetaldehyde
- [4] Furancarboxaldhyde
- [6] Methyl ethyl ketone
- [33] Hexanal
- [36] 2-Furancarboxaldehyde
- [46] Benzaldhyde
- [48] Acetophenone
- [54] 1-Phenyl-1-pentanone

醚、酯類：(2 個化合物)
- [42] n-Butyl ether
- [57] Methyl benzoate

有機鹵化物：(6 個化合物)
- [1] Chloromethane
- [38] Chlorobenzene
- [61] n-Heptyl bromide
- [66] 1,2,4-Trichloro benzene
- [69] Tetrachloro benzene
- [70] Tetrachloro benzene

矽烷物：(2 個化合物)
- [37] Dimethyl siloxane cyclictrimer
- [50] Octamethyl cyclotetrasiloxane

由於本研究所選定之濃縮倍率爲 15000 倍，所以前述濃度尚需再除以 15000，以獲得其在大氣中之實際濃度。運用圖 13 與 14 之相對感應係數與檢量線結果，將 HC 採樣分析所得繪製於圖 15~18 中，而由這些圖獲知大台中地區大氣中存在物種以烷與環烷最多，其次爲烯與二烯類，再其次爲有機鹵化物、醇類、芳香族類，以及醛、酮類。但在單一化合物的濃度上，常見的苯、乙基苯、甲苯、二甲苯(Benzene [21], Ethyl benzene[40], Toluene [30] and Xylene [41, 43], BETX)則均有相當的濃度存在各高程大氣中。一般而言，雖然有許多的烯類與醛、酮類化合物被檢測出，但它們的濃度大都不高。另外，有二矽烷[37, 50]被檢測出，且濃度亦不低，其來源值得深入探討。各採樣點分析結果之詳細說明於后。

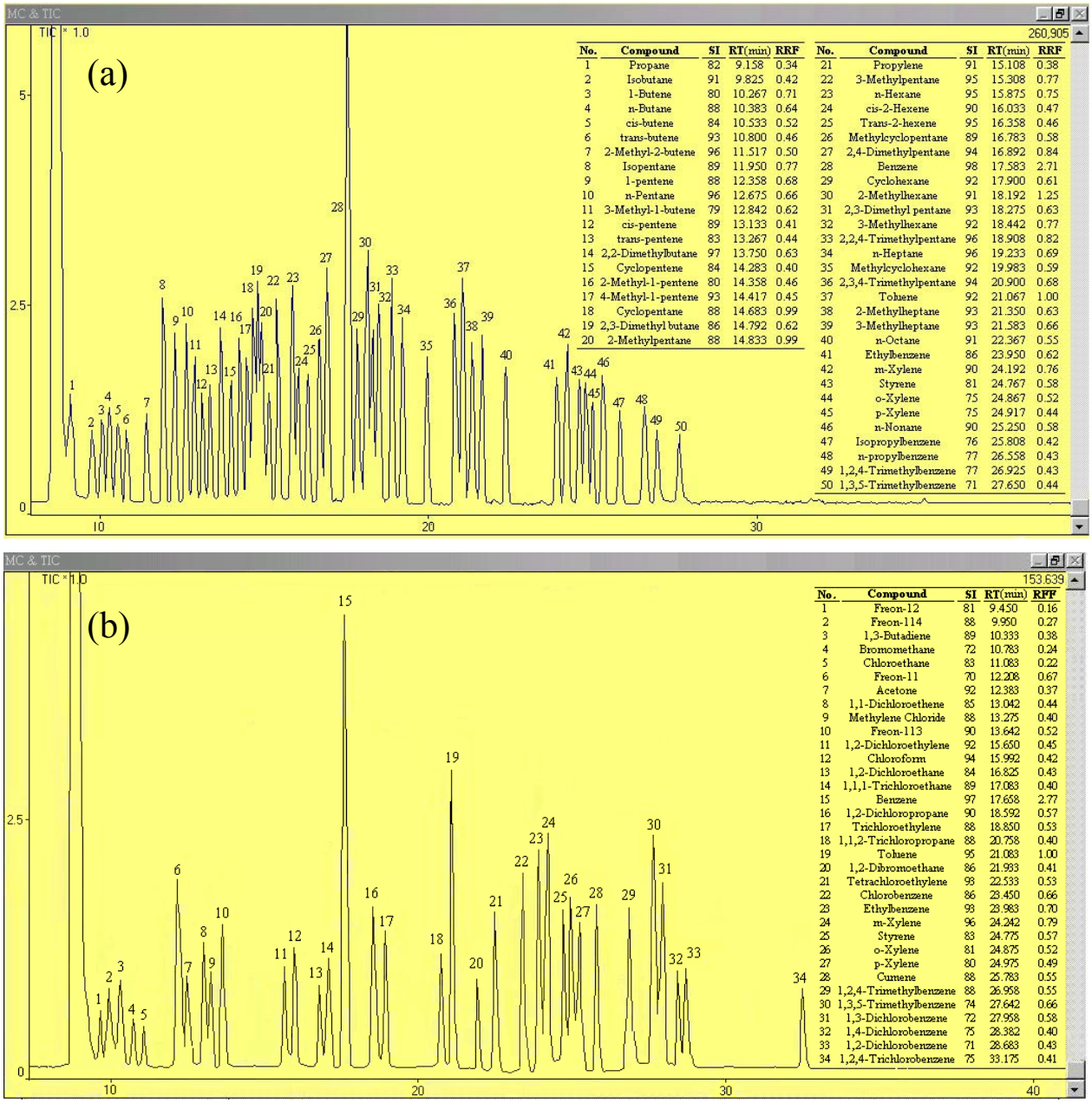

Figure 13 Chromatogram and RRF of the standard gases separation obtained after collecting VOCs in a concentrator with Tenax-TA. (a) TO-15 Ozone Precursor Mixtures (RESTEK, cat.#34420) and (b) TO-14A Calibration Mixtures (RESTEK, cat.#34400).

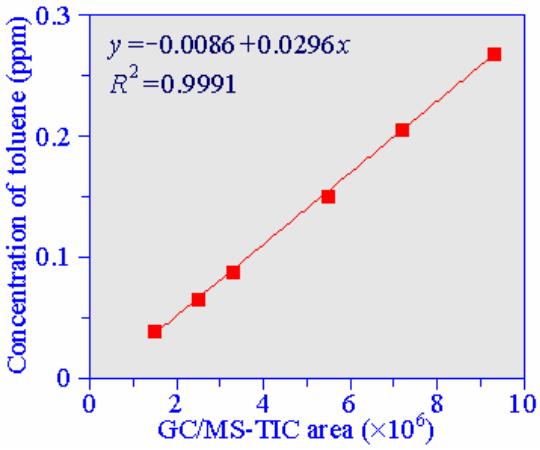

Figure 14 Toluene standard curve.

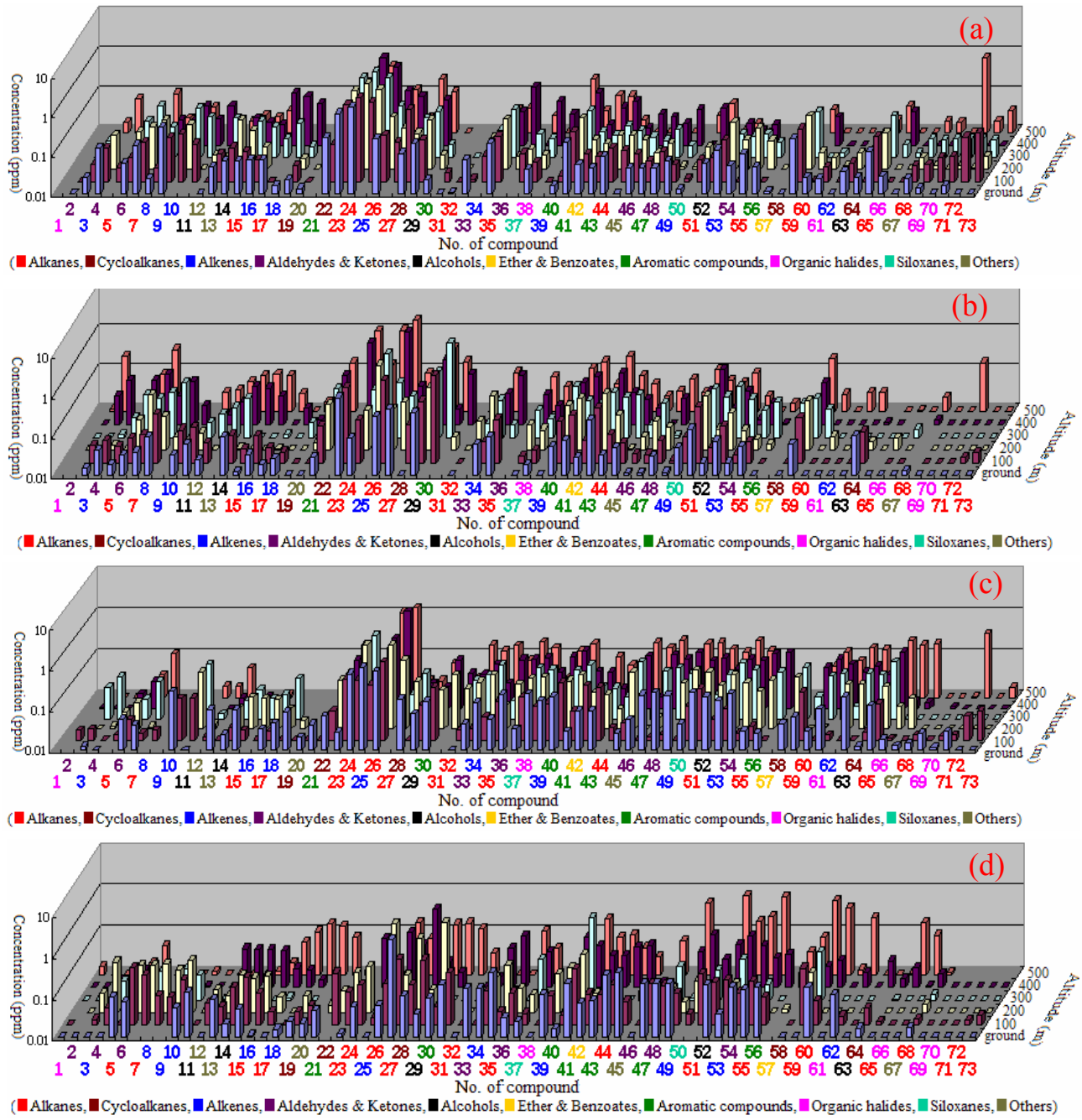

Figure 15　Plot of concentration and compound distribution at different altitude at (a) S1, (b) S2, (c) S3, and (d) S4, in the coastal area on June 27 and 28, 2002.

圖 15 顯示各採樣位置均以[22]~[32]之烷類、烯類與醇類有較高的濃度，尤其是庚烷[23, 24, 26]與辛烷[27]，其次是[38]~[55] 之各種化合物，再者爲[4]~[18] 之各種化合物。S1 採樣點之 BETX 濃度約在 0.01~0.05 ppm 間，而 L2、L3 與 L4 採樣點之 BETX([21]、[30]、[40]、[41]、[43]) 濃度約在 0.06~0.12 ppm 間。L3 之[23]~[65]間各 HC 濃度大小最爲相近，各高程之 HC 總濃度也高於其他三採樣點。基本上各採樣點均以 500 m 高程存在最高之 HC 濃度，而地面之 HC 濃度略低些。整體而言，本次採樣分析結果顯示沿海地區各採樣點與各高程，均有相當的 HC 存在大氣中，且上空大氣中之 HC 物種數量與濃度均較地面高。由於 L1 與 L2 位置之交通量與人口數遠少於其他二處，但 HC 物種數量與濃度亦不低，顯示空氣中 HC 主要來源爲環境中的傳輸。此點可與後面的研究成果來一併討論。

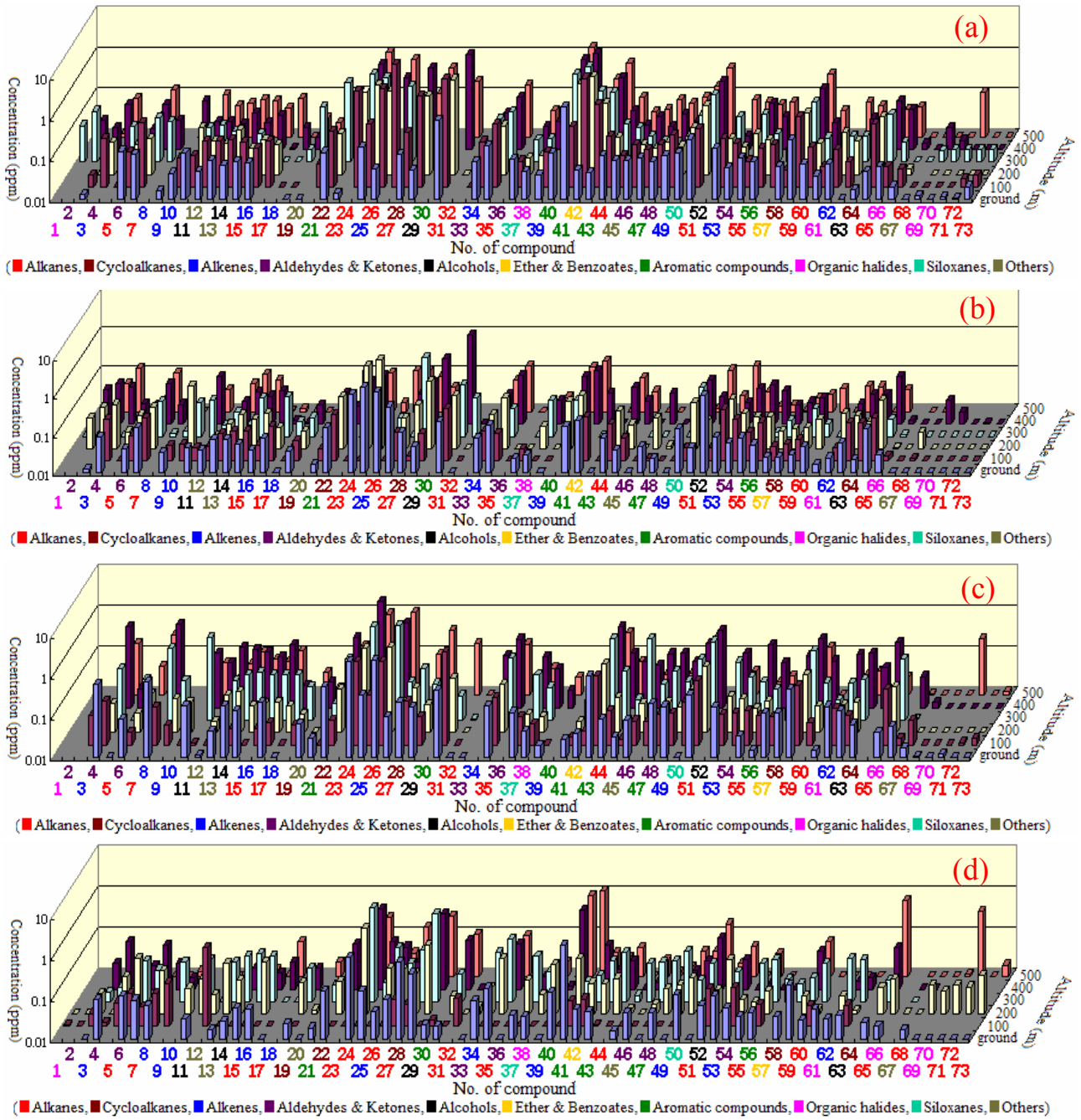

Figure 16　Plot of concentration and compound distribution in the different altitude at (a) L1, (b) L2, (c) L3, and (d) L4, in Taichung Basin on July 1 and 2, 2002.

圖 16(a)中顯示 L1 採樣點地面 HC 物種與濃度較其他高程少與低。100~500 m 高程之 HC 物種與濃度大小均十分相似，其中以 [22]~[32]之烷類、烯類與醇類有較高的濃度，芳香族類苯與甲苯的濃度小，但有 0.1 ppm 左右的乙基苯與二甲苯存在各高程。L2 採樣點地面與 200 m 處之各 HC 濃度略高於其他高程(見圖 16(b))，而 BETX 的濃度均很小，而以[24]~[32]之烷類、烯類與醇類有較高的濃度。圖 16(c)顯示 L3 採樣點各高程之 HC 物種與濃度與 L1 採樣點相似，但地面之 HC 濃度較 L1 處高。L2 樣點的 HC 濃度低於其他採樣點，尤其是[12]~[20]與[55]~[63]之化合物濃度明顯較低，但 300 m 高處有較高 [69]~[73]之烷類與芳香族類存在。

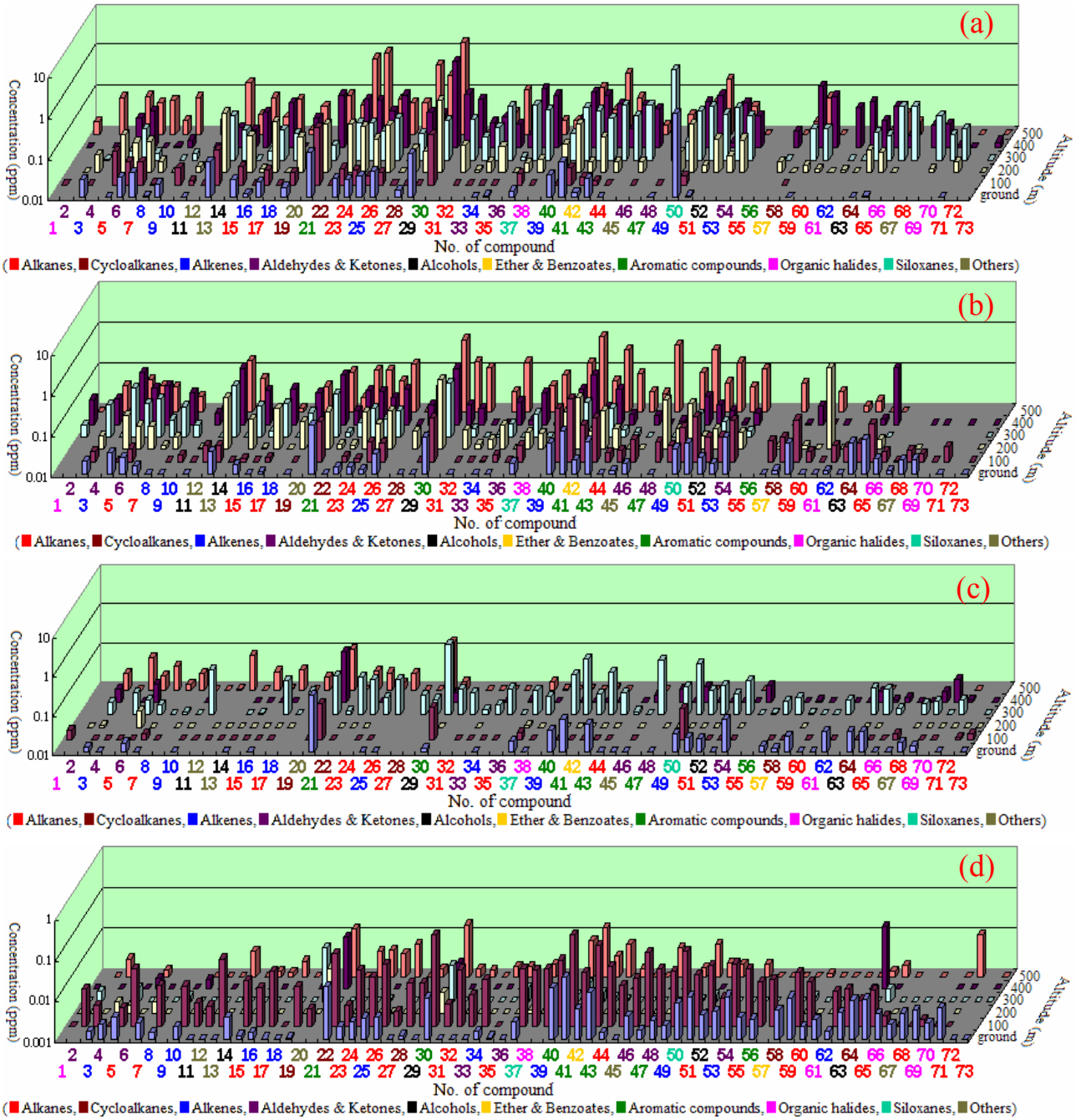

Figure 17　Plot of concentration and compound distribution in the different altitude at (a) S1, (b) S2, (c) S3, and (d) S4, in the coastal area on August 1 and 2, 2002.

圖 17(a)中顯示 S1 採樣點 300~500 m 高程有著較多之 HC 物種與濃度，其中不乏芳香族類，尤其是各高程都存在有相當濃度的 BETX。另外，也有相當的矽烷與各種烷、烯類。S2 採樣點各高程之 HC 物種與濃度較 S1 處少些(見圖 17(b))，但的濃度亦相當高，其餘物種與濃度相似於 S1，但地面處的 HC 亦較少。圖 16(c)顯示 S3 採樣點各高程之 HC 非常少，僅 300 m 高處有高之濃度，但除甲苯[30]外，其餘化合物濃度均< 0.1 ppm。四個沿海地區各高程之 HC 濃度，均以 S4 採樣點最低(見圖 17(d)，注意濃度尺度不同於其他圖)，僅少數幾個化合物濃度> 0.01 ppm，而濃度最高者是 300 m 高程之甲基異丁酮[6]、環己烷[20]、甲苯[30]與二甲苯[41, 43]。

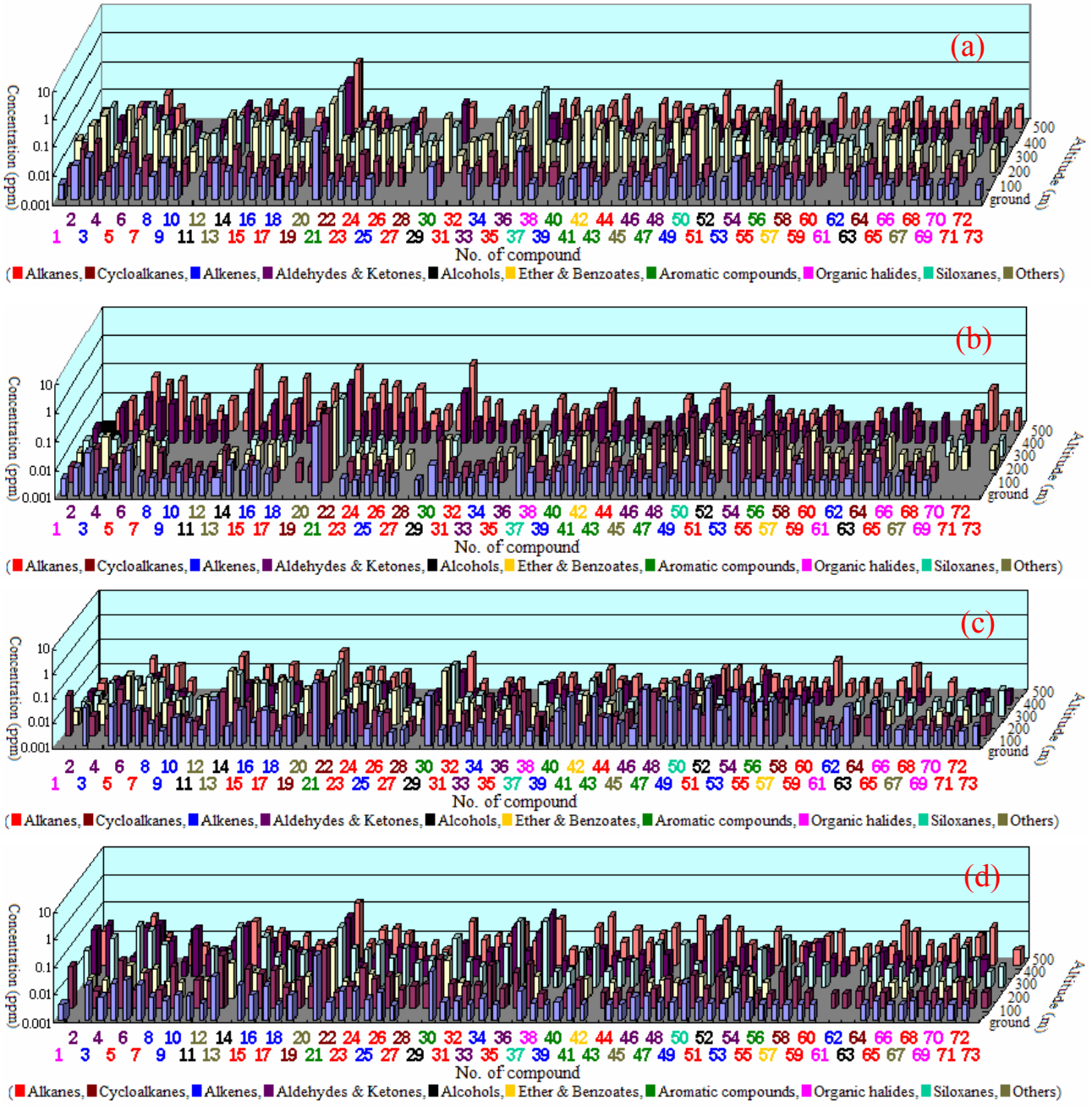

Figure 18　Plot of concentration and compound distribution in the different altitude at (a) L1, (b) L2, (c) L3, and (d) L4, in Taichung Basin on September 14 and 15, 2002.

圖 18(a)中顯示各採樣點雖均可分析得大部份的 HC，但其濃度並非很高，其中以 L2 採樣點除 500 m 高程處之 HC 外，300 m 高程處的 HC 濃度最低，但的 HC 濃度最低其他高程的 HC 濃度亦較小。而 L4 採樣點各高程之 HC 較高，尤其是[64]~[73]之一些有機鹵化物與高分子量烷類有較高的濃度。雖然各採樣點之地面 HC 濃度均較低，但各 HC 之濃度亦未明顯隨高程改變，而有確切的遞增或遞減變化，HC 物種與濃度大小均十分相似。其中本次採樣分析中，[1]~[10]之低分子量 HC 濃度顯現增加的現象，此是否受季節改變所致，值得再深入探討。另外。L1 與 L2 兩採樣點其[22]~[32]之烷類、烯類與醇類濃度亦有減少情形。四個採樣點各高程之芳香族類苯[21]、甲苯[30]、乙基苯[40]、二甲苯[41, 43, 47]均存有相當的濃度。

高空採樣當時之地面各種空氣污染物濃度分布與風場變更，亦非常的重要。因此，本研

究亦蒐集採樣時段大台中地區各監測站之監測資料，經整理並繪製地面風場與臭氧變化圖，如此得以與各項實測結果相比較，以釐清大台中地區各種空氣污染物之貢獻量與承受量。圖 19 顯示第一次沿海地區採樣時，北部位置各高程均吹東南風，南部則吹西南風，風速隨高程漸增，最大風速在 4 m/sec 左右。O_3、NO、NO_2 與 HC 最高濃度之出現位置(UTM-N, Altitude)，分別在(2684000, ground)、(2679000, 400)、(2679000, ground)與(2684000, 500)處之 60、7.0、20 ppb 與 7.0 ppm。O_3 在全區垂直濃度分布並無大差異，水平上則以中段明顯變動，向南、北快速遞減。NO 與 NO_2 的濃度分布高近似，垂直上無大變動，而水平上則由北向南逐漸快速增高濃度。HC 的濃度分布曲線與前三者不同，濃度隨位置的變動性較大，且呈現由南往北濃度遞減，以及中段 300 m 高以上有較高之濃。

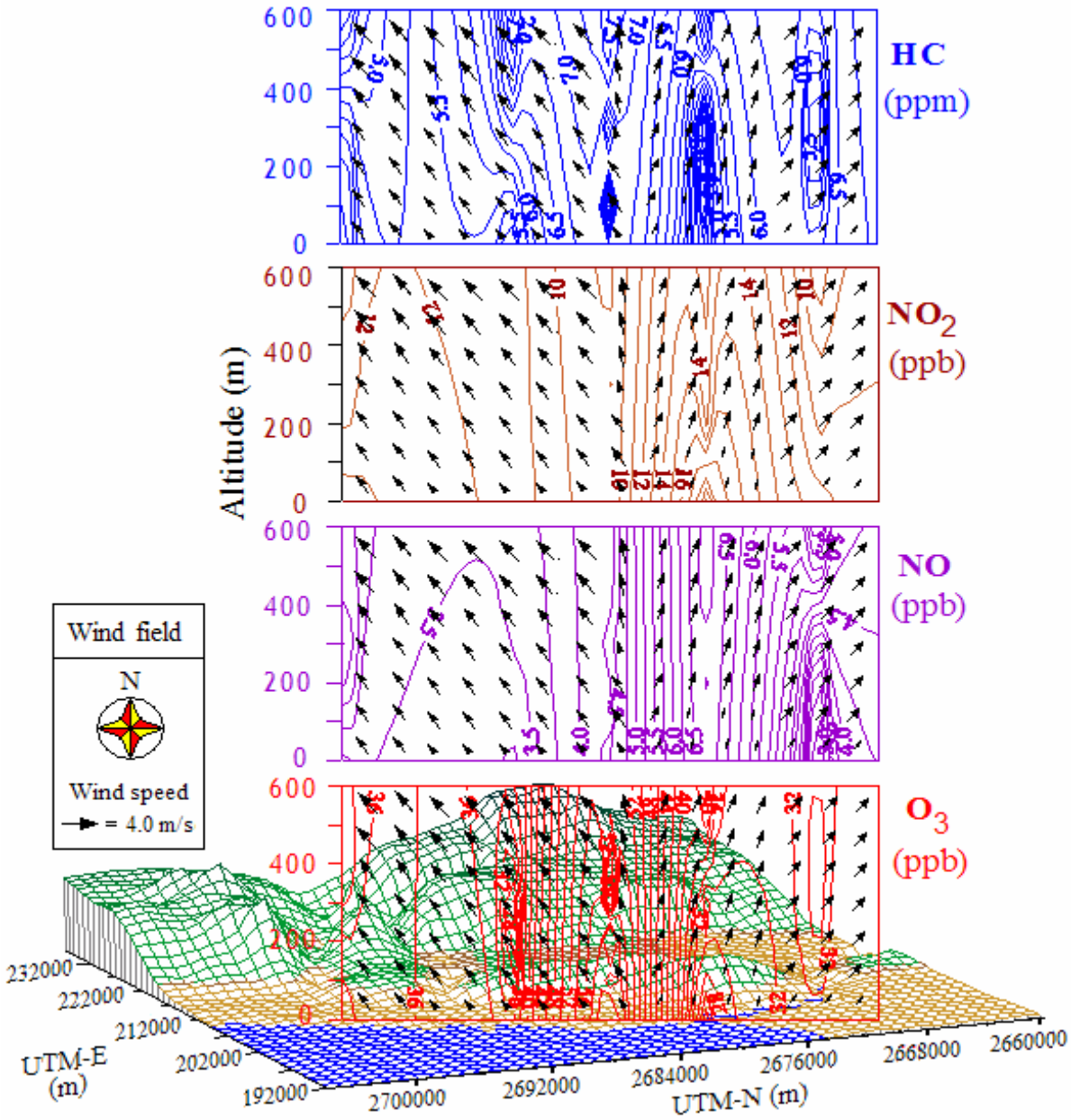

Figure 19 Concentration distribution of O_3, NO, NO_2 and HC and wind field, in the coastal area on June 27 and 28, 2002.

圖 20 顯示 11: 00 出現高、中、低三個臭氧中心，高臭氧中心位於盆地東北側，濃度約 68 ppb。

中臭氧中心在彰化市北側，濃度約 53 ppb。低臭氧中心在海邊，濃度約 23 ppb。地面吹南風，風速 3.5 m/sec 左右。風向在逐漸靠近內陸山區時轉爲西南。此時盆地東北側位處下風，因風場傳輸而造成較高之臭氧濃度。12:00 仍出現高、中、低三個臭氧中心，位置與 11: 00 約略相同，濃度值略有變動，爲 75、54 與 21 ppb。13:00 時山區臭氧(>70 ppb)明顯增多，區域往東南增大。低臭氧中心略向南移動，濃度再降至 18 ppb。12:00 與 13:00 時地面風場，顯現與 11: 00 時大致相同，風速略增至 3.8 與 4.0 m/sec 左右。

14: 00 時低臭氧中心範圍由港區向東南延伸至龍井鄉，濃度約 26 ppb。其餘地區臭氧濃度由西向東漸增。除彰化地區吹東南風外，其餘地區吹東南風，風速約 4.7 m/sec，顯現臭氧濃度與風場無關。15:00 時出現五個臭氧中心，二個高臭氧中心分別在盆地東邊，中臭氧中心位於盆地中心處，而二低臭氧中心則港區與西南側地區。前者範圍相當小，臭氧濃度約在 28 ppb 左右，後者濃度略低於 22 ppb。此時風場與 14:00 相同，東側內陸地區均吹西南風，但 15: 00 風速降爲 3.7 m/sec 左右。

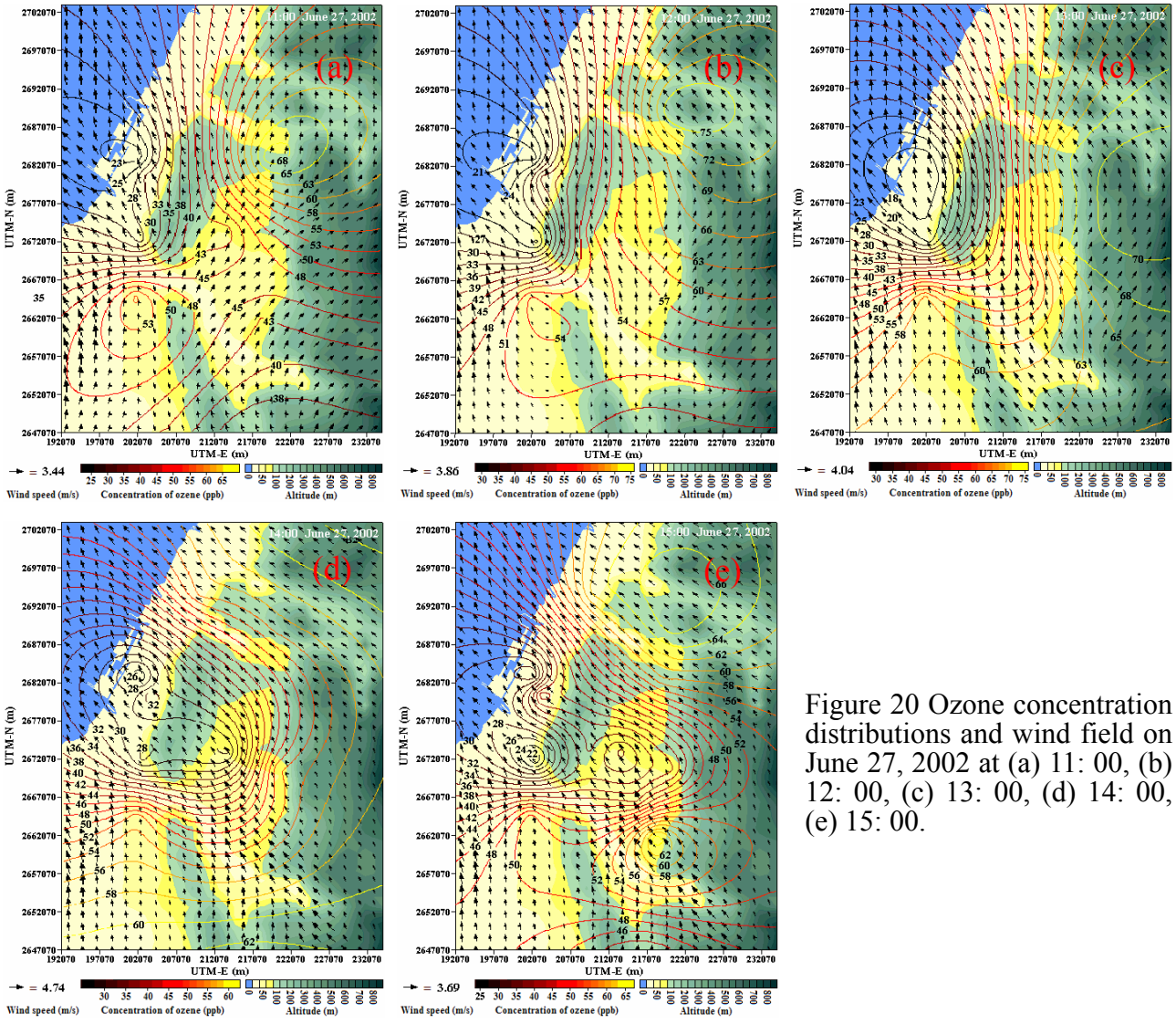

Figure 20 Ozone concentration distributions and wind field on June 27, 2002 at (a) 11: 00, (b) 12: 00, (c) 13: 00, (d) 14: 00, (e) 15: 00.

圖 21 顯示 6 月 28 日 11: 00 與 6 月 27 日近似，二個中臭氧濃度中心分別位於后里鄉近山區處與彰化市內南側，濃度均約 42 ppb。低中臭氧中心在港區沿海處，濃度低於 6 ppb。全區

呈現西南與東北方臭氧濃度較高，而西北與東南方較低之現象。地面風向則西側爲南風，靠山區則爲西風，風速約 4.4 m/sec，而臭氧濃度明顯與地面風場無關。

12: 00 時中臭氧中心消失。低臭氧中心位置不變，亦維持 10 ppb 左右。而東北地區又出現高臭氧中心，濃度高於 58 ppb。靠海地區風向由南風往北轉吹西南風，而靠山區則仍吹西風，風速約 4.6 m/sec。13:00 之臭氧濃度分布與風向維持與 12:00 時相同，高臭氧中心在后里，低臭氧中心在港區西側，風速略增至 5.0 m/sec 左右。

14: 00 與 15: 00 時二臭氧中心範圍均明顯逐漸向東南方擴大，濃度先上升(約 70 ppb)再略降(約 63 ppb)。地面風場與 13:00 時大致相同，但風速增至 5.6 m/sec 左右。值得一提的是 11:00 至 15:00 時，港區均出現 10 ppb 左右之低臭氧中心。另外，由於本日內陸風場大都爲吹東風，所以可以約略觀察出與臭氧濃度分布有稍許之關聯性存在。

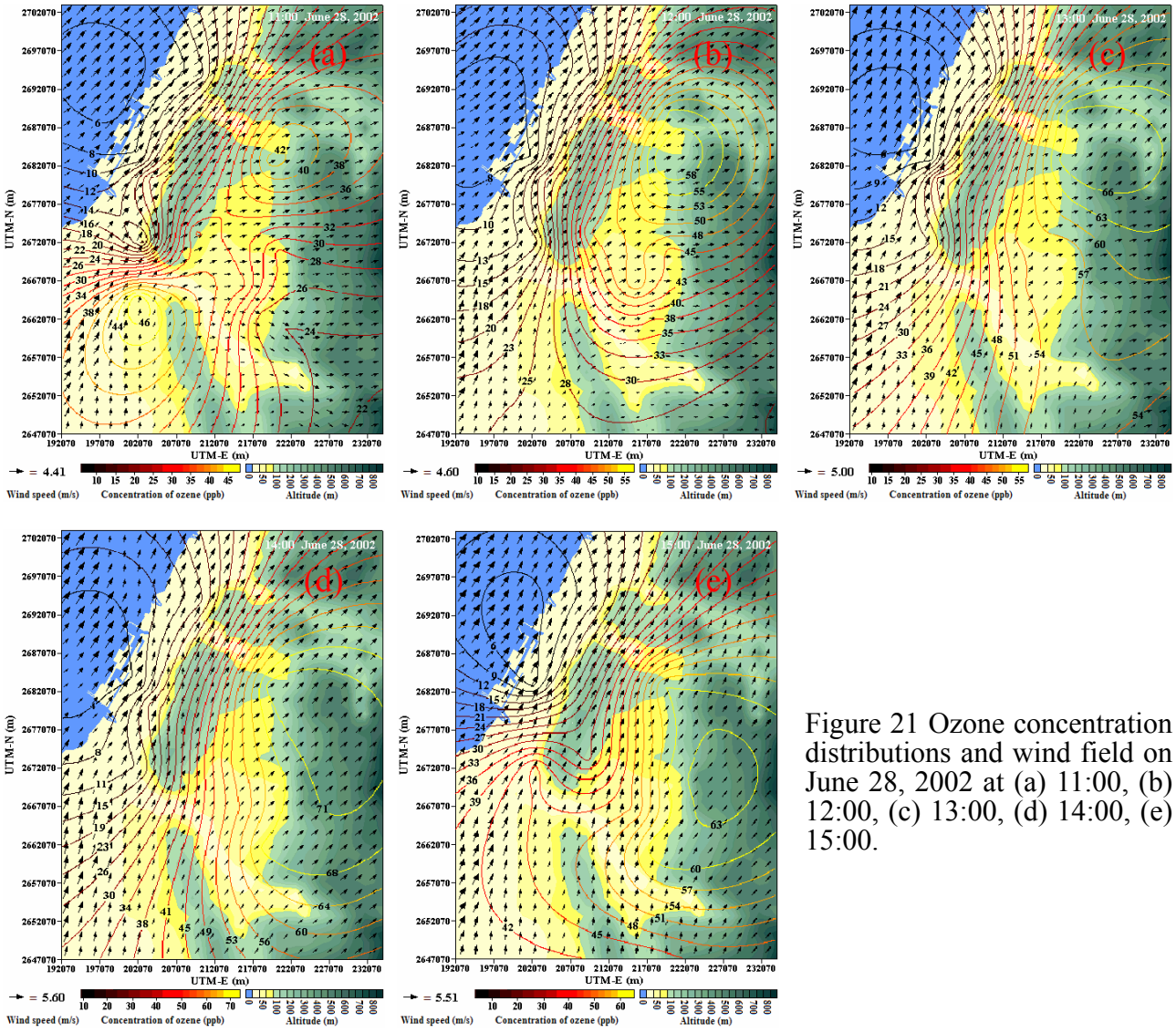

Figure 21 Ozone concentration distributions and wind field on June 28, 2002 at (a) 11:00, (b) 12:00, (c) 13:00, (d) 14:00, (e) 15:00.

第一次盆地內採樣時，各高程均呈現由北部之吹南風，逐漸轉至南部吹西南風，風速均隨高程漸增，最大風速在 4.5 m/sec 左右(圖 22)。另外，中間位置之風速略低於南北兩端。分析結果顯示 O_3、NO、NO_2 與 HC 之最高濃度位置，分別出現在(2684000, 500)、(2652000, ground)、(2663000, ground)與(2688000, 500)處之 80、6.6、14 ppb 與 6.2 ppm。O_3 在全區垂直濃度分布

並無大差異，水平上則呈現由北方低處向南方高處逐漸快速增高濃度。全區之 NO 濃度分布相當均勻，垂直與水平上之均無大變動。NO_2 則大半北部均約 13 ppb，小半的南部則濃度遞減。HC 除最北端有較高與較大的濃度變化外，其餘地方與濃度僅隨位置與高度略爲變動。

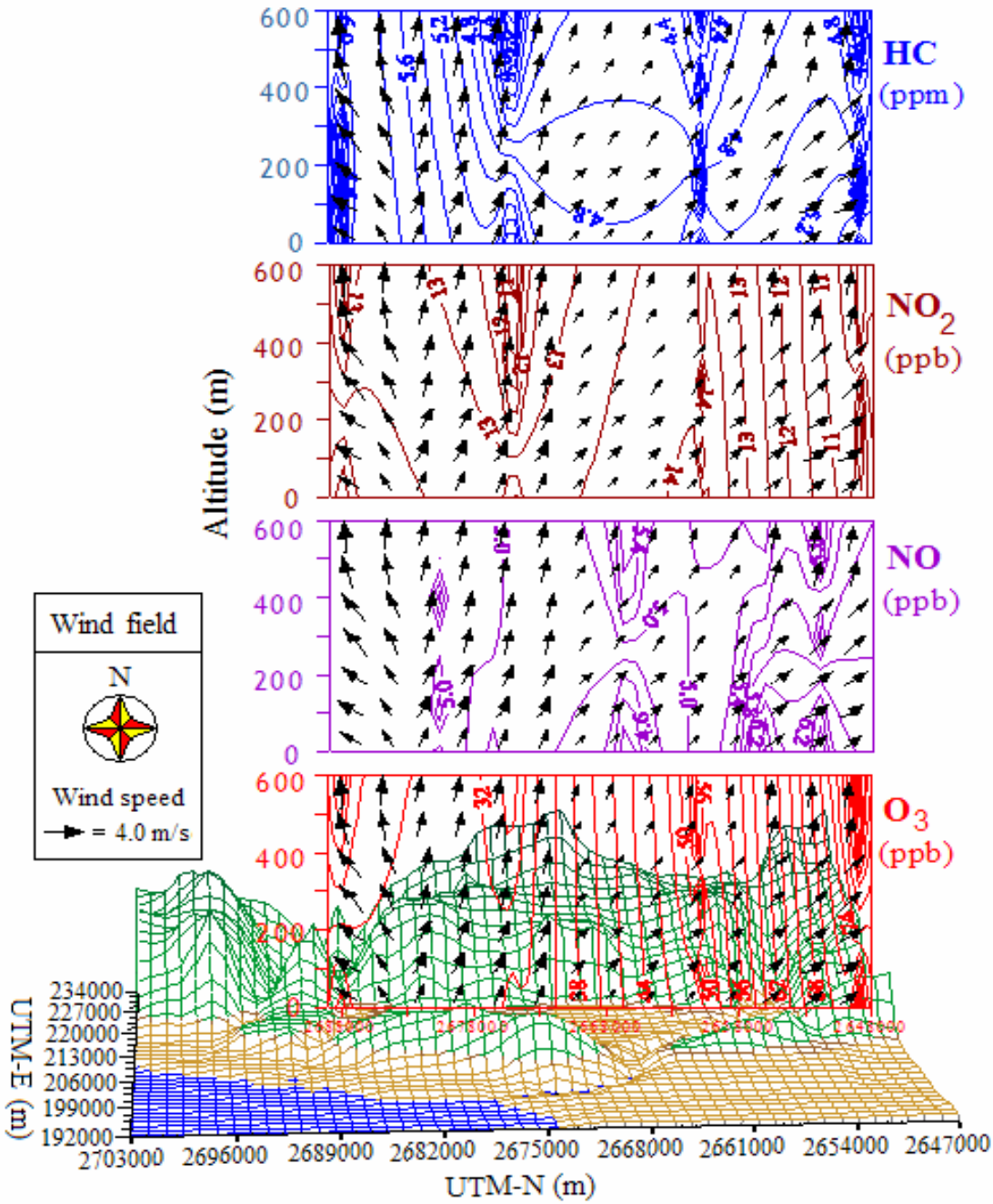

Figure 22　Concentration distribution of O_3, NO, NO_2 and HC and wind field, in Taichung Basin at July 1 and 2, 2002.

圖 23 顯示 11: 00 時臭氧濃度分布無明顯異常。位於港區之低臭氧中心濃度約 20 ppb；盆地東南地區之高臭氧中心濃度大於 70 ppb。此時地區風場，大致吹東南風，海邊之風速略大。12: 00 時地區風場相似但稍爲增強，霧峰地區之高臭氧中心濃度增至 96 ppb，而低臭氧中心之濃度也略爲增高。13:00 與 14:00 區域內風向仍無明顯改變，但風速明顯增大，尤其是位處盆地內東測與東南測。此時，霧峰地區之高臭氧中心濃度均已超過 120 ppb，達到臭氧事件日(臭

氧濃度大於 120 ppb)之標準。但值得注意的是港區之低臭氧中心濃度並無明顯增高。15:00 時靠海區域之低臭氧中心濃度僅 18 ppb，位置維持不變。盆地內東南側之高臭氧中心位置風速略降，且濃度也已降至 78 ppb 左右。

本日已具備臭氧事件日之條件，而綜合上述結果得知：(1).臭氧能於東南地區迅速增高，且維持 2~3 小時後再逐漸降低；(2).高臭氧產生明顯受來自區域外之東南風所影響，但濃度與風速無明顯關係，且影響似乎不能擴及大肚山台地以西地區；(3).大台中全區之臭氧濃度分布呈現由西北往東南方遞增，並且與當地風場流向完全相反。(4).來自東南測上風處山區生物源和高幅射所產生之臭氧量，不能忽視與低估，值得日後深入研究。

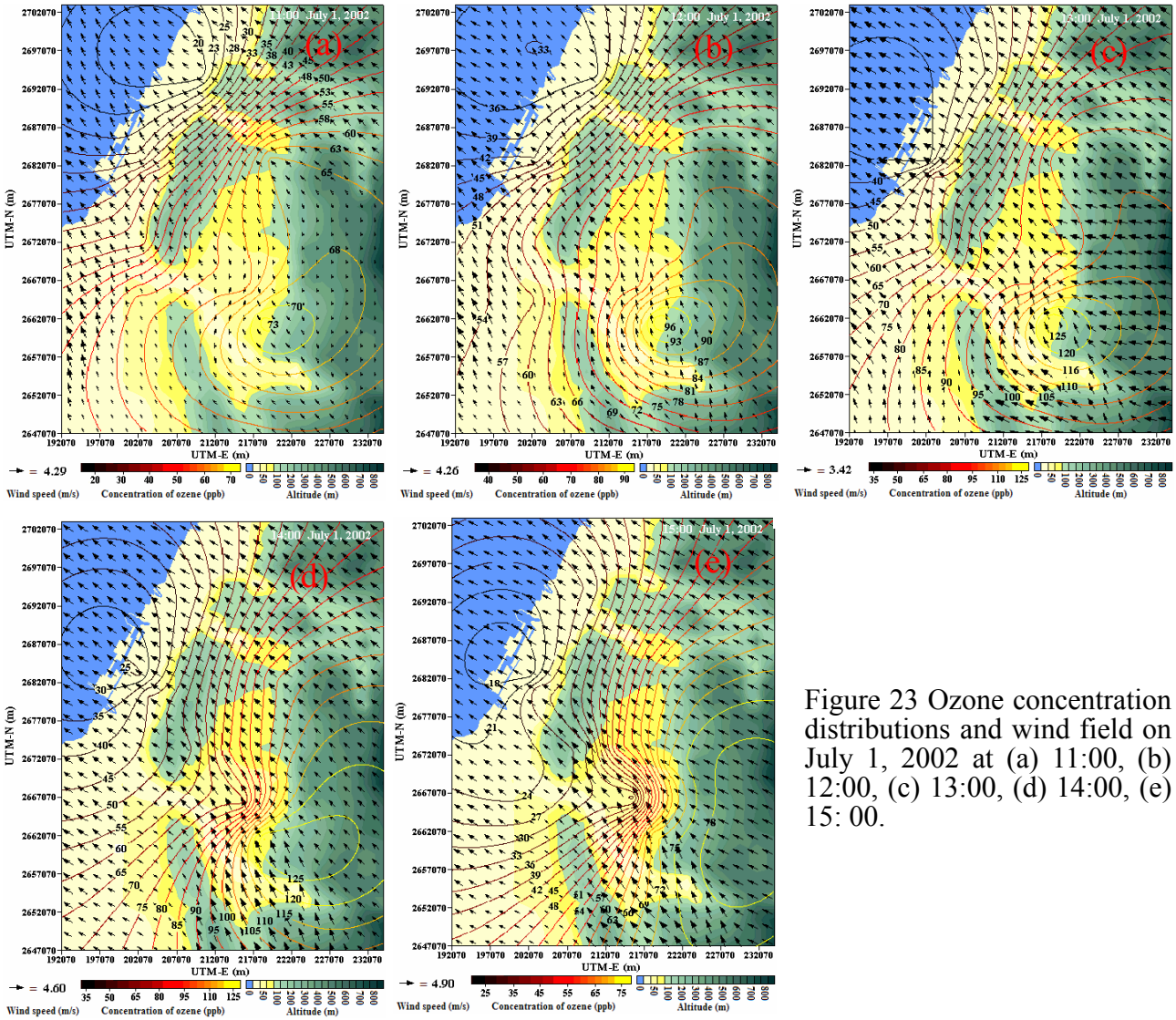

Figure 23 Ozone concentration distributions and wind field on July 1, 2002 at (a) 11:00, (b) 12:00, (c) 13:00, (d) 14:00, (e) 15: 00.

7 月 2 日 11: 00 與 12: 00 時之臭氧濃度分布與前一日相似(參見圖 23 與 24)，全區之臭氧濃度分布呈現由西北往東南方遞增，但濃度略高 5~10 ppb。因此，12:00 時位於霧峰與盆地南邊地區之高臭氧中心濃度，出現大於 100 ppb 現象。此二小時之地面風場，以吹東風爲主，均高於 5 m/sec。12:00 時起，盆地內東南測逐漸轉爲吹東南風，但風速未明顯改變。13:00 與 14:00 區域內風向仍無明顯改變，但風速增大。此二時段，大台中圈全區之臭氧濃度均明顯下降，位於(217070, 2662070)之周圍地區高臭氧中心均降至 90 ppb 以下。而值得注意台中港區之低

臭氧中心濃度更降至 12 ppb 左右。

15: 00 時靠海區域之低臭氧中心濃度僅 8 ppb 左右，位置維持不變。盆地內東南側之高臭氧中心位置風向與風速無明顯變化，但濃度卻又增至 100 ppb 左右。7 月 1、2 二日天氣型態相近，使二日之地面風場與臭氧濃度分布亦約略相同。7 月 2 且有著稍高的風速，雖有著略低的濃度，但尚不足以證明風速會影響濃度。以及東南側之高臭氧濃度，似乎不能擴及臨海地區，臨海區域日間濃度可低於 10 ppb 左右。

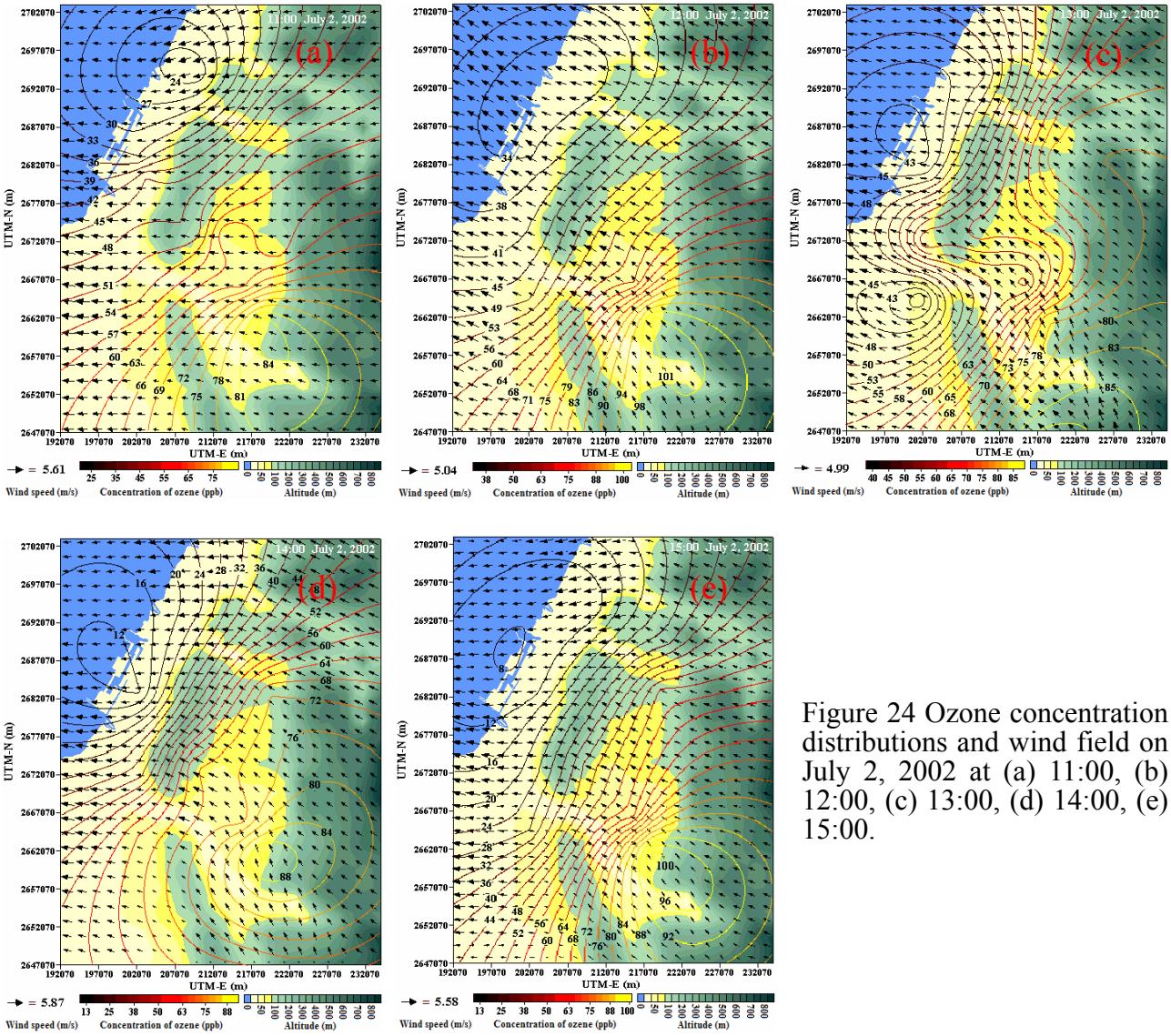

Figure 24 Ozone concentration distributions and wind field on July 2, 2002 at (a) 11:00, (b) 12:00, (c) 13:00, (d) 14:00, (e) 15:00.

圖 25 顯示第二次沿海地區採樣時，全區在 300 m 以上高程均吹東風，而 300 m 以下則吹東風，且風速明顯變小。最大風速在 5 m/sec 左右。O_3、NO、NO_2 與 HC 之最高濃度出現位置，分別在(2684000, 500)、(2681000, 200)、(2681000, 200)與(2698000, 500)處之 56、5.0、14.5 ppb 與 6.0 ppm。O_3 濃度分顯現由北向南漸增，南半部上空出現一些高濃度小區塊。NO 與 NO_2 的濃度均呈現由 UTM-N 爲 268100 m 處向南北兩方向逐漸遞減，而地面濃度稍高於上空。HC 的濃度分布呈現與最北端 500 m 高處，向南部與低處遞減，至 UTM-N 爲 2687000 m 處濃度已低於 1.0 ppm，但在 UTM-N 爲 2681000 m 的地面，小範圍濃度約 1.5 ppm

左右。

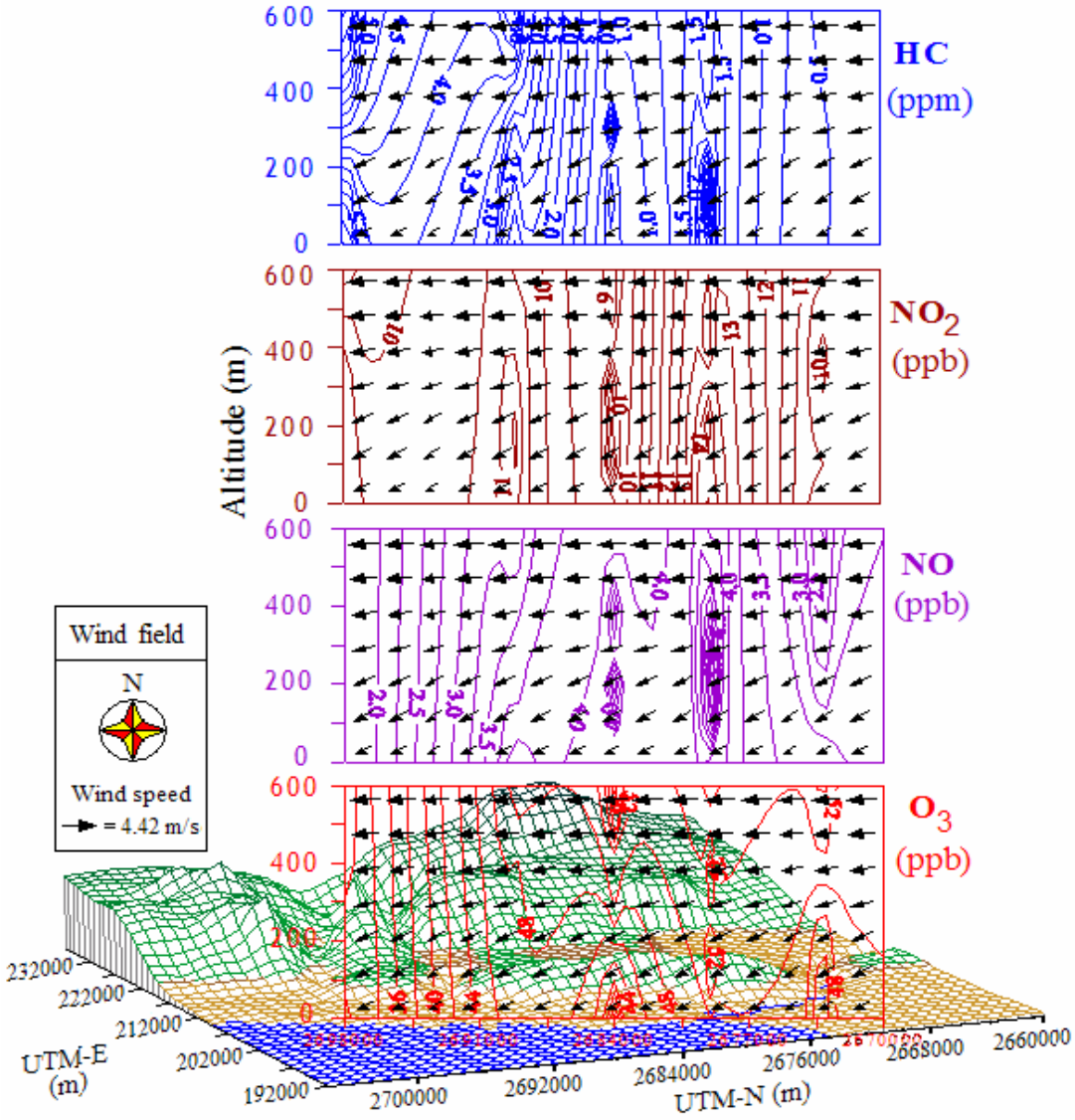

Figure 25　Concentration distribution of O_3, NO, NO_2 and HC and wind field, in the coastal area on August 1 and 2, 2002.

圖 26 顯示 8 月 1 日 11: 00 之風場，北方是吹東風，南方吹南風或吹東南風。11:00 至 13: 00 均出現一個高臭氧中心於霧峰地區，一個低臭氧中心於台中港區。高臭氧中心由 68 ppb 升至 88 ppb。低臭氧中心則不僅逐漸東移，濃度由 15 ppb 逐漸升至 44 ppb。值得注意的是 13:00 開始在台中市南屯區形成一中臭氧中心，濃度約 54 ppb 左右，隨後明顯往東增大範圍，但濃度變化不大。至 15:00 時，此中臭氧中心位移至台中市與烏日鄉間，而濃度維持在 50 ppb 左右。

14: 00 時高臭氧中心南移至草屯地區，同時範圍與濃度均增大，且濃度已近 100 ppb，即使 15:00 陽光已稍減弱，濃度仍居高不下。13:00 至 15:00 之風場以吹東南風爲主，風速 4 m/sec 以下。而 15:00 時由於南投、草屯地區吹著較強的東南風(風速約 4 m/sec)，似乎起了一些作用，使高臭氧中心略爲北移，且臭氧濃度不再升高。整體而言，8 月 1 日之大台中地區無論地面風場與臭氧濃度分布，均與 6 月 27、28 二日不同。有著較低的風速，卻有著較高的臭氧濃度，

而風向也明顯不同，其原因值得深入探討。

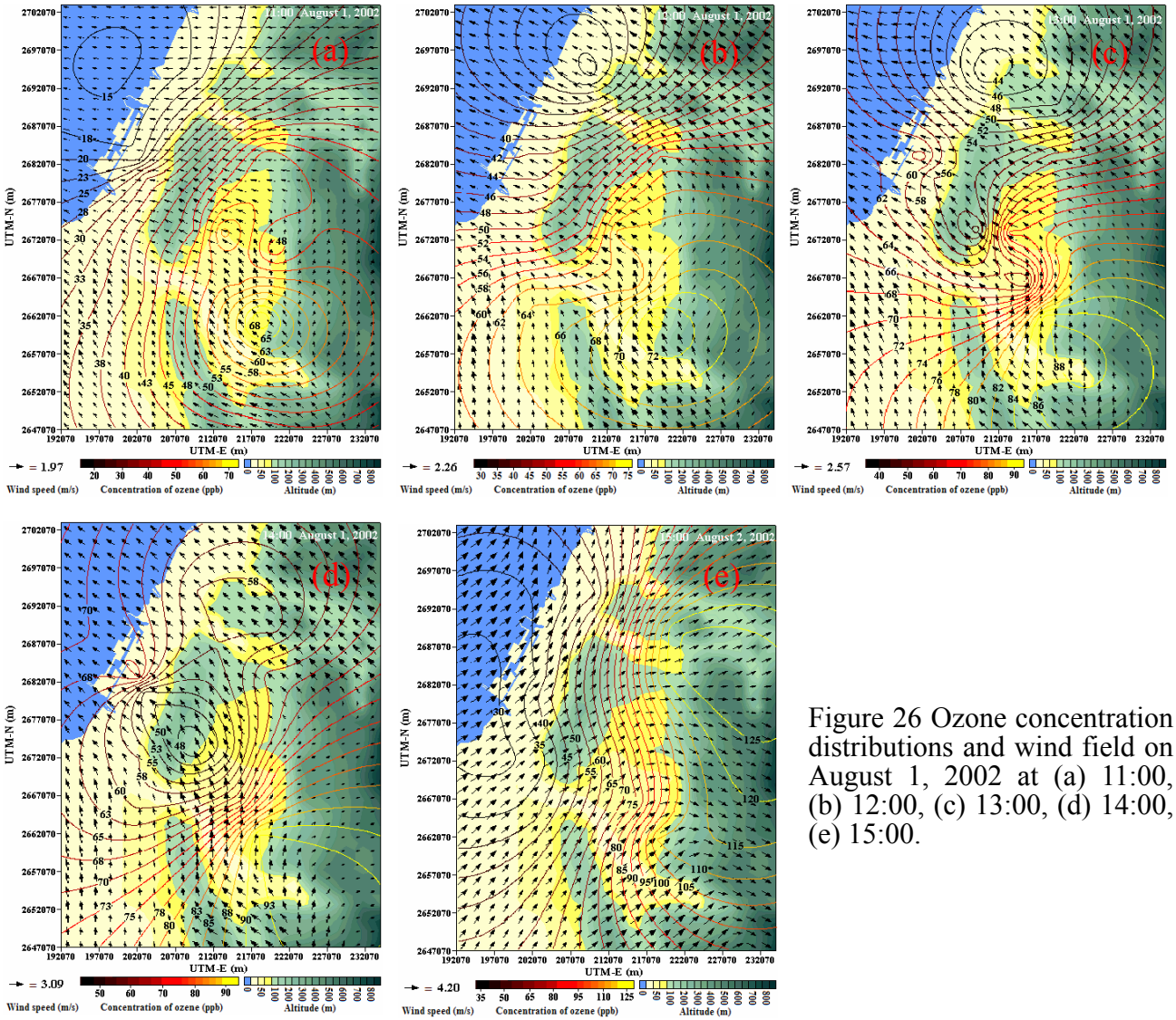

Figure 26 Ozone concentration distributions and wind field on August 1, 2002 at (a) 11:00, (b) 12:00, (c) 13:00, (d) 14:00, (e) 15:00.

圖 27 顯示大台中地區持續著前一日之高臭氧濃度現象，且已達臭氧事件日標準。自 11: 00 臭氧濃度就已相當高，即時平時濃度不高的台中港區也出現 68 ppb。而位於清水鎮之低臭氧中心也有 36 ppb。11:00 之最高臭氧值(126 ppb)出現在霧峰地區之高臭氧中心。此時地區風場，由南投地區先向東北方吹，進入台中縣南端後，山區仍吹正南風，但另一股風則由八卦山台地與大肚山台地間，沿著大肚溪吹向西方，或沿大甲溪與大安溪河床吹向西方。12:00 時之臭氧濃度分布與 11:00 時大致相似，但台中盆地內東側與東南側臭氧濃度均高過 100 ppb。風場也有些微的改變，海邊風向改爲東南風，但風速沒有明顯增大。值得一提的是台中港與鄰近地區之臭氧濃度，並無明顯增加。反而是原先之 68 ppb 的龍井地區，此時降爲 50 ppb 以下。

13:00 靠海區域之低臭氧中心濃度僅 25 ppb，但位置南移至台中港北堤方上方。另外，台中盆地內東側與東南側，則臭氧濃度大都已高出 120 ppb，霧峰地區更大於 150 ppb。值得注意的是此時風場有明顯轉變，彰化靠海處先吹正南風，再被大肚山台地分割成二股氣流。一股沿大肚山台地西側轉吹西南風；另一股吹向台中市之西南風，而遇到太平地區山緣後，轉向吹西北風，致使太平、霧峰、草屯與南投地區臭氧濃度異常之高。但此時之風速僅 2.8 m/sec

左右。14:00 與 15:00 時之地面風場除風速增大外，整個風場變化相近。可能由於風速略爲增大，使高臭氧中心位置移至台中縣新社鄉地區，中心地區濃度仍有 144 與 125 ppb 以上。且往南逐漸降低至南投市的約 110 與 100 ppb。低臭氧中心一直出現在台中港區南端，濃度也維持在較低的 30 ppb 左右。

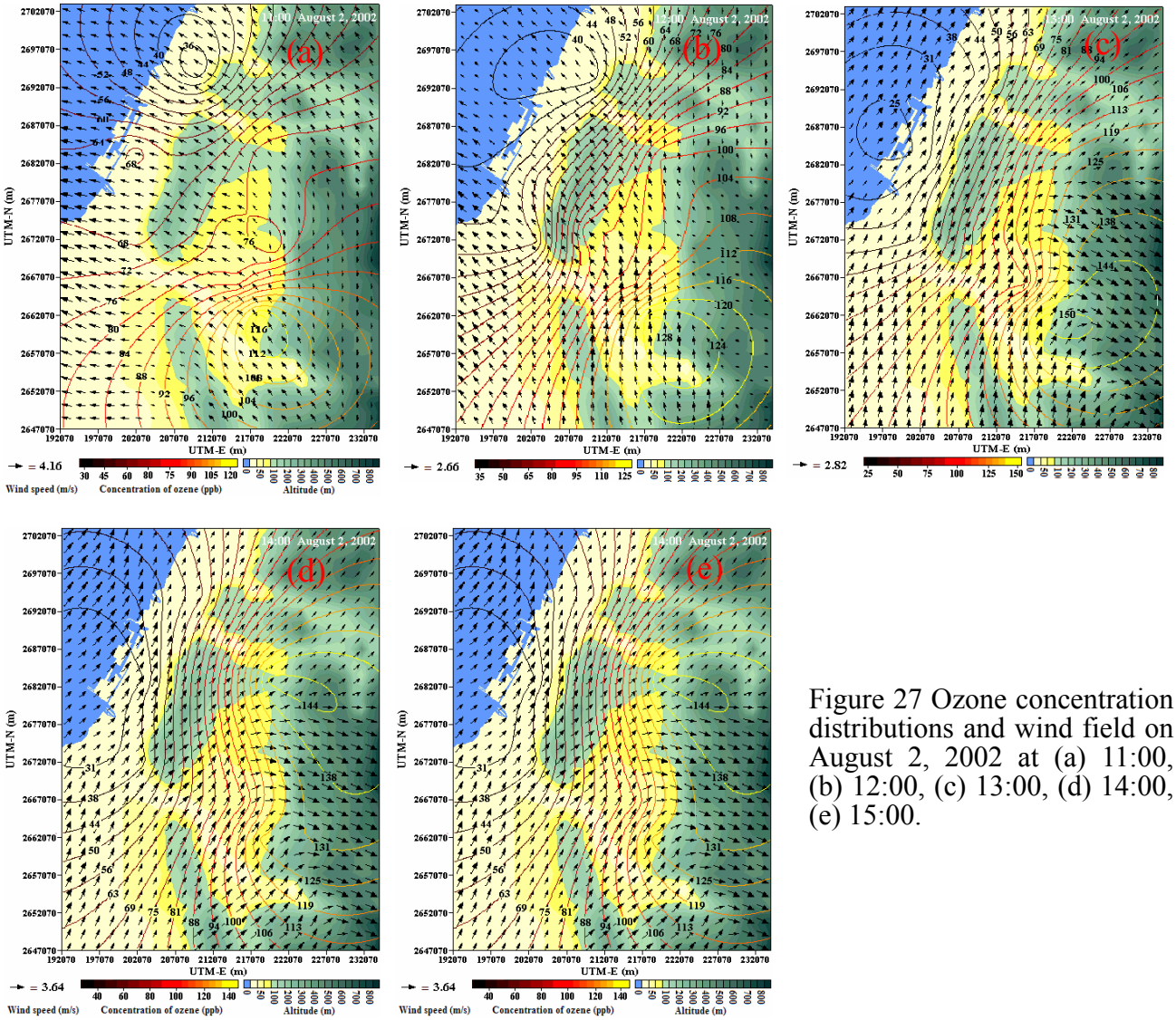

Figure 27 Ozone concentration distributions and wind field on August 2, 2002 at (a) 11:00, (b) 12:00, (c) 13:00, (d) 14:00, (e) 15:00.

8 月 2 日確定爲大台中地區之臭氧事件日，但綜合上述結果得知：(1).11:00 左右即足以產生相當高之臭氧值，(2).高臭氧的區域出現在盆地內東測之人口與經濟活動較少區域，(3).盆地內效應會使風場明顯改變，尤其造成由西南風轉成吹西北風，使盆地內東測之臭氧濃度居高不下，(4).台中港區與鄰近鄉鎮之臭氧濃度，並不會受臭氧事件日之影響，仍保持一定的低濃度值，(5).因無由台中港區之風吹向內陸，亦即應無 HC 由台中港區吹向內陸，來加深大盆地內臭氧濃度。

第二次盆地內採樣時，各採樣點之風向隨高程變化相近，300 m 高程以下主要吹東南風或南南東風，400 與 500 m 高程處則北方轉爲吹東風或東南東風，風速不大，均約在 4 m/sec 左右(圖

21)。分析結果顯示 O_3、NO、NO_2 與 HC 之最高濃度位置，分別出現在(2657000, 各高程)~(2662000, 各高程)、(2674000, ground)、(2674000, ground)與(266000, ground)處之 130、5.0、26 ppb 與 2.5 ppm。雖然 2002 年 9 月 15 日並非臭氧事件日，但 O_3 在盆地南部(採樣點 L3 與 L4 二處)的濃度均相當高，且各高程臭氧濃度均相近，維持在 130 ppb 左右。水平上則呈現由北方低處向南方高處逐漸快速增高濃度。全區之 NO 濃度分布相當均勻，垂直與水平上之均無大變動。NO_2 則北部均約 20 ppb，中段位置約 25 ppb，南部則濃度遞減，逐漸降至 10 ppb 左右。HC 除最中段位置有較高與較大的濃度變化外，其餘地方與濃度僅隨位置與高度略爲變動。

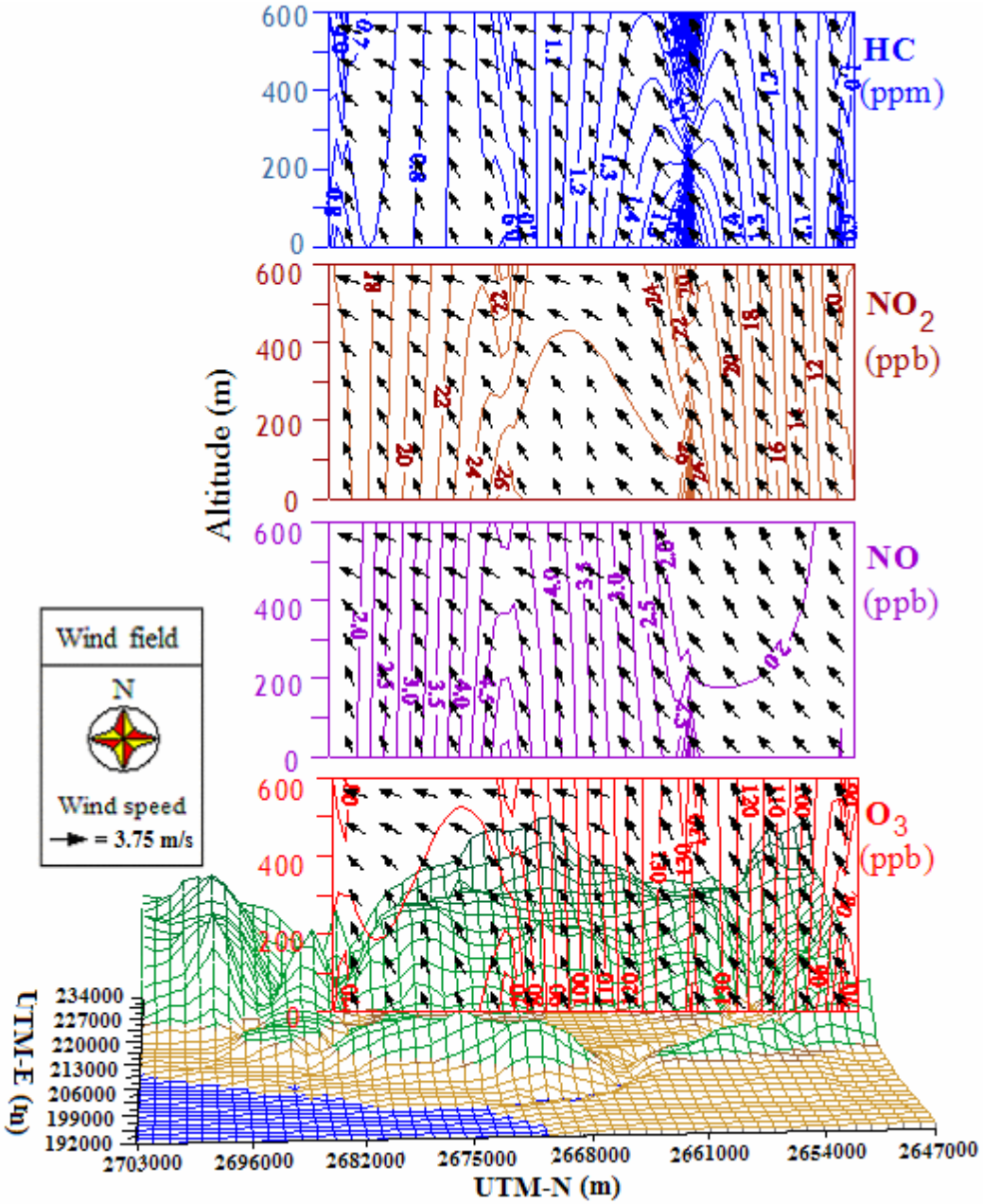

Figure 28 Concentration distribution of O_3, NO, NO_2 and HC and wind field, in Taichung Basin on September 14 and 15, 2002.

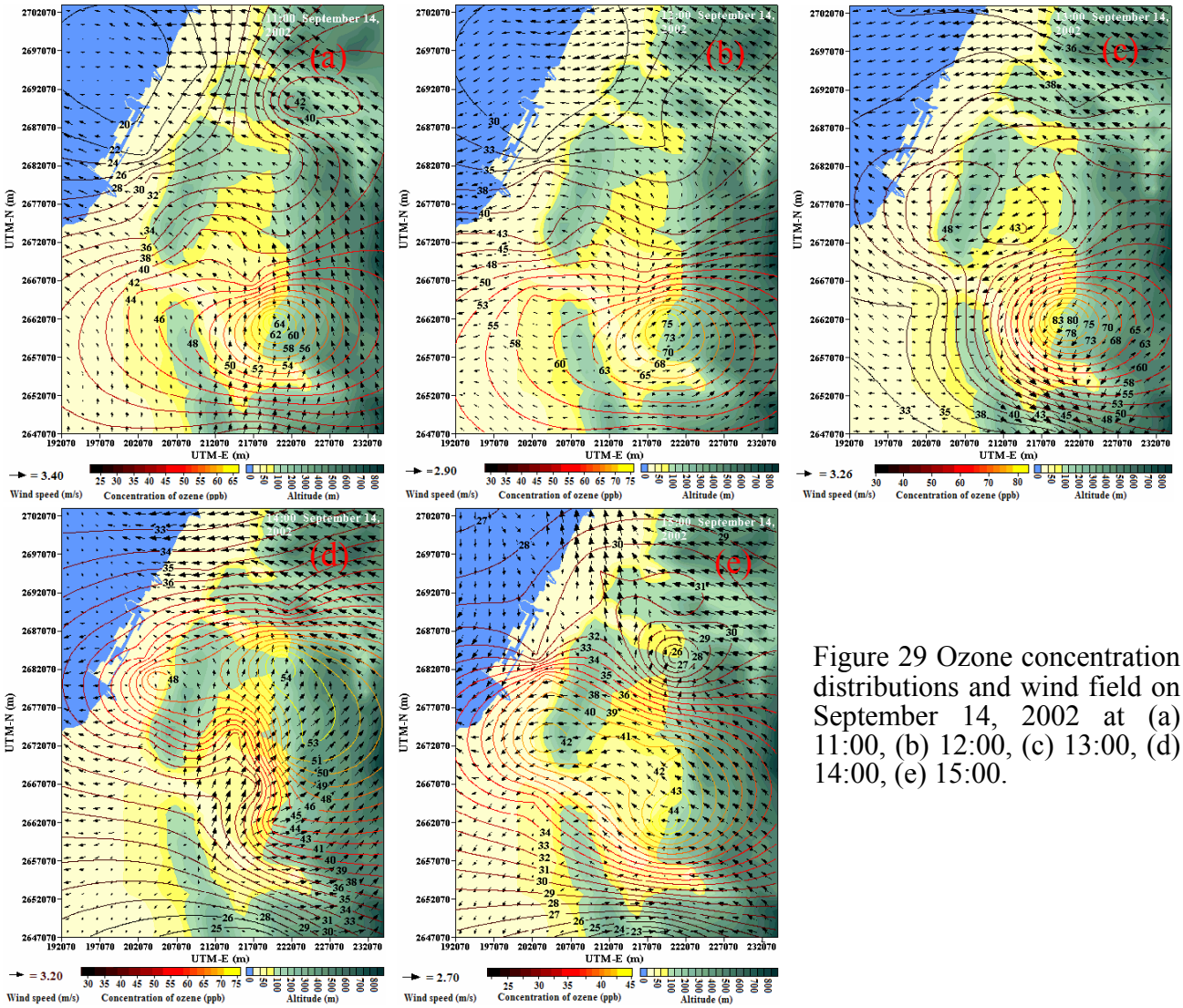

Figure 29 Ozone concentration distributions and wind field on September 14, 2002 at (a) 11:00, (b) 12:00, (c) 13:00, (d) 14:00, (e) 15:00.

圖 29 顯示 2002 年 9 月 14 日 11: 00 出現高、中、低三個臭氧中心，高臭氧中心位於盆地內東南處，濃度約 66 ppb。中臭氧中心在盆地內東北處，濃度約 40 ppb。低臭氧中心在台中港區，濃度約 20 ppb。12: 00~15: 00 則變爲高、低二個臭氧中心，其中高臭氧中心位置大致維持不變。所有時間之地面風場僅盆地東南處由吹南風逐漸轉爲西南風與東南風，風速均約在 3 m/sec 左右。臭氧最高濃度出現在 13:00 時之盆地內東南處，而該地區正是盆地效應造成地面風場最大變動之處。14:00 之後，高臭氧中心位置略爲北移，且全區域之臭氧濃度開始明年降低，15:00 時最高濃度僅 44 ppb。另外本日 11:00~15:00 時，沿海地區的臭氧濃度均保持低濃度，臭氧濃度在 30 ppb 左右。圖 30 顯示 2002 年 9 月 14 日 11:00 出現多個臭氧中心，但每個臭氧中心的臭氧濃度並無太大的差異，濃度均低於 51 ppb。

12:00 時臭氧中心數量有增無減，濃度並未較 11: 00 時明顯升高，最高濃度僅 56 ppb。13:00 時各處臭氧濃度均顯現降低現象。13: 00~15:00 間之最高濃度僅 45 ppb，臭氧中心位置大都不變。所有時間地面風場僅盆地東北處由吹東南風，其餘地區都維持吹西南風或南風，最大風速則由 11:00 之 3.4 m/sec 左右，逐漸增大至 15:00 時之 5 m/sec 左右，最大風速亦出現在盆地東北端。臭氧最高濃度出現在 12:00 時之盆地內東南處，同樣的該地區正是盆地效應造成地面風場最大變動之處。11:00~15:00 時，沿海區臭氧濃度亦保持低濃度，濃度低於 40 ppb。

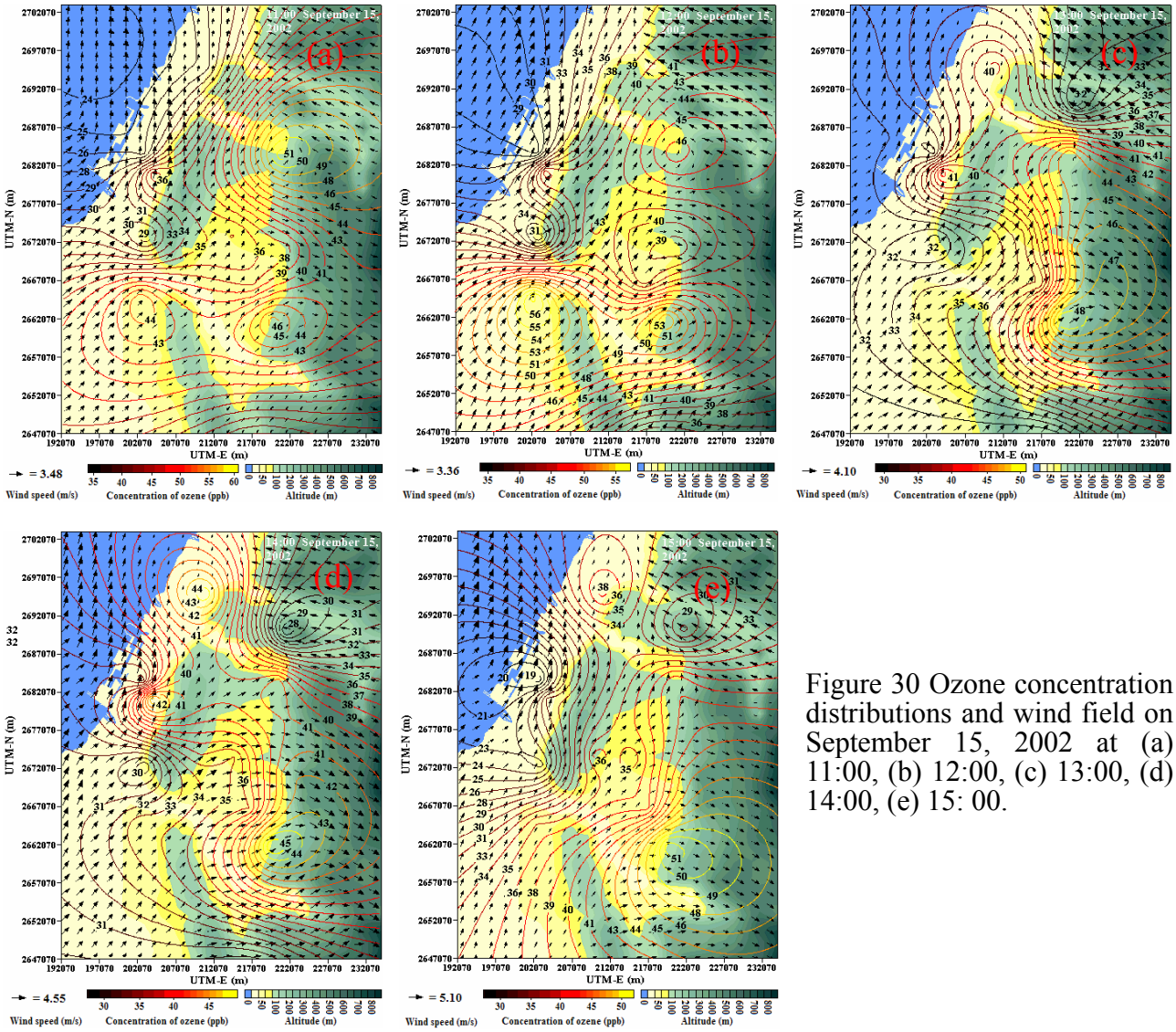

Figure 30 Ozone concentration distributions and wind field on September 15, 2002 at (a) 11:00, (b) 12:00, (c) 13:00, (d) 14:00, (e) 15: 00.

由圖 19~30 顯示除 6 月 27、28 二日風向略有不同外，其餘各次採樣期間之風場均相近。因此採行每天 11:00~14:00 間於二個採樣點進行高空採樣，且連續二天來完成四個採樣點的方法，證實足以代表各污染物不同高程之濃度分布，同時所獲得的結果，可以被用來闡釋該地區之風場、時間、地形對臭氧傳輸之影響。圖 19, 22, 25 與 28 均顯示大部分地區無明顯濃度的高程梯度，但存在明顯濃度之水平梯度。僅分別於盆地內之 L3 與沿海地區之 S3 位置在各二次的結果，均出現明顯之濃度隨高程變動，由其是 HC，前者可能受地型與風場之盆地效應影響所致，後者可能因靠近台中電廠與港區大油槽區的污染物排放所致。因此，盆地效應與工廠的存在均會明顯影響污染物之濃度的高程梯度。

爲比較沿海地區與盆地內在採樣期間上空空氣品質之差異，本研究將上列結果詳加彙整，並繪出圖 31 與 32 之兩地區各污染物於不同高程之濃度變動圖。比較圖 31(a)與 32(a)獲知盆地內 O_3 除平均濃度較沿海地區高外，各高程之濃度變動亦均較沿海地區明顯，而 NO 與 NO_2 濃度變動也與臭氧近似(圖 31(b), (c)與 32(b), (c))，即濃度較高與變動較大。在 HC 上，沿海地區 HC 濃度明顯隨高程增加而增高(圖 32(d))，但盆地內則相反，且盆地除地面有較高的 HC 外，其餘各高程平均 HC 濃度均低於沿海地區。盆地內 O_3 濃度亦呈現隨高程增加而增高。

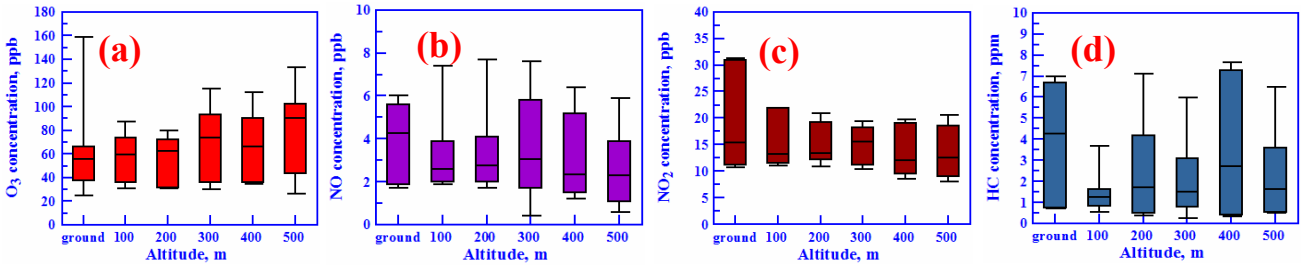

Figure 31 The Box-whisker plots of the analysis data in Taichung Basin. (a) O_3, (b) NO, (c) NO_2, (d) HC.

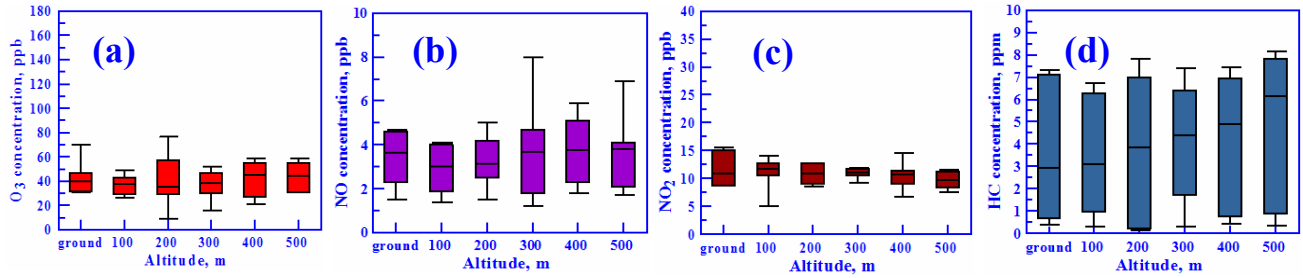

Figure 32 The Box-whisker plots of the analysis data in the coastal area. (a) O_3, (b) NO, (c) NO_2, (d) HC.

同樣本研究亦將各類 HC 之分析結果彙整，繪出圖 33 與 34 之兩地區各類 HC 於不同高程之濃度變動圖，以瞭解沿海地區與盆地內在採樣期間上空各類 HC 之差異。

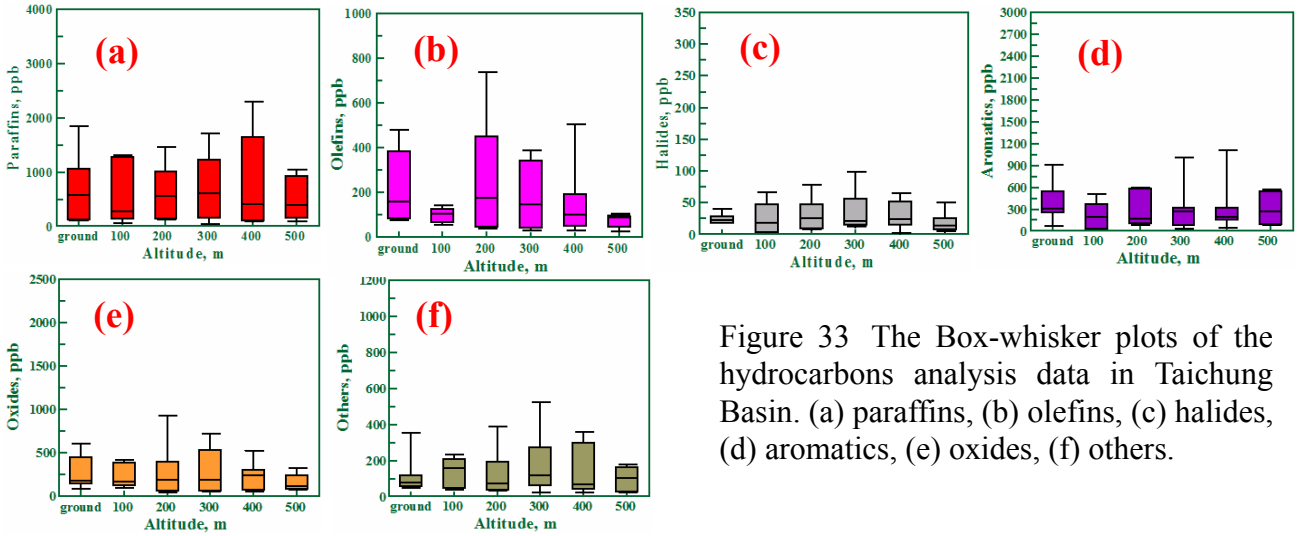

Figure 33 The Box-whisker plots of the hydrocarbons analysis data in Taichung Basin. (a) paraffins, (b) olefins, (c) halides, (d) aromatics, (e) oxides, (f) others.

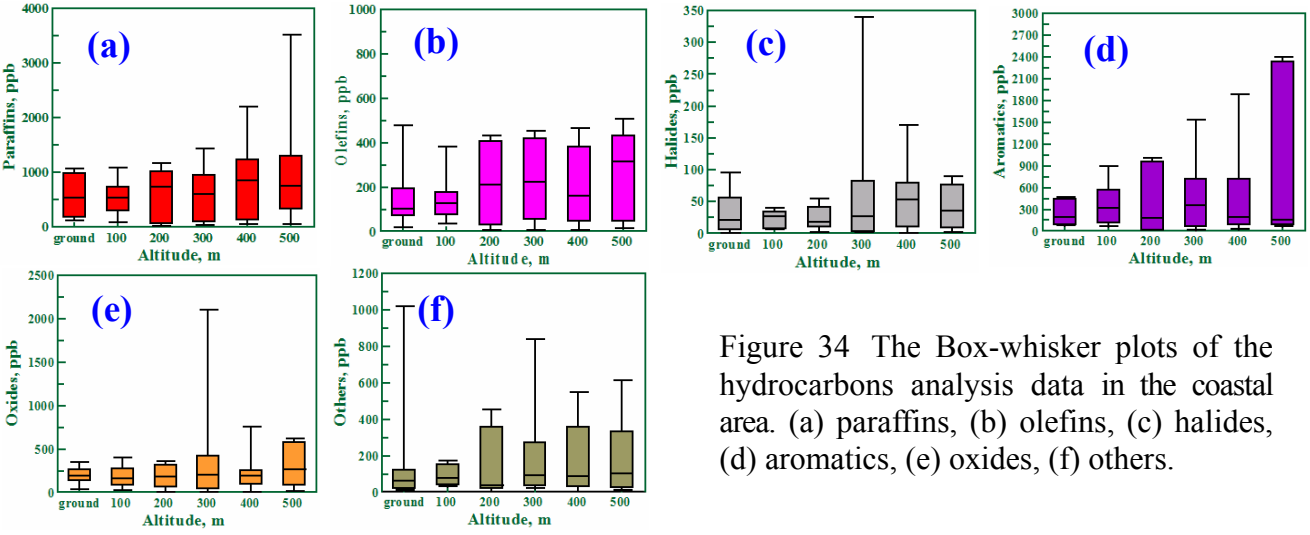

Figure 34 The Box-whisker plots of the hydrocarbons analysis data in the coastal area. (a) paraffins, (b) olefins, (c) halides, (d) aromatics, (e) oxides, (f) others.

比較沿海地區與盆地之烷類隨高程變動情形，獲知進海地區之烷類與烯類均隨高程增高而略爲增加(圖 34(a), (b))，但在盆地內則恰爲相反(圖 33(a), (b))。二地區各高程之有機鹵化物濃度均不高(圖 33(c), 34(c))，僅在沿海地區 300 m 高處有較大的變動。盆地內芳香族化合物之濃度低且變動小(圖 33(d))，但在進海地區則芳香族化合物雖然濃度不高，但隨高程增加而變動加大(圖 34(d))。二地區之有機氧化物各高程之平均濃度均在 250 ppb 以下(圖 33(e), 34(e))，但沿海地區在 300 m 高處出現較大的變動。其他有機物則二地區各高程平均濃度均低於 200 ppb，但盆地內濃度略大於沿海地區。

綜合前述結果得：(1).盆地內 O_3 、NO 與 NO_2 平均濃度不僅較沿海地區高，且於各高程之變動亦較大，(2).沿海地區 HC 濃度明顯隨高程增加而增高，但盆地內則相反，且沿海地區除地面外，其餘各高程平均濃度均較高。(3).沿海地區之烷類與烯類均隨高程增高而略爲增加，但在盆地內則恰爲相反。(4).二地區各高程之有機鹵化物、芳香族化合物、有機氧化物與其他有機物之平均濃度相近，但在濃度變動性上，沿海地區大於盆地內。

考慮臭氧在大氣中之穩定狀態與一維的傳輸與反應作用，則(2)式可改寫爲

$$\frac{u_i[\mathrm{O_3}]_i - u_{i-1}[\mathrm{O_3}]_{i-1}}{\Delta x_{i\leftrightarrow i-1}} = R - L[O_3]_i \qquad (4)$$

綜合圖 20~30 之結果，顯現二種傳輸現象，一爲風由外往盆地內吹，且臭氧濃度是隨風向遞增；另一爲風由盆地內往外吹，而臭氧濃度是隨風向遞減。因此，本研究選用 6 月 28 日與 7 月 1 日之 12:00 與 14:00 地面風場與臭氧濃度資料，並如圖 35(a)~(d)選定四條與風向平行之直線位置，整理其這些數據列於表 4，並運用此數據配合(4)式以 $\left(\frac{u_i[\mathrm{O_3}]_i - u_{i-1}[\mathrm{O_3}]_{i-1}}{\Delta x_{i\leftrightarrow i-1}}\right)$ 對 $[\mathrm{O_3}]_i$ 做圖，即可得此二種傳輸現象下的斜率 $-L$ 與截距 R 值，所得結果亦列於表 4 中。探討結果得：(1).風由外往盆地內時常(6 月 28 日)，R 與 L 會由 12:00 之正值，轉爲 14:00 之負值，此結果與表 2 所列相同，但而非遞減，(2).風改由盆地內向外吹時(7 月 1 日)，R 與 L 值提前於 12:00 即爲大的負值，但 14:00 時 R 之負值變小(臭氧之消失作用縮小)與 L 轉爲正值

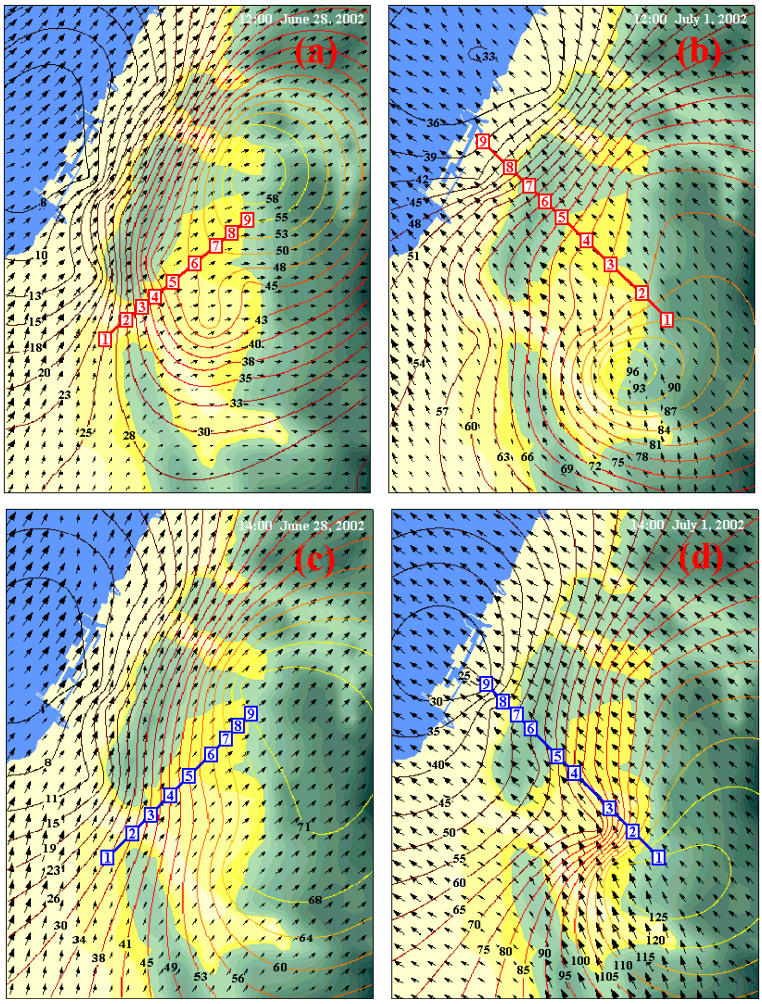

Figure 35 Air parcel trajectory arriving at Taichung area. (a) 12:00, June 28, 2002, (b) 12:00, July 1, 2002, (c) 14:00, June 28, 2002, (d) 14:00, July 1, 2002.

(–L[O_3]恢復爲消失項)，(3).風向並非決定臭氧濃度的主要因素，地形與一些需再深入探討環境因素與才是要因。

Table 4　The data of two lines of Figure 35 to calculate R and L values

Point-1		Point-2		Point-3		Point-4		Point-5		Point-6		Point-7		Point-8		Point-9		R	L
[O_3]	u	[O_3]	u	[O_3]	u	[O_3]	u	[O_3]	u	[O_3]	u	[O_3]	u	[O_3]	u	[O_3]	u		
Surface wind blew into the basin at 12:00, June 28, 2002																			
48	6120	58	6840	67	9180	77	9360	86	9180	91	8820	92	7200	101	8280	106	8280	**109.622**	**0.913**
$\Delta x_{1\leftrightarrow2}$=3284 m, $\Delta x_{2\leftrightarrow3}$=2512 m, $\Delta x_{3\leftrightarrow4}$=1932 m. $\Delta x_{4\leftrightarrow5}$=2512 m, $\Delta x_{5\leftrightarrow6}$=3478 m, $\Delta x_{6\leftrightarrow7}$=3284 m. $\Delta x_{7\leftrightarrow8}$=2125 m, $\Delta x_{8\leftrightarrow9}$=2318 m																			
Surface wind blew out of the basin at 12:00, July 1, 2002																			
167	7380	156	8280	150	10080	144	11520	132	12960	121	13140	109	12960	92	12240	75	11520	**–202.561**	**–1.621**
$\Delta x_{1\leftrightarrow2}$=4250 m, $\Delta x_{2\leftrightarrow3}$=3090 m, $\Delta x_{3\leftrightarrow4}$=2473 m. $\Delta x_{4\leftrightarrow5}$=2705 m, $\Delta x_{5\leftrightarrow6}$=3864 m, $\Delta x_{6\leftrightarrow7}$=3980 m. $\Delta x_{7\leftrightarrow8}$=4753 m, $\Delta x_{8\leftrightarrow9}$=4250 m																			
Surface wind blew into the basin at 14:00, June 28, 2002																			
58	6900	65	6650	73	6480	86	7410	102	7410	115	7880	123	7880	131	9500	136	9970	**–52.083**	**–0.968**
$\Delta x_{1\leftrightarrow2}$=3719 m, $\Delta x_{2\leftrightarrow3}$=2819 m, $\Delta x_{3\leftrightarrow4}$=3054 m. $\Delta x_{4\leftrightarrow5}$=2936 m, $\Delta x_{5\leftrightarrow6}$=3602 m, $\Delta x_{6\leftrightarrow7}$=2036 m. $\Delta x_{7\leftrightarrow8}$=1957 m, $\Delta x_{8\leftrightarrow9}$=1957 m																			
Surface wind blew out of the basin at 14:00, July 1, 2002																			
240	15120	211	14760	163	14500	144	14400	125	14050	106	13680	96	13500	86	12960	58	12600	**–76.411**	**0.244**
$\Delta x_{1\leftrightarrow2}$=4064 m, $\Delta x_{2\leftrightarrow3}$=3861 m, $\Delta x_{3\leftrightarrow4}$=5690 m. $\Delta x_{4\leftrightarrow5}$=2845 m, $\Delta x_{5\leftrightarrow6}$=4268 m, $\Delta x_{6\leftrightarrow7}$=2439 m. $\Delta x_{7\leftrightarrow8}$=2032 m, $\Delta x_{8\leftrightarrow9}$=2642 m																			

The unit of [O_3], u, R, and L are μg/m^3, m/hr, μg/m^3-hr, and 1/hr.

陸、多變量關係方程式

利用各氣象與空氣品質測站之數據來求取關係方程式時，最小平方估計法(Least square approximation method)不能滿足所需，而需採用多變量迴歸法(Multiple regression)。多變量迴歸法爲因變數 y 具有 m 個變數 $x_1, x_2, x_3 \ldots x_m$，且具有如下之關係方程式：

$$y = a_o + a_1 x_1 + a_2 x_2 + \cdots + a_m x_m \tag{5}$$

則當具有 n 組數據時，可依(5)式寫出 n 個線性聯立方程式：

$$y_i = a_o + a_1 x_{1i} + a_2 x_{2i} + \cdots + a_m x_{mi} \tag{6}$$

其中 $i = 1, 2, \ldots, n$。(7)式改以矩陣方程式：

$$\mathbf{Y} = \mathbf{X}\vec{\alpha} \tag{7}$$

其中 $\mathbf{Y} = \begin{bmatrix} y_1 \\ y_2 \\ y_3 \\ \vdots \\ y_n \end{bmatrix}$, $\mathbf{X} = \begin{bmatrix} 1 & x_{11} & x_{21} & \cdots & x_{m1} \\ 1 & x_{12} & x_{22} & \cdots & x_{m2} \\ 1 & x_{13} & x_{23} & \cdots & x_{m3} \\ \vdots & \vdots & \vdots & & \\ 1 & x_{1n} & x_{2n} & \cdots & x_{mn} \end{bmatrix}$, $\vec{\alpha} = \begin{bmatrix} \alpha_o \\ \alpha_1 \\ \alpha_2 \\ \vdots \\ \alpha_m \end{bmatrix}$

則由最小平方偏差和可推導出正規化(normal)方程式

$$\vec{\alpha} = (\mathbf{X}^\mathbf{T}\mathbf{X})^{-1}(\mathbf{X}^\mathbf{T}\mathbf{Y}) \tag{8}$$

經由(8)式計算結果，即可求出 m+1 個係數$\alpha_o, \alpha_1, \alpha_2, \alpha_3 \ldots \alpha_m$，進而獲得(4)式之多變量關係方程式，係數值之大小反映出所對應變數之重要性。利用實測所得之數據來求取包含日照、絕對濕度與臭氧之各種前軀物的多變量關係方程式如下：

$$\begin{aligned}[O_3] = {} & 77.6 + 17.994[\text{Radiation}] - 6.408[\text{Humidity}] - 2.703[NO] + 1.752[NO_2] \\ & - 4.22\times10^{-3}[\text{Paraffins}] - 1.01\times10^{-2}[\text{Olefins}] - 9.45\times10^{-3}[\text{Aromatics}] \\ & - 8.147\times10^{-3}[\text{Organicoxides}] - 1.56\times10^{-2}[\text{Organichalides}] - 9.96\times10^{-3}[\text{Others}]\end{aligned} \tag{9}$$

其中臭氧、日照、絕對濕度與各前軀物的單位分別爲 ppb、MJ/m^2、g/m^3 與 ppb。(9)式顯示高

日照與低濕度下易產生高臭氧濃度，而所有臭氧前驅物 NO 與各類 HC 之係數均爲負值，則說明當它們濃度高時，意味著未進一步生成臭氧。Jeffries 與 Crouse 氏進行數學模式的研究，亦顯示相似的結果[21, 23]。

柒、臭氧之基礎反應實驗

爲充分瞭解諸如濕度、日照度與一些有機物對臭氧生成與傳輸之影響，亦進行實驗工作，採用之反應裝置如圖 36。反應器爲厚 5 mm 方形強化玻璃，長、寬、高分別爲 60、50、50 cm，內部體積 150 公升。實驗時，玻璃反應器除頂部供紫外線照射爲唯一透明面外，底部置於黑色橡皮墊上，其餘四面外部均再外加亮面不銹鋼薄片以加強反光，提高光照效果。實驗是於室內採用六支波長 300~400 nm (以 365 nm 爲代表)、強度 90 μW/cm^2 之紫外線燈管(EAST ASIA, FL 20BL/18W)做爲替代光源，並配合量測範圍相同之紫外線強度計(UVX Digital Radiometer)來進行。

反應操作程序如下：1.將反應器中氣體以高純度空氣置換之，2.開啓分析儀進行熱機(至少二小時)後，以零值與標準氣體來校正之，3.由叉管中通入已知濃度與體積之 NO 或 O_3，並使之充分混合。4.由注入口注入定量之 HC 或水份，並使之完全蒸發。5.開啓分析儀與反應器氣體進出口連接閥，使所有設備串聯成一氣流迴路，以連續分析反應過程中日照度、溫度、HC、O_3 與 NO_X 之濃度變化。所有儀器分析結果之輸出訊號，均連接至數據處理機。

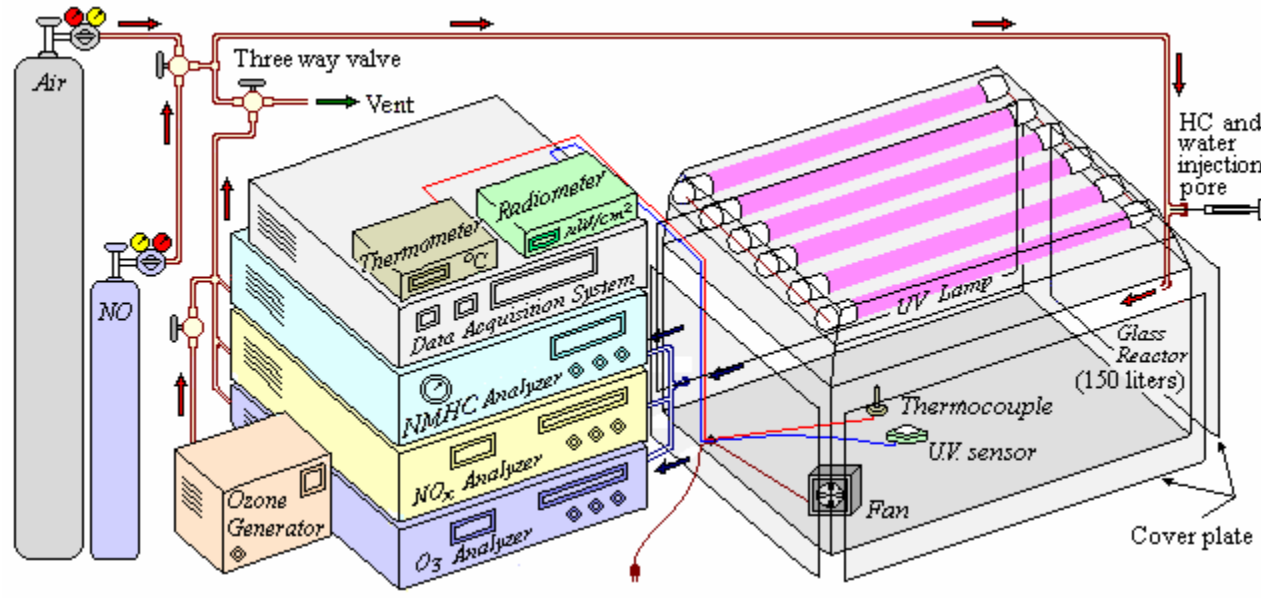

Figure 36 Experimental arrangement for the photochemical reaction.

一、.HC 種類之影響

選擇以甲苯與異辛烷來進行不同種類 HC 對臭氧生成與消失之影響實驗，所得結果如圖 37(a)與(c)所示，由圖中獲知戊烯最易於參與光化學反應，甲苯次之，異辛烷最末，使得 O_3 與戊烯濃度遞減均明顯較快。值得一提的是 NO 在反應中，迅速氧化轉變成 NO_2，但 NO_2 在反應中亦會反應而逐漸減少。此結果顯示不同種類 HC 對臭氧生成與消失有明確之影響。

二、NO 啓始濃度之影響

由於 NO 在反應之初即迅速氧化生成 NO_2(參見圖 37)，因此 NO 啓始濃度($[NO]_o$)對臭氧

濃度之影響，值得深入探討。圖 38 顯示不同$[NO]_o$對臭氧濃度改變之影響不大，且臭氧濃度下降的趨勢相近。但較高的$[NO]_o$會使得臭氧濃度下降略緩。此可能因 NO 爲臭氧之前軀物，而較高之 NO 亦會生成較多的臭氧所致，所以臭氧濃度下降之速率隨$[NO]_o$的增加而略爲變慢。

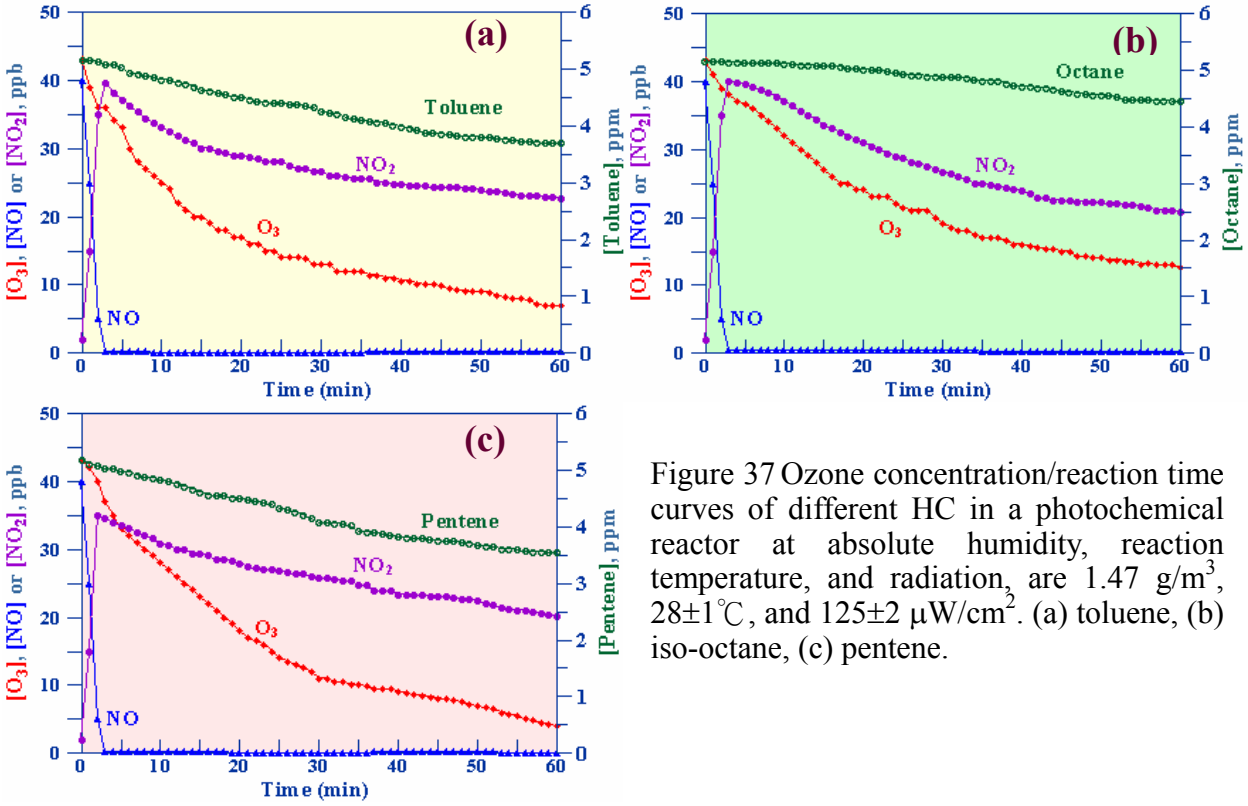

Figure 37 Ozone concentration/reaction time curves of different HC in a photochemical reactor at absolute humidity, reaction temperature, and radiation, are 1.47 g/m^3, 28±1℃, and 125±2 μW/cm^2. (a) toluene, (b) iso-octane, (c) pentene.

三、濕度之影響

前面結果顯示高濕度有助於臭氧的反應消失，其反應可能爲 $O_3+H_2O \rightarrow H_2O_2+O_2$。因此探討濕度對臭氧的影響，是實驗工作之探討重點，而改變光化反應中之含水量所得結果如圖 39(a)~(c)所示。由圖 39(a)中獲知在低臭氧啓始濃度($[O_3]_o$=47±2 ppb)下，通入少量水份即可以明顯增加臭氧之衰減，但增加水量對臭氧衰減影響不大。但當臭氧之濃度增高時，臭氧衰減量明顯隨水量的增加而增大(參見 39(b)與(c))。比較不同臭氧量下之無水與濕度($\mathcal{H}$) 10.0 g/m^3 二曲線間的差值，在反應 60 min 後均約爲 20 ppb，但逐步提高臭氧濃度後，亦顯示逐漸增加四條曲線的間距。

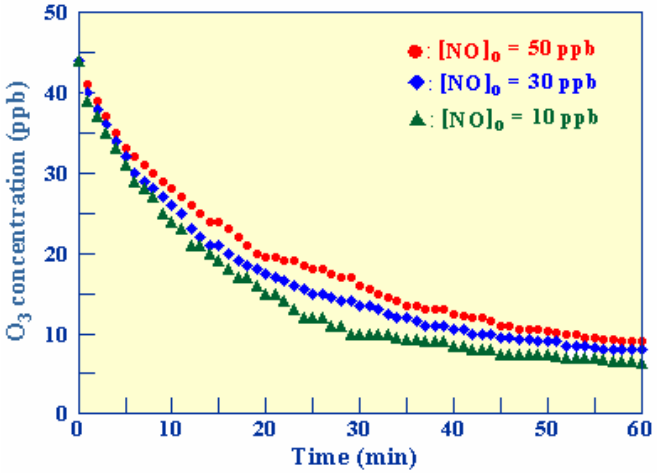

Figure 38 Ozone concentration/reaction time curves of different NO initial concentration in a photochemical reactor at absolute humidity, reaction temperature, radiation, and toluene initial concentration are 5±0.2 ppm, 14.7 g/m^3, 28±1℃, and 125±2 μW/cm^2.

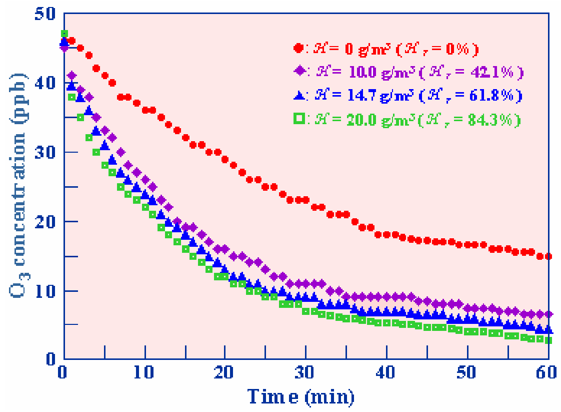

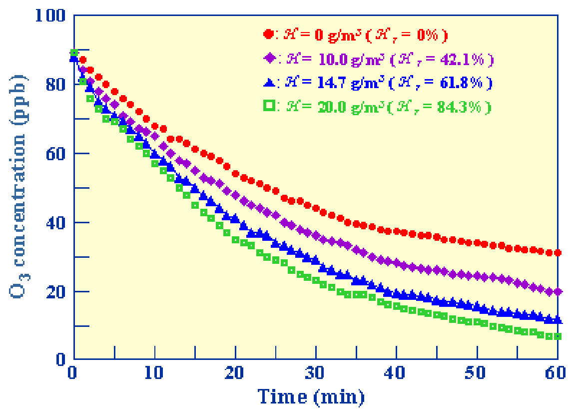

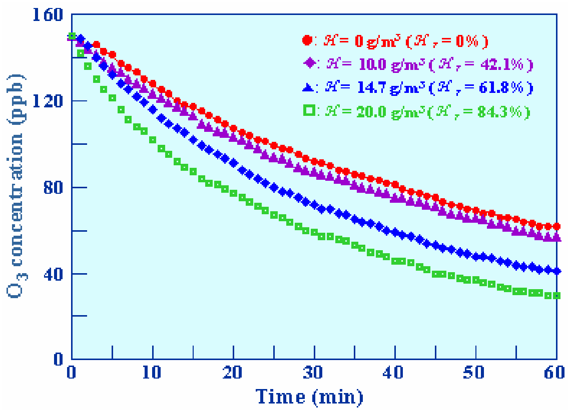

Figure 39 Ozone concentration/reaction time curves of different O_3 initial concentration and absolute humidity, in a photochemical reactor at reaction temperature, radiation, and toluene initial concentration are 28±1℃，125±2 μW/cm^2, and 5±0.2 ppm. (a) $[O_3]_o$ = 47±2 ppb, (b) $[O_3]_o$ = 90±2 ppb, (c) $[O_3]_o$ = 150±2 ppb.

圖 40 為以 H =14.7 g/m^3 下，不同臭氧量下之$[O_3]/[O_3]_o$對時間做圖所得。其中$[O_3]_o$=185 ppb 之$[O_3]/[O_3]_o$比值最大，顯示其臭氧之衰減率最差，即相同濕度下，臭氧之衰減率隨臭氧濃度之增加而降低。造成此現象可能的原因，由於常壓下大氣密度低，臭氧與水份或其他反應物反應，會受空間效應的影響，使高臭氧濃度需高的反應時間所致。此現象可藉助諸動力學參數與反應速率式來解釋之。

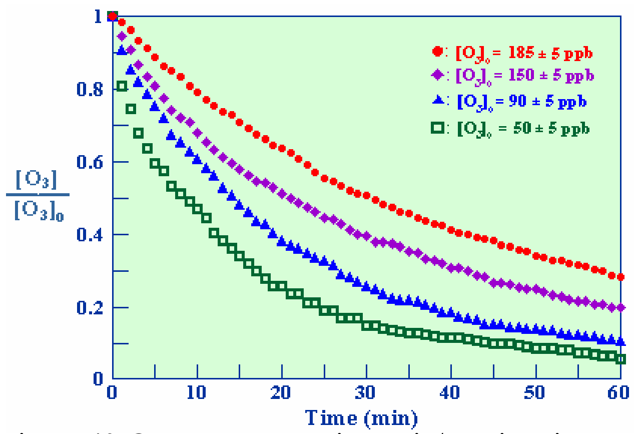

Figure 40 Ozone concentration ratio/reaction time curves of different ozone initial concentration in a photochemical reactor at absolute humidity, reaction temperature, and toluene initial concentration, radiation are 1.47 g/m^3, 28±1℃, 125±2 μW/cm^2, and 5±0.2 ppm.

綜合前述結果，顯示降低 HC 與 NOx 濃度雖可使臭氧濃度略降，但提高大氣水份含量，最能抑制臭氧濃度。實驗結果亦顯示在臭氧的衰減量上，臭氧隨濕度的增加而快速降低；但在臭氧的衰減率上，則隨臭氧濃度的增加而降低。

圖 37~39 結果顯示臭氧濃度隨時間的變化，可滿足(10)式之動力方程式：

$$\frac{d[O_3]}{dt} = -k_{observed}[O_3] \tag{10}$$

其中 $k_{observed}$ 為外觀速率常數。積分(10)式可得

$$\ln\frac{[O_3]_o}{[O_3]} = k_{observed} \cdot t \tag{11}$$

運用(11)式及圖 38(b)之數據，以 $\ln\frac{[O_3]_o}{[O_3]}$ 對 t 做圖，則可求得斜率 $k_{observed}$，所得結果如圖 41 所繪。若考慮所有與臭氧作用之參數，則 $k_{observed}$ 可寫成

$$k_{observed}=\sum_{i=1}^{N}k_i[\text{Parameter}]_i=k^*+k_H\mathcal{H} \tag{12}$$

其中 $k^*=\sum_{j=1}^{N-1}k_j[\text{Parameter}]_j$，$k_H$ 爲與水有關之速率常數。再以 $k_{observed}$ 對 $\mathcal{H}$ 做圖可求得截距(k^*)與斜率(k_H)，所得結果如圖 42 所繪，k^*=2.07×10^{-2} 與斜率 k_H=1.08×10^{-3}，但 k_T 是在本研究反應條件所得，而 k^* 會隨不同反應條件而變。最後建立臭氧之反應速率式(13)或(14)式，其中[O_3]、H 與 t 之單位分別爲 ppb、g/m^3 與 min。

$$\frac{d[O_3]}{dt}=-(k^*+1.08\times10^{-3}\mathcal{H})[O_3] \tag{13}$$

$$[O_3]=[O_3]_o\exp[-(k^*+1.08\times10^{-3}\mathcal{H})t] \tag{14}$$

(14)式證實提高環境大氣中水份含量，可以降低臭氧之濃度。另外，在海島型氣候的台灣地區，$\mathcal{H}$ 值通常大於 14.5g/m^3(相對濕度約 60%)，使 1.08×10$^{-3}\mathcal{H}$ 乘積與 k^* 值相近，顯見大氣中水份的存在可以有效的降低臭氧之濃度。而提高環境大氣中水份含量的方法可藉助提高植栽、綠地與池塘、水道等面積比例，以增加水份之蒸發量。

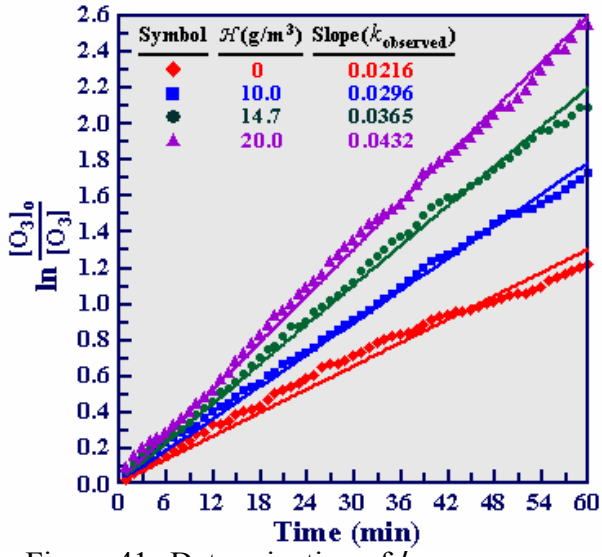

Figure 41 Determination of $k_{observed}$

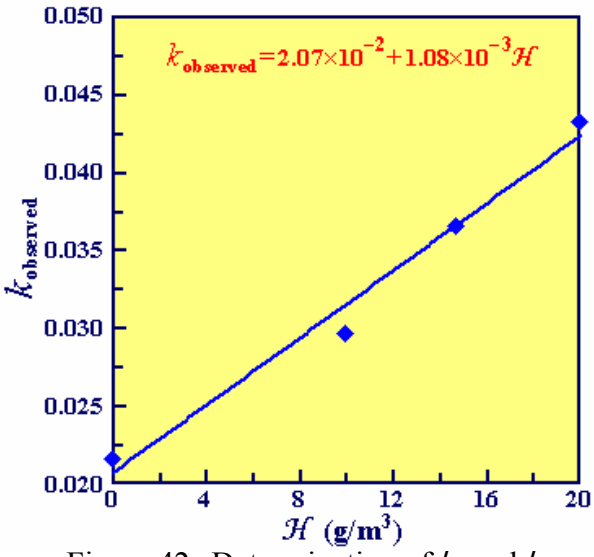

Figure 42 Determination of k and k_H

捌、結論

1.運用相關係數式求出各參數與臭氧濃度的相關係數值，獲知各月份與全年之日間，相對濕度與臭氧濃度之相關度最高，日照次之。提高環境中水份，最能抑制臭氧濃度。夜間臭氧仍會與水份、HC、NO、NO_2 作用，其中 NO 與臭氧的相關度最高，相對濕度次之。

2.歷年臭氧事件日時：(1).11:00 左右即足以產生相當高臭氧，(2).盆地內效應會明顯改變風場，使盆地內東測之臭氧濃度居高不下，(3).沿海地區因具有較高濕度，即使在臭氧事件日仍可保持一定低的臭氧濃度。(4).位處下風處之沿海地區，會因臭氧不斷輸入，臭氧濃度於傍晚時顯現出較慢之下降速率。

3.探討臭氧事件日裏，臭氧在大氣中之非穩定狀態與一維的傳輸與反應作用，獲知：(1).14:00後之臭氧產生速率 R 與消失速率常數 L 均由正值轉爲負值，顯示大氣反應有明顯轉變。(2).R 與 L 值在 12:00~13:00 間最大，14:00~15:00 間最小，(3).14:00 前因 NOx 與 HC 反應使臭氧增高，14:00~15:00 間，因光化學煙霧產量最大，消耗臭氧使 R 與 L 由正轉爲負，(4).16:00 後又出現另一大的 R 與 L 負值，顯現另一種臭氧之消耗反應在進行，但此反應是否是臭氧與大氣中之微粒或水份反應，則有待深入探討。

4.經濃度採樣分析，不同高程之大氣均可分析出 73 種主要碳氫化合物，其中烷類有 26 種、烯類有 12 種、芳香族類有 6 種、有機鹵化物有 6 種、醛酮類有 8 種、醇類有 5 種、醚酯類有 2 種、其他有 7 種。低層大氣會有較多低分子量之 HC 存在，而高層大氣則有較多高分子量之 HC。

5.採樣分析結果顯示各污染物的濃度，會隨高程而略爲增加，最高濃度會通常出現在 300~500 m 處。整理各項結果獲知：(1).盆地內 O_3、NO 與 NO_2 平均濃度不僅較沿海地區高，且於各高程之變動亦較大，(2).沿海地區 HC 濃度隨高程增加而增高，但在盆地內則相反，另外沿海地區 100 m 高程以上平均濃度均較高。(3).沿海地區之烷、烯類均隨高程增高而增加，但在盆地內則恰爲相反。(4).二地區各高程之有機鹵化物、芳香族化合物、有機氧化物與其他有機物之平均濃度相近，但沿海地區之濃度變動性較大。

6.採樣時日出現二種傳輸現象，一爲風由外往盆地內吹，且臭氧濃度是隨風向遞增；另一爲風由盆地內往外吹，而臭氧濃度是隨風向遞減。探討此二傳輸現象獲知：(1).風由外往盆地內時，R 與 L 會由 12:00 之正值，轉爲 14:00 之負值，顯現此結果與表 2 所列相同，(2).風改由盆地內向外吹時，R 與 L 值提前於 12:00 即爲大的負值，但 14:00 時 R 之負值變小(臭氧之消失作用縮小)與 L 轉爲正值($-L[O_3]$恢復爲消失項)，(3).風向並非決定臭氧濃度的主要因素，地形與一些需再深入探討環境因素與才是要因。

7.由多變量關係方程式獲知高日照與低濕度下最容易產生高臭氧濃度，而所有臭氧前軀物 NO 與各類 HC 之係數均爲負值，則說明當它們濃度高時，意味著未進一步生成臭氧。

8.實驗結果證實不同的 HC 會影響臭氧之生成與消失。改變 NO 啓始濃度對臭氧濃度變動趨勢影響不大，但高 NO 會使得臭氧濃度下降略緩。

9.降低 HC 與 NOx 濃度雖可使臭氧濃度略降，但提高大氣水份含量，最能抑制臭氧濃度。實驗結果亦顯示在臭氧的衰減量上，臭氧隨濕度的增加而快速降低；但在臭氧的衰減率上，則隨臭氧濃度的增加而降低。

10.完成光化反應之動力學研究，獲得水份之速率常數參數與反應速率式。

參考文獻

1.Sillman, S., *The Relation Between Ozone, NO_x and Hydrocarbons in Urban and Polluted Rural Environments*, Atmospheric Environment, **33**, 1821- 1845, 1999.

2.Wakamatsu, S., Uno, I., Ohara, T., and Schere, K. L., *A Study of the Relationship Between Photochemical Ozone and Its Precursor Emissions of Nitrogen Oxides and Hydrocarbons in Tokyo and Surrounding Areas*, Atmospheric Environment, **33**, 3097-3108, 1999.

3.Uno, I., Ohara, T., and Wakamatsu, S., *Analysis of Wintertime NO_2 Pollution in the Tokyo Metropolitan Area*, Atmospheric Environment, **30**(5), 703-713, 1996.

4.Skov, H., Egeløv, A. H., Granby K., and Nielsen, T., *Relationships Between Ozone and Other Photochemical Products at Li Valby, Denmark*, Atmospheric Environment, **31**(5), 685-691, 1997.

5.Kim, J. Y. and Ghim Y. S., *Effects of the Density of Meteorological Observations on the Diagnostic Wind Fields and the Photochemical Modeling in the Greater Seoul Area*, Atmospheric Environment, **36**, 201-212, 2002.

6.Elkamel, A., Abdul-Wahab, S., Bohamra, W., and Alper, E., *Measurement and Prediction of Ozone levels Around a Heavily Industrialized Area*, Adv. in Environ. Res., **5**, 47-59, 2001.

7.Huang, H., Akustu, Y., Arai, M., and Tamura, M., *Analysis of Photochemical Pollution in Summer and Winter Using a Photochemical Box Model in the Center of Tokyo, Japan*, Chemosphere, **44**, 223-230, 2001.

8.Rabl, A. and Eyre, N., *An Estimate of Regional and Global O_3 Damage from Precursor NO_x and VOC Emissions*, Environment International, **24**(8), 835-850, 1998.

9.Trainer, M., Parrish, D. D., Goldan, P. D., Roberts, J., and Fehsenfeld, F. C., *Review of Observation-based Analysis of the Regional Factors Influencing Ozone Concentrations*, Atmospheric Environment, **34**, 2045-2061, 2000.

10.Lal, S., Naja, M., and Subbaraya, B. H., *Seasonal Variations in Surface Ozone and its Precursors over an Urban Site in India*, Atmospheric Environment, **34**, 2713-2724, 2000.

11.Chu, S. H., *Meteorological Considerations in Siting Photochemical Pollutant Monitors*, Atmospheric Environment, **29**(21), 2905-2913, 1995.

12.Sistla, G., Zhou, N., Hao, W., Ku, J. Y., Rao, S. T., Bornstein, R., Freedman, F., and Thunis, P., *Effects of Uncertainties in Meteorological Inputs on Urban Airshed Model Predictions and Ozone Control Strategies*, Atmospheric Environment, **30**(12), 2011-2025, 1996.

13.Sebnem, A. A., Lu, C. H., Keller, J., Prévôt, A. S. H., and Chang, *Variability of Indicator Values for Ozone Production Sensitivity: a Model Study in Switzerland and San Joaquin Valley (California)*, Atmospheric Environment, **35**, 5593-5604, 2001.

14.Blanchard, C.L. and Stoeckenius, T., *Ozone Response to Precursor Controls: Comparison of Data Analysis Method with the Predictions Photochemical Air Quality Simulation Models*, Atmospheric Environment, **35**, 1203-1215, 2001.

15.Pryor, S. C., *A case Study of Emission Changes and Ozone Responses, Atmospheric Environment*, **32**(2), 123-131, 1998.

16.Pohlmann, B., Scharf, H. D., Jarolimek, U., and Mauermann, P., *Photochemical Production of Fine Chemicals with Concentrated Sunlight*, Solar Energy, **61**(3), 159-168, 1997.

17.Shih, J. S., Russell, A. G., and McRae, G. J., *An Optimization Model for Photochemical Air Pollution Control*, European Journal of Operational Research, **106**, 1-14, 1998.

18.Jenkin, M. E. and Clemitshaw, K. C., *Ozone and Other Secondary Photochemical Pollutants: Chemical Processes Governing Their Formation in the Planetary Boundary Layer*, Atmospheric Environment, **34**, 2499-2527, 2000.

19.Chang, T. Y., Chock, D. P., Nance, B. I., and Winkler, S. L., *A Photochemical Extent Parameter to Aid Ozone Air Quality Management*, Atmospheric Environment, **31**(17), 2787-2794, 1997.

20.Geisse, S. M. and Doebner, H. D., *Dynamical Systems Based on a Mesospheric Photochemical Model*, Physics Letters A, **241**, 269-273, 1998.

21.Seinfeld, J. H. and Pandis, S. N., *Atmospheric Chemistry and Physics*, JOHN WILEY & SONS, INC. 1217-1230 (1998).

22.Botkin, D. B. and Keller, E. A., *Environmental Science*, 3rd Edition, JOHN WILEY & SONS, INC. 474-477 (2000).

23.Jeffries, M. E., and Crouse, R. (1990), Scientific and technical issues related to the application of incremental reactivity. Department of Environmental Science and Engineering, University of North Carolina, Chapel Hill, NC.

評 語

1.能充分利用周邊人力與儀器設備資源(逢甲大學理工所)進行野外臭氧之垂直分布觀測，並能利用氣象觀測資料，分析彼此相關。

2.能在實驗室設計光化學反應之設備，並進行實驗分析結果。

3.能由野外實測與實驗室量測，推論近地面臭氧濃度與相對溼度之相關性。

Ozone Event Days–
The Effects of Meteorology and Topography on Formation and Transformation of Ozone in the Lower Atmosphere

Chen-Jui Liang
National Taichung Second Senior High School, Taichung, Taiwan

Abstract

The monitoring data were used to investigate the effect of surface wind, time, and terrain on the transformation of ozone. The sampling and the analysis in the coastal and in the Taichung basin were completed. The vertical distribution of O_3, NO_X and HC and the different altitude wind were investigated. The contour of O_3 and surface wind with 3D map were plotted. The results show that the correlation behaves relativity of relative humidity with ozone is the best, and solar radiation is the next. Enhancing environmental moisture can efficiently decrease ozone concentration. In each ozone event day are: (1) the high [O_3] always starts from 11:00, (2) the ozone concentration on the coastal is always low due to the high humidity, (3) the high [O_3] in the east of the basin is due to the basin effect which causes changes the surface wind, and (4) in the evening, the descend rate of [O_3] in the coastal area is lower because ozone blows into the coastal area. The formation rate (R) and disappear rate constant (L) of the ozone event day were obtained. The values of R and L change from plus to minus before 14:00. The values of R and L are lower at 14:00~15:00 due to the photochemical smog formation. And another lower R and L value before 16:00 may be due to ozone react with particle or water. The results of analysis indicate that: (1) the concentration increases with increasing altitude, and the maximum is at 300-500 m height, (2) 73 kinds of hydrocarbons were identified, and the concentration variation with altitude was also investigated, and (3) most of low molecular weight HC are at lower altitude, otherwise high molecular weight HCs are at higher altitude. The results also show that: (1) [O_3], [NO], and [NO_2] on the basin are not only lower than on the coastal, but also their variability of concentration are big, (2) THC, paraffin, and olefins on the coastal are higher than on the basin, and the concentrations increase with increasing altitude on the coastal, but on the basin is decreasing, (3) the average concentrations of halides, aromatics, oxides, and others are similar on both area, but concentration variability on the coastal is obvious. The results of the reaction experiment show that: (1) ozone formation or disappearance depends on different HC, (2) the effect of $[NO]_o$ is small for ozone photochemical reaction, but [O_3] decreases with increasing [NO], (3) the descend rate of O_3 depends on high humidity more than different kinds of HC or [NO], and (4) the descend amount of ozone increases with increasing humidity strongly, and the descend rate of ozone decreases with enhancing [O_3]. The reaction rate and rate constant of ozone reaction with water were also obtained.

Keyword: Ozone, Meteorology, Terrain, Formation, Transformation

1. Introduction

High concentration of ozone is a major environmental concern in Taiwain because of its adverse impacts on human health. Taiwain, with warm and high humidity climates, is especially likely to experience high ozone. But the effect of meteorology and topography on formation and transformation of ozone in the lower atmosphere on an island is seldom studied[1~9]. The Taichung basin is a special area, which combines coast, basin and mountain topography. The high concentration of air pollution accumulates easily in the Taichung basin because of the basin effect. So this study does not only discuss the above influential factors but also includes the correlation with mass and concentration of HC vertical distribution in the atmosphere, wind field and topography effect. This helps discern the mechanism of ozone formation.

2. Study process

Fig. 1 shows the observed steps in the study process. First, the analysis of monitoring data from 2001 to 2002. Second, field measurements by means of Tenax-TA column concentrations and GC-MS analysis. Finally, some of the approaches have been developed in the laboratory.

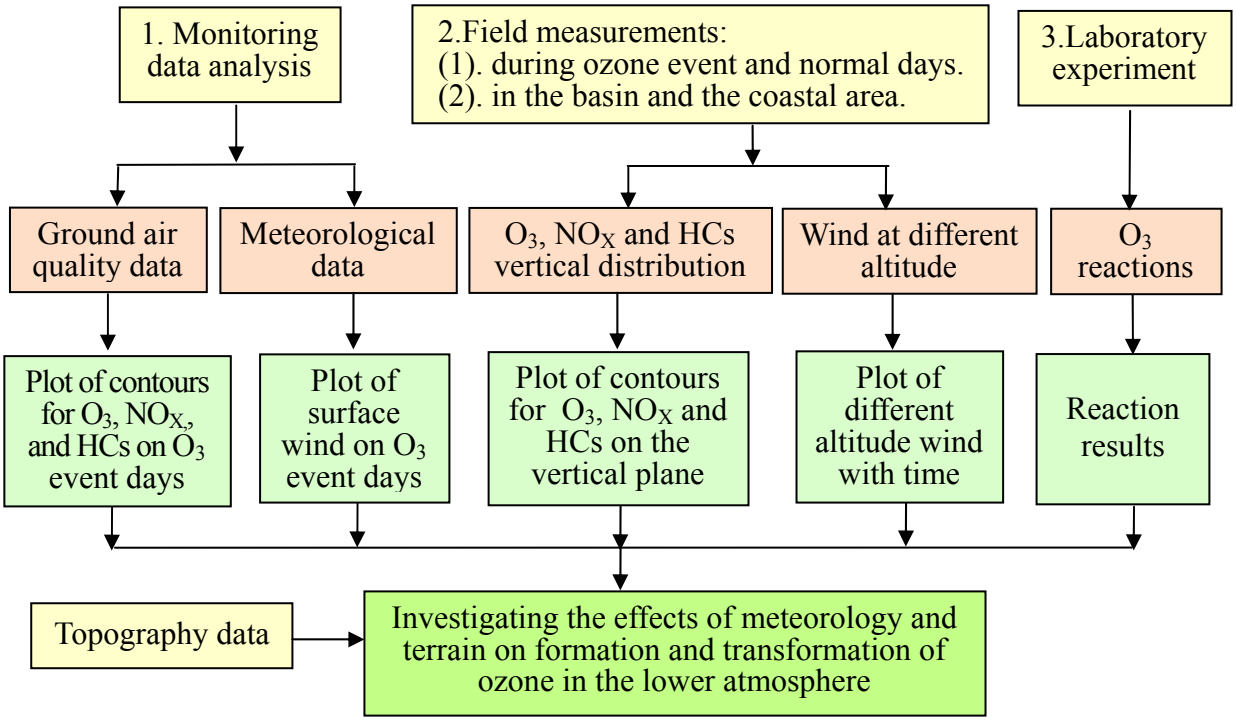

Figure 1 Steps in the study process

3. Taichung basin digital maps

It has been necessary to set up digital maps for this study. Therefore, these two maps have been developed. Both use UTM scales. One is a three-dimensional contour map in which the visual angles are changeable; the other is a color differential map.

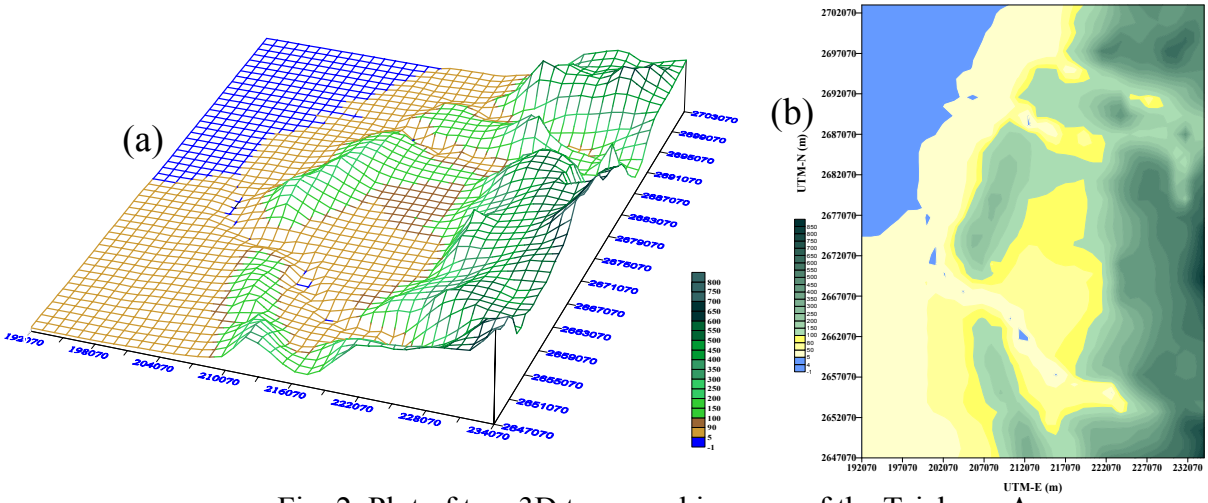

Fig. 2. Plot of two 3D topographic maps of the Taichung Area

4 Monitoring data analysis

There are 22 ambient air-quality monitoring stations in the Taichung area (Fig. 3). The monitoring were taken during the daytime of four event days and eight field measurement days, were

used to plot ozone contour and wind field maps.

Annual data for 2001 were only taken from C2 station (Fig. 3) to calculate the correlation coefficients between ozone and parameters. This station monitored the most parameters.

These air quality-monitoring stations are divided into three groups depending on their distance from the Taichung coastal area\Line-1, mountainside area\Line-2, and between the coastal and mountain\Line-3. The field measurement sampling positions for this study are also show in Fig. 3. These sampling positions are divided into two sets, i.e. coastal area\green flags and mountain side\red flags.

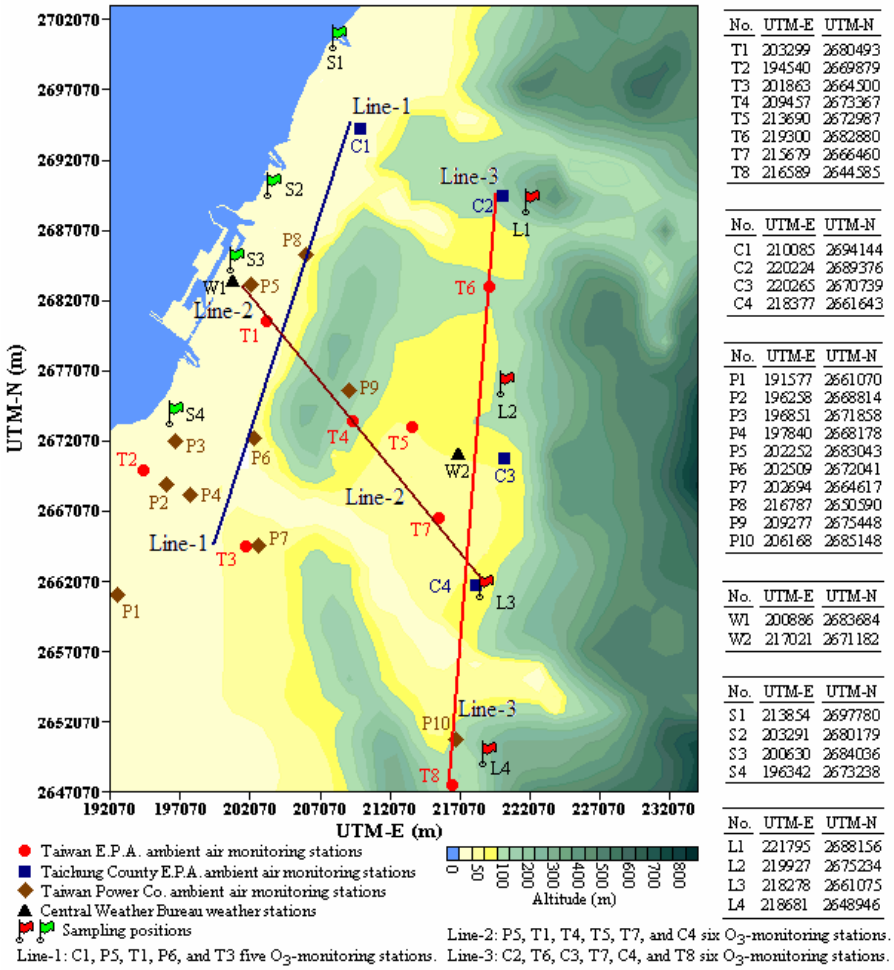

No.	UTM-E	UTM-N
T1	203299	2680493
T2	194540	2669879
T3	201863	2664500
T4	209457	2673367
T5	213690	2672987
T6	219300	2682880
T7	215679	2666460
T8	216589	2644585

No.	UTM-E	UTM-N
C1	210085	2694144
C2	220224	2689376
C3	220265	2670739
C4	218377	2661643

No.	UTM-E	UTM-N
P1	191577	2661070
P2	196258	2668814
P3	196851	2671858
P4	197840	2668178
P5	202252	2683043
P6	202509	2672041
P7	202694	2664617
P8	216787	2650590
P9	209277	2675448
P10	206168	2685148

No.	UTM-E	UTM-N
W1	200886	2683684
W2	217021	2671182

No.	UTM-E	UTM-N
S1	213854	2697780
S2	203291	2680179
S3	200630	2684036
S4	196342	2673238

No.	UTM-E	UTM-N
L1	221795	2688156
L2	219927	2675234
L3	218278	2661075
L4	218681	2648946

Fig. 3. Map of monitoring stations and sampling positions in the Taichung Area

(1) Factor analysis

For understand the role of the major parameters in the ozone formation, a statistical factor analysis method was used to assess the correlation coefficient between ozone with the different concentrations of precursors and variable meteorological factors, the following equation was used:

$$r_{xy} = \frac{\sum_{i=1}^{n}(x_i - \bar{x})(y_i - \bar{y})}{\sqrt{\sum_{i=1}^{n}(x_i - \bar{x})^2}\sqrt{\sum_{i=1}^{n}(y_i - \bar{y})^2}} \quad (1)$$

As can be seen, during daytime (06:00~18:00) in monthly and annul data, solar radiation,

relative humidity and ambient temperature have high relative importance with ozone (Table 1 and Fig. 4). They are generally higher than the other 6 parameters. The importance of relative humidity is the highest of the variables. With the r_{xy} all at negative values, indicating that O_3 concentration decreases with increasing relative humidity. High solar radiation is always coupled with high temperature, so they seem to be of equal importance, both of their coefficients present high positive correlation with ozone. Relative humidity exhibits the most major contribution. The correlation coefficients of other precursors are relatively low, especially as no relationship is obvious for CH_4 and NMHC concentration variation during the day hours. The importance of NO is the highest of the other precursors (annul data is −0.36), but presents a negative correlation. Ozone will react with moisture, CH_4, NO, or NO_2 in the nighttime (18:00~06:00), so their correlation coefficients are negative values. However, the correlation coefficient between NO and O_3 is the maximum, and relative humidity is the second.

Table 1 Results of the relative coefficients between some parameters and ozone.

Parameters	Jan.	Feb.	Mar.	Apr.	May	June	July	Aug.	Sep.	Oct.	Nov.	Dec.	Annual
Solar radiation													
daytime	0.546	0.596	0.693	0.672	0.564	0.409	0.654	0.520	0.719	0.628	0.484	0.445	0.578
Relative humidity													
daytime	-0.683	-0.737	-0.752	-0.633	-0.615	-0.410	-0.542	-0.455	-0.785	-0.665	-0.527	-0.416	-0.602
nighttime	-0.576	-0.532	-0.551	-0.333	-0.334	-0.135	-0.185	-0.110	-0.226	-0.177	-0.410	-0.295	-0.322
Ambient temperature													
daytime	0.333	0.452	0.479	0.496	0.679	0.631	0.604	0.638	0.674	0.753	0.431	0.314	0.540
nighttime	-0.404	-0.387	-0.297	0.032	0.268	0.148	0.235	0.247	-0.044	-0.077	-0.315	-0.345	-0.078
Methane, CH_4													
daytime	-0.314	-0.046	-0.097	-0.400	-0.052	-0.132	-0.144	-0.010	0.012	-0.181	0.081	-0.044	-0.111
nighttime	-0.295	-0.488	-0.528	-0.447	-0.162	-0.248	-0.159	-0.149	-0.200	-0.188	-0.373	-0.066	-0.275
Non-methane hydrocarbon, NMHC													
daytime	-0.034	-0.167	-0.032	0.202	-0.017	-0.242	-0.375	-0.342	-0.256	-0.033	-0.138	-0.078	-0.126
nighttime	-0.228	-0.342	-0.230	-0.201	-0.160	-0.133	0.021	-0.069	-0.106	-0.106	-0.253	-0.096	-0.159
Sulfur dioxide, SO_2													
daytime	0.161	0.233	0.250	0.082	0.222	-0.024	-0.107	-0.097	0.340	0.269	0.329	0.181	0.153
nighttime	-0.130	-0.270	0.184	0.011	0.173	0.083	0.188	-0.178	0.312	-0.060	-0.163	-0.104	0.004
Carbon monoxide, CO													
daytime	-0.183	0.081	-0.117	-0.078	0.009	-0.076	0.013	-0.072	0.048	-0.026	0.111	0.041	-0.021
nighttime	-0.355	-0.316	-0.213	-0.162	-0.093	-0.252	0.126	-0.052	0.015	-0.247	-0.287	-0.311	-0.179
Nitric oxide, NO													
daytime	-0.348	-0.151	-0.482	-0.336	-0.186	-0.329	-0.470	-0.350	-0.445	-0.447	-0.444	-0.389	-0.365
nighttime	-0.395	-0.474	-0.492	-0.254	-0.171	-0.288	-0.227	-0.309	-0.410	-0.417	-0.364	-0.511	-0.359
Nitrogen dioxide, NO_2													
daytime	-0.076	-0.060	-0.188	-0.247	0.027	-0.066	0.101	0.053	0.301	0.092	0.080	-0.048	-0.003
nighttime	-0.547	-0.534	-0.318	-0.148	-0.056	-0.253	-0.030	-0.198	-0.129	-0.397	-0.547	-0.388	-0.295

Note: Daytime and nighttime are at 06:00-18:00 and 18:00-06:00 next day.

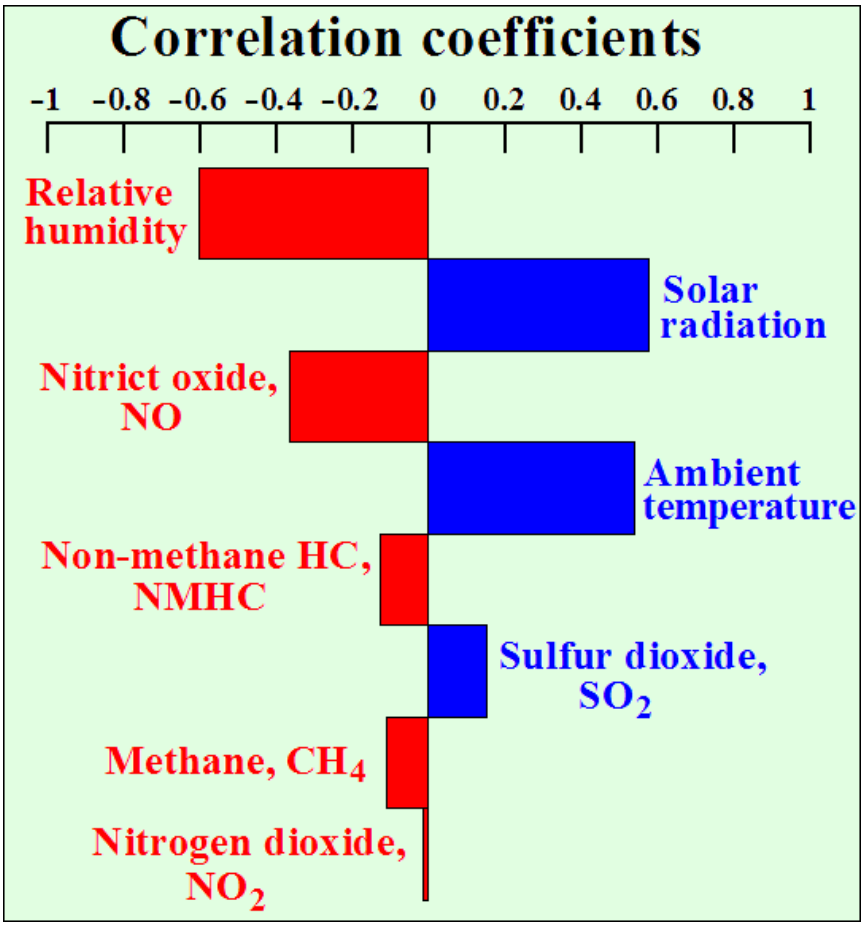

Fig. 4 Results of correlation coefficients between ozone and parameters during the daytime (C2, 2001 annual data)

(2) The effect of wind field, time and topography on transformation of ozone

Fig. 5~8 show that: (1) the ozone event day always occur at low surface wind speed (about 3 m/sec), and wind direction always comes from south-east, south, or east in the southern area of the Taichung; (2) the ozone concentrations of T7 and C4 are always the maximum due to heavy traffic and some location industry; (3) ozone and it's precursors will come from south-east, so the ozone concentration at the downwind position of the Taichung area is high especially on May 25, 2002; (4) the surface wind in the coastal area is different from the basin, so the ozone concentration is always kept low even on the ozone event day.

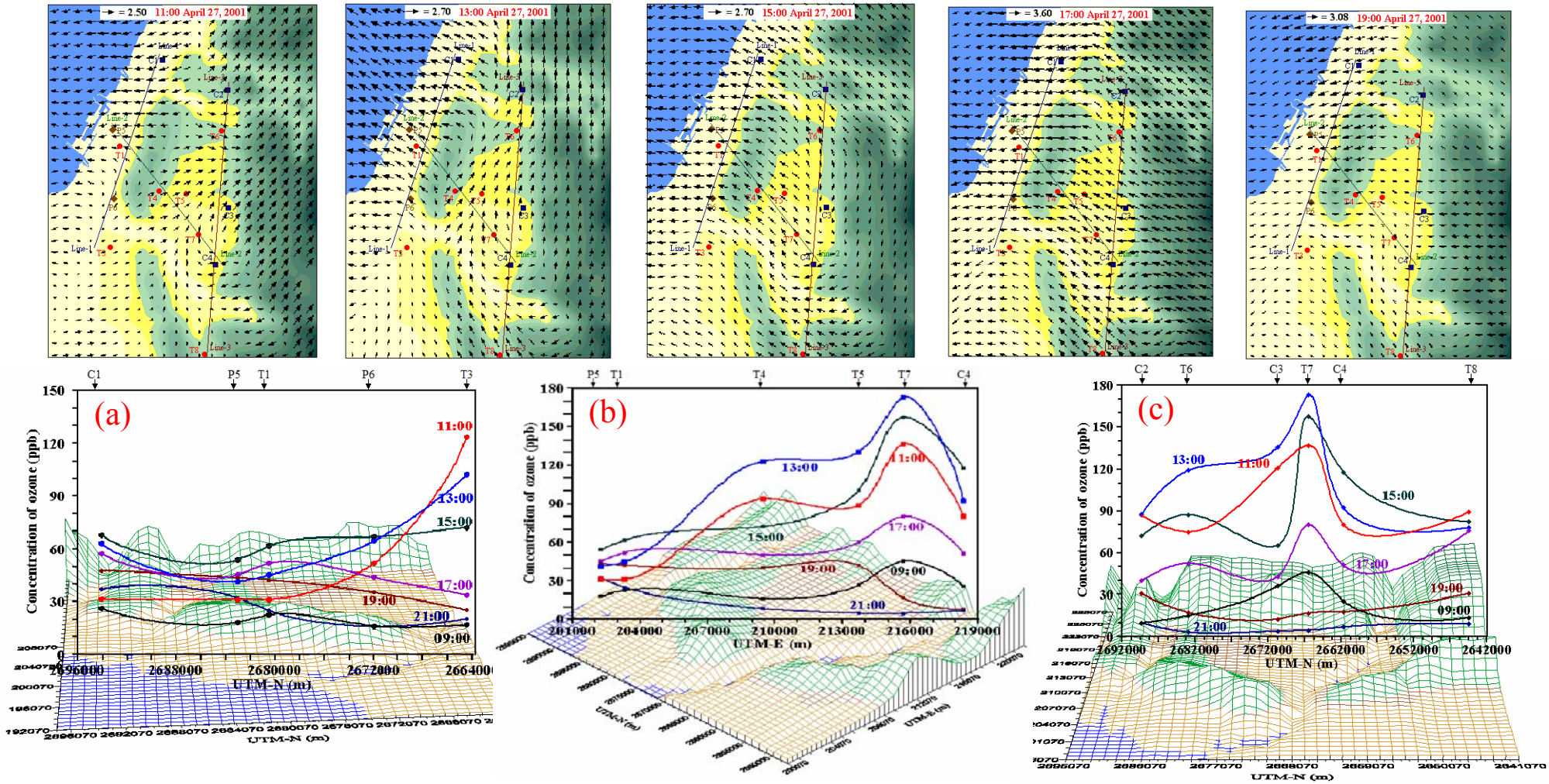

Fig. 5. Measurements of ozone and surface wind from air-monitoring stations of the Taichung Area on April 27, 2001. (a) five air-monitoring stations in the coastal area. (b) six air-monitoring stations from sea side to the east of basin. (c) six air-monitoring stations in the Taichung Basin.

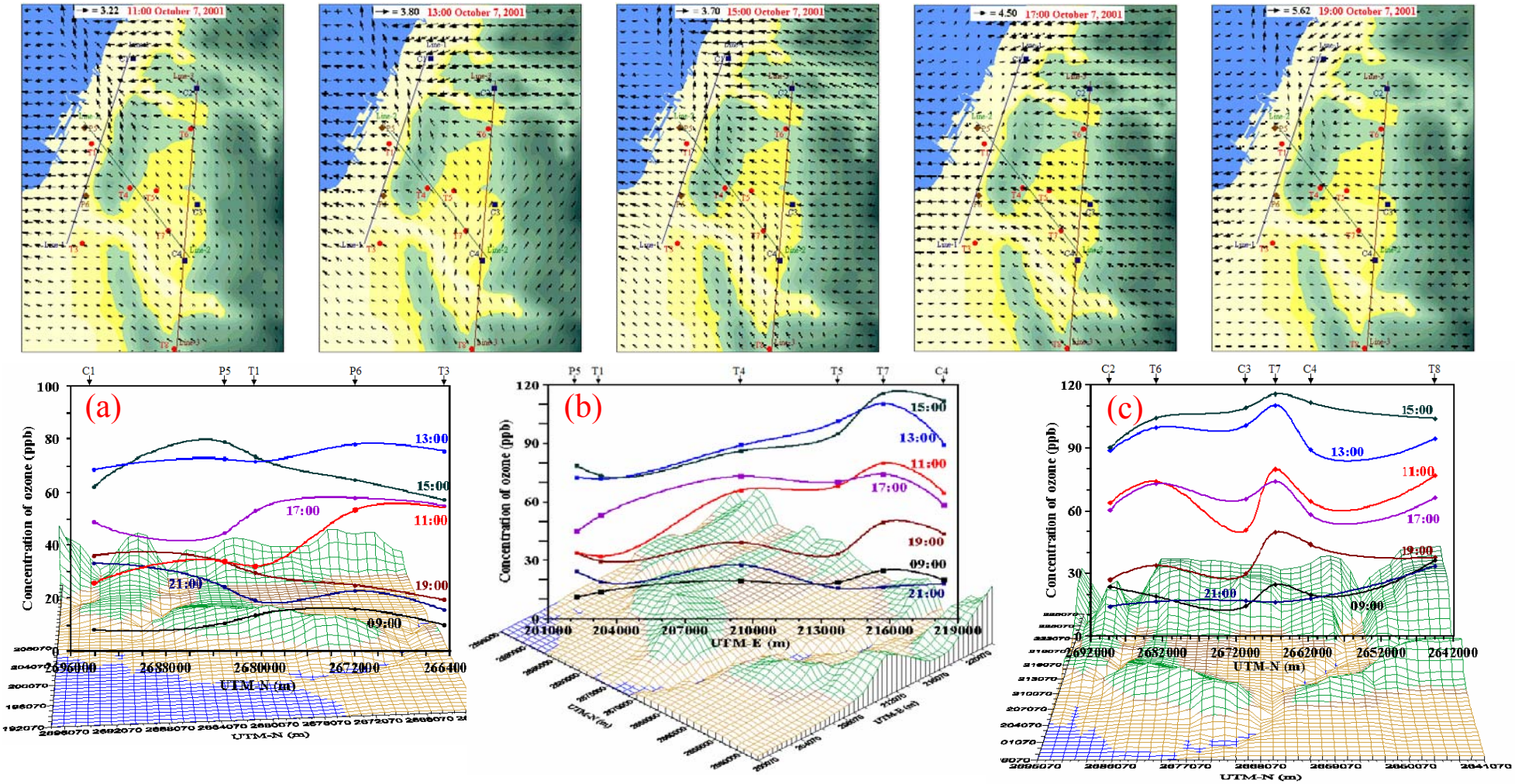

Fig. 6. Measurements of ozone and surface wind from air-monitoring stations of the Taichung Area on October 7, 2001. (a) five air-monitoring stations in the coastal area. (b) six air-monitoring stations from sea side to the east ofbasin. (c) six air-monitoring stations in the Taichung Basin.

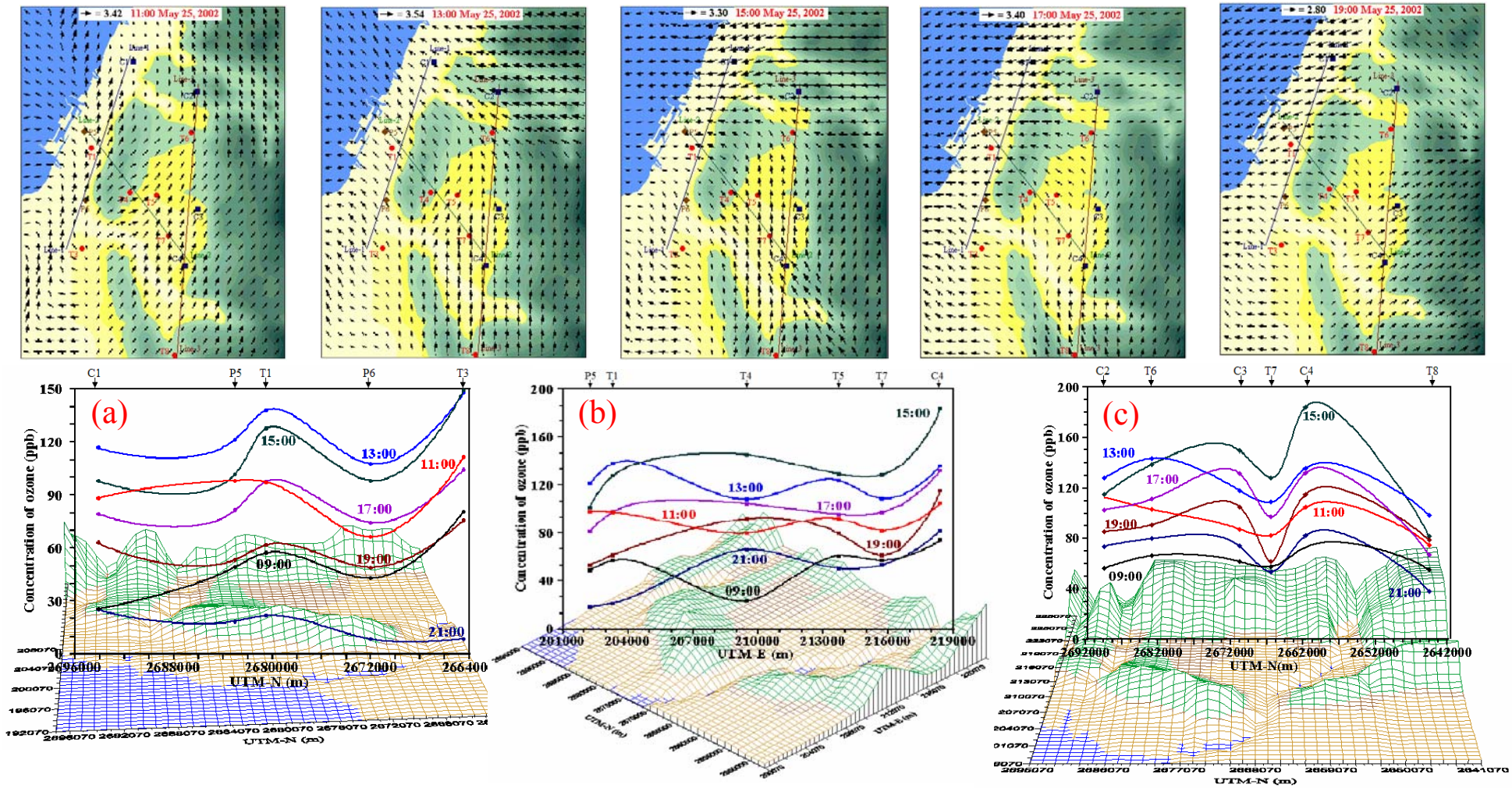

Fig. 7. Measurements of ozone and surface wind from air-monitoring stations of the Taichung Area on May 25, 2002. (a) five air-monitoring stations in the coastal area. (b) six air-monitoring stations from sea side to the east of basin. (c) six air-monitoring stations in the Taichung Basin.

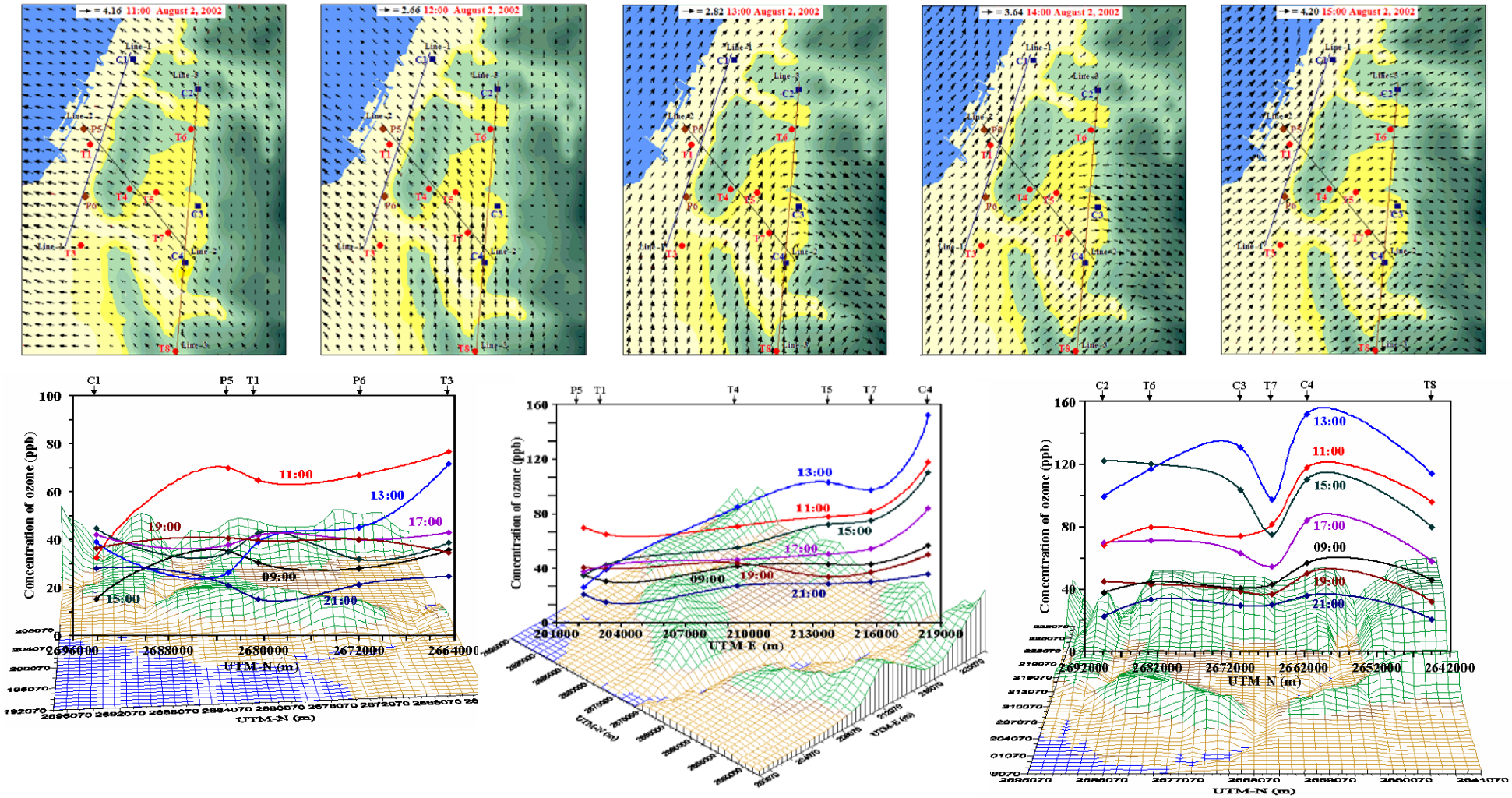

Fig. 8. Measurements of ozone and surface wind from air-monitoring stations of the Taichung Area on August 2, 2002. (a) five air-monitoring stations in the coastal area. (b) six air-monitoring stations from sea side to the east of basin. (c) six air-monitoring stations in the Taichung Basin.

(3) Numerical analysis

An unsteady state and one-dimensional atmospheric transport equation[10] for ozone in

$$\frac{\partial[O_3]}{\partial t}+\frac{\partial(u[O_3])}{\partial x}=R-L[O_3] \tag{2}$$

where u, R, and $L[O_3]$ are wind speed, ozone generation rate, and loss rate. The simplest method for the solution of Eq.(2) is base on the finite difference approach. Writing

$$\frac{[O_3]_i^{n+1}-[O_3]_i^n}{\Delta t}+\frac{u_i^n[O_3]_i^n-u_{i-1}^n[O_3]_{i-1}^n}{\Delta x_{i\leftrightarrow i-1}}=R^n-L^n[O_3]_i^n \tag{3}$$

The air quality monitoring stations of Line-2 are parallel with wind direction at 11:00~17:00 on October 7, 2001 (see Fig. 6), so the data of these stations are satisfy the conditions of Eq.(2). Summary of the data of the air quality monitoring stations of Line-2 are listed in Table 2. Plot the $[O_3]_i^n$ value against $\left(\frac{[O_3]_i^{n+1}-[O_3]_i^n}{\Delta t}+\frac{u_i^n[O_3]_i^n-u_{i-1}^n[O_3]_{i-1}^n}{\Delta x_{i\leftrightarrow i-1}}\right)$, the slope is $-L^n$ and the intercept R^n. The results are shown in Table 2.

Table 2 Observed ozone concentrations and surface wind speeds and calculated R and L values in T7, T4, T1, and P5 on October 7, 2001.

i	1 (T7)		2 (T4)		3 (T1)		4 (P5)		R	L
t_n	$[O_3]$ (μg/m^3)	u (m/hr)	$[O_3]$ (μg/m^3)	u (m/hr)	$[O_3]$ (μg/m^3)	u (m/hr)	$[O_3]$ (μg/m^3)	u (m/hr)	(μg/m^3-hr)	(1/hr)
11:00	154.6	4680	127.9	3600	62.1	6840	65.6	5760		
12:00	200.1	6480	152.5	4320	105.5	7200	107.8	6840	80.27	0.657
13:00	213.9	6120	172.5	6840	139.0	7920	140.5	7920	238.26	1.883
14:00	228.6	5760	180.0	8640	143.2	7200	145.5	6480	30.98	0.215
15:00	223.9	8280	166.8	9000	142.3	7200	152.5	6120	–213.05	–1.262
16:00	184.3	11160	149.2	12600	124.6	7920	116.3	7920	–128.87	–0.468
17:00	143.6	9360	141.7	11880	102.8	11160	86.9	7920	–201.03	–1.082

$\Delta x_{1\leftrightarrow 2}$=9296 m, $\Delta x_{2\leftrightarrow 3}$=9418 m, $\Delta x_{3\leftrightarrow 4}$=2757 m.

Fig. 9 shows the value of R and L change from positive to negative before 14:00. The maximum ozone concentration of each station is always at 14:00. The values of R and L are lower from 14:00~15:00 due to the photochemical smog formation[22]. And another lower R and L value before 16:00 may be due to ozone reaction with particles or moisture.

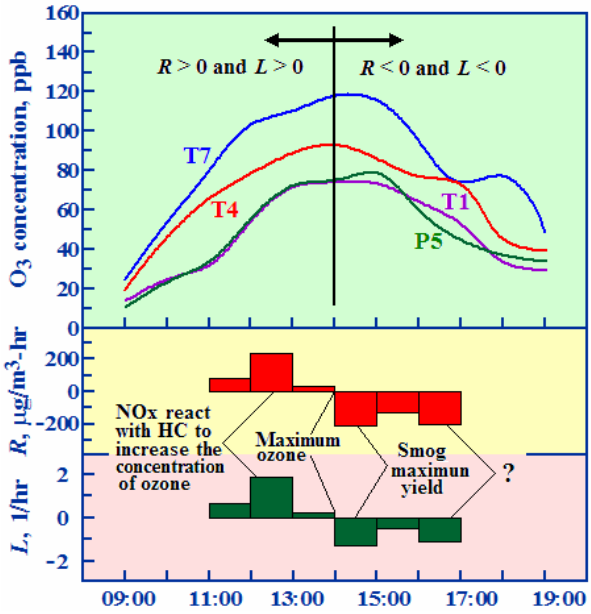

Figure 9 O_3 concentrations, R and L values of the Taichung Area on October 7, 2001.

5 Vertical sampling and analysis

This vertical sampling arrangement is set up by using a big balloon (2.2 m diameter) filled with hydrogen gas, one electro-motion capstan with rope and several automatic sampling apparatuses shown in Fig. 10. The automatic sampling apparatus combines a preset initiation timer, auto-pump and 10 L

Tedler sampling bag. When the balloon floats up high into the atmosphere it will drag several automatic sampling apparatuses, tied with rope, up to different altitudes. For the safety of the air-line, the highest sampling position is limited; six differential altitude positions are at ground, 100, 200, 300, 400 and 500 m. After vertical sampling, some air from the Tedler sampling bags were analyzed for NO, NO_2, and O_3 by monitors immediately, and the rest were concentrated by a Tenax-TA column in liquid nitrogen bath for HC analysis. While a GPS and a laser range-finder were used to determine the sampling height.

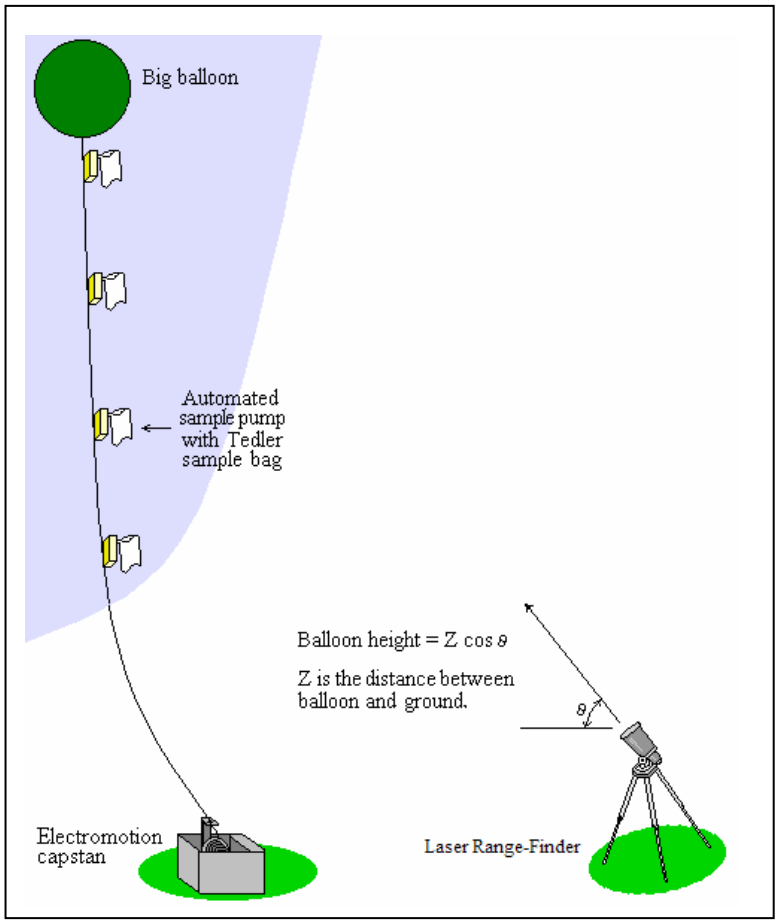

Fig. 10. Schematic of the sampling apparatus for air pollutant at different altitude.

(1) Primary concentration process for HC

It is necessary to concentrate samples for analysis because of the lower mass of HC in the atmosphere. This process follows U.S. EPA TO-10 and TO-14A methods. The concentration arrangement is shown in Fig. 11. Air samples from Tedler bag was concentrated by a Tenax-TA adsorption column in liquid nitrogen bath. The volume concentration is 15,000 times, so the detection limit of HC mass can be expected in ppb range

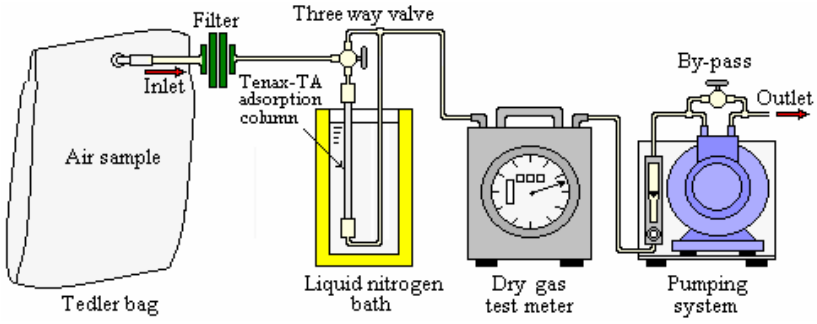

Fig. 11. Air sample being concentrated with Tenax-TA column in a liquid nitrogen bath for HC analysis.

(2) Analysis for O_3, NO_X and HC

The monitors for O_3 and NO_X are API Model-200A and DASIBI Model-1008-PC O_3 Analyzer. The following methods are NIEA A417.10T and NIEA A420.10T. After sampling, O_3, NO_X were analyzed from bag air by above instruments immediately, and then the other air gases were concentrated by Tenax-TA. The quality and quantity analysis of HC was conducted in the laboratory by Shimadzu QP-5050A GC–MS with heat-desorption equipment. The Tenax-TA adsorption column was kept in liquid nitrogen bath before analysis to prevent leaking. The first step of analysis is that Tenax-TA column desorption in heat-desorption equipment to 150℃ then sample accumulation and inlet to GC–MS to –20℃ by liquid carbon dioxide cooling. The analysis column is 0.25 mm Chrompack DB-1 60 m-length capillary column. The GC operation conditions are: (1) initial temp.: –20℃ (inlet liquid CO_2 controlled by GC-MS automatically); (2) 8℃/min temperature rate to 200℃; (3) carry gas flow rate: 3mL/min; (4) split rate:1/10. The MSD analysis conditions were:(1) range: 33-300 mass; (2) detector volts: 1.1 kV; (3) scan interval: 0.5 sec; (4) scan speed: 500.

(3) Wind field determination

Meteorological conditions especially in wind-speed and direction below 1000 m atmosphere are favorable for O_3 dispersion. Wind speed and direction at differential altitudes were determined by pilot balloon and digital theodolite (World Z105-8). To keep the floating rate, the mass of Pilot balloon is less than 100g. During floating, the degrees of balloon projection was measured every 20 seconds till the balloon disappeared. The data of wind speed and direction at differential altitudes was determined by single-theodolite functions (see Fig. 12).

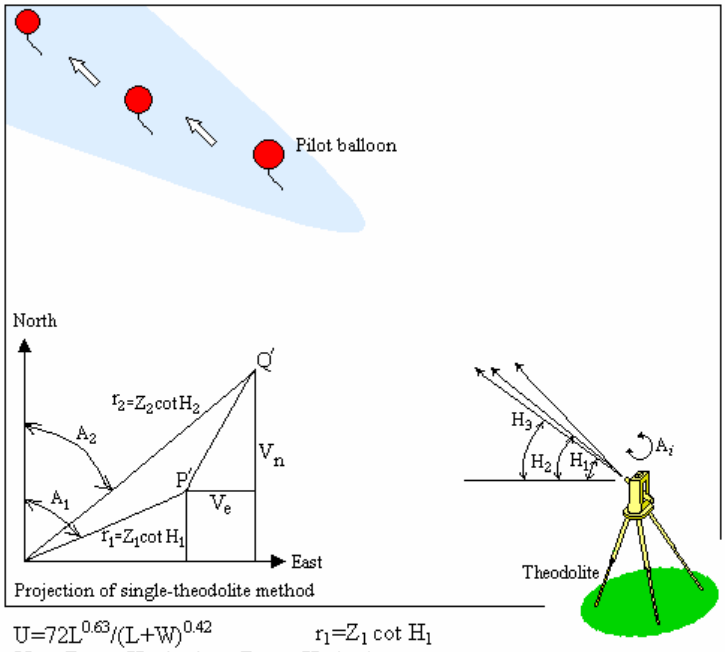

$U=72L^{0.63}/(L+W)^{0.42}$ $\quad r_1=Z_1\cot H_1$

$V_e=Z_2\cot H_2\sin A_2-Z_1\cot H_1\sin A_1$

$V_n=Z_2\cot H_2\cos A_2-Z_1\cot H_1\cos A_1$

$\phi=\tan^{-1}(V_e/V_n)$ $\quad P'Q'=V_e/\sin\phi$ $\quad V=P'Q'/t$

where U, W, L, and Z_1 are uprise speed, weight, buoyance, and height of balloon, r_1 is the projection on the ground of balloon at point P, V_e and V_n are the projection of wind speed on east and north, ϕ is the degree between V_e and V_n, $P'Q'$ is the projection of PQ on the ground, and V is mean wind speed.

Fig. 12. Schematic of the wind field measure apparatus at different altitude.

(4) Results of analysis

Four field measurements and chemical analyses had been conducted, two in the coastal area (June 27-28, 2002 and August 1-2, 2002) and another two in mountain area (July 1-2, 2002 and

September 14-15, 2002). Each field measurement run needs two days because four sampling positions in a run could not be conducted in a day, the distance between positions of at least 30 km and the sampling period must be during high ozone concentration time (11:00~14:00). A set of two sampling days must be sequential with similar weather conditions.

Fig. 13 shows the result of chromatograph by GC-MS. 73 hydrocarbons were identified, and their name and the number (in red) of each compound are showed in Fig. 12 and Table 3. And the real ambient concentration of each compound is from the result data divide by 15,000.

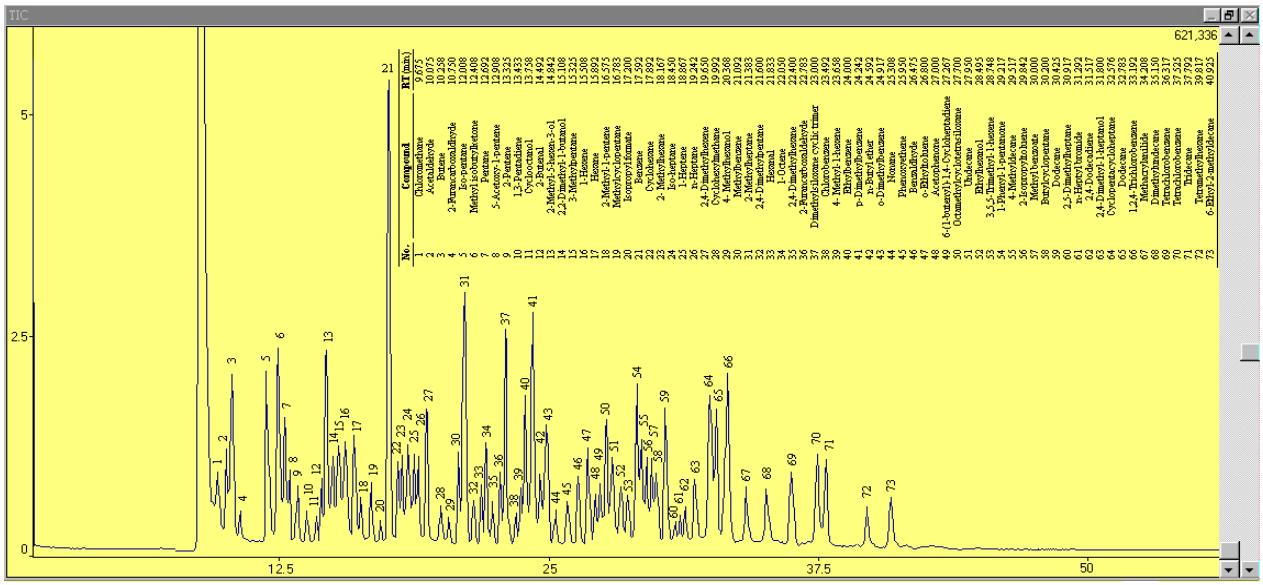

Fig. 13. Chromatogram of air pollutant (HCs) separation obtained after collecting HCs in a concentrator with Tenax-TA.

Table 3 Summary of the qualitative analysis

Paraffins:
- [5] Iso-pentane
- [7] Pentane
- [15] 3-Methyl pentane
- [17] Hexane
- [23] 2- Methyl hexane
- [24] Iso-heptane
- [26] n-Heptane
- [27] 2,4-Dimethyl hexene
- [31] 2-Methyl heptane
- [32] 2,4-Dimethyl pentane
- [35] 2,4-Dimethyl hexane
- [44] Nonane
- [51] Undecane
- [55] 4-Methyldecane
- [59] iso-Dodecane
- [60] 2,5-Dimethyl heptane
- [65] Dodecane
- [68] Dimethyl undecane
- [71] Tridecane
- [72] Tetramethyl hexane
- [73] 6-Ethyl-2-methyl decane

Multi-function group:
- [12] 2-Butenal
- [13] 2-Methyl-5-hexen-3-ol
- [20] Isopropyl formate
- [45] Phenoxy ethane
- [67] Methacryl anilide

Olefins:
- [3] Butene
- [8] 5-Acetoxy-1-pentene
- [9] 2-Pentene
- [10] 1,3-Pentadiene
- [16] 1-Hexene
- [18] 2-Methyl-1-pentene
- [25] 1-Heptene
- [34] 1-Octene
- [39] 4-Methyl-1-hexene
- [49] 6-(1-butenyl)-1,4-Cycloheptadiene
- [53] 3,5,5-Trimethyl-1-hexene
- [62] 2,4-Dodecadiene

Aromatics:
- [21] Benzene
- [30] Toluene
- [40] Ethyl benzene
- [41] p-Xylene
- [43] o- and m-Xylene
- [47] o-Ethyl toluene
- [56] Isopropyl toluene

Alcohols:
- [11] Cyclooctanol
- [14] 2,2-Dimethyl-1-butanol
- [29] 4- Methyl hexanol
- [52] Ethylhexanol
- [63] 2,4-Dimethyl-1-heptanol

Aldehydes and Ketone
- [2] Acetaldehyde
- [4] Furancarboxaldhyde
- [6] Methyl ethyl ketone
- [33] Hexanal
- [36] 2-Furancarboxaldehyde
- [46] Benzaldhyde
- [48] Acetophenone
- [54] 1-Phenyl-1-pentanone

Ether and Benzoztes:
- [42] n-Butyl ether
- [57] Methyl benzoate

Organic halides:
- [1] Chloromethane
- [38] Chlorobenzene
- [61] n-Heptyl bromide
- [66] 1,2,4-Trichloro benzene
- [69] Tetrachloro benzene
- [70] Tetrachloro benzene

Siloxanes:
- [37] Dimethyl siloxane cyclictrimer
- [50] Octamethyl cyclotetrasiloxane

Spectrum Gases for standard curve in quantities are following standard gas of U.S. EPA Method TO-14A Calibration Mix (RESTEK, cat.#34400) and Method TO-15 Ozone Precursor Mixtures (RESTEK, cat.#34420). Standard curve was developed by the same process of real ambient samples. The analysis results are an average of testing three times using the standard gases concentrated into three Tenax TA columns, and then analyses by GC-MS under the same conditions. The relative response factor, RRF of each compound was estimated based on the RRF of toluene (Figure 13) and the real ambient concentration of each compound is from the result data divide by 15,000.

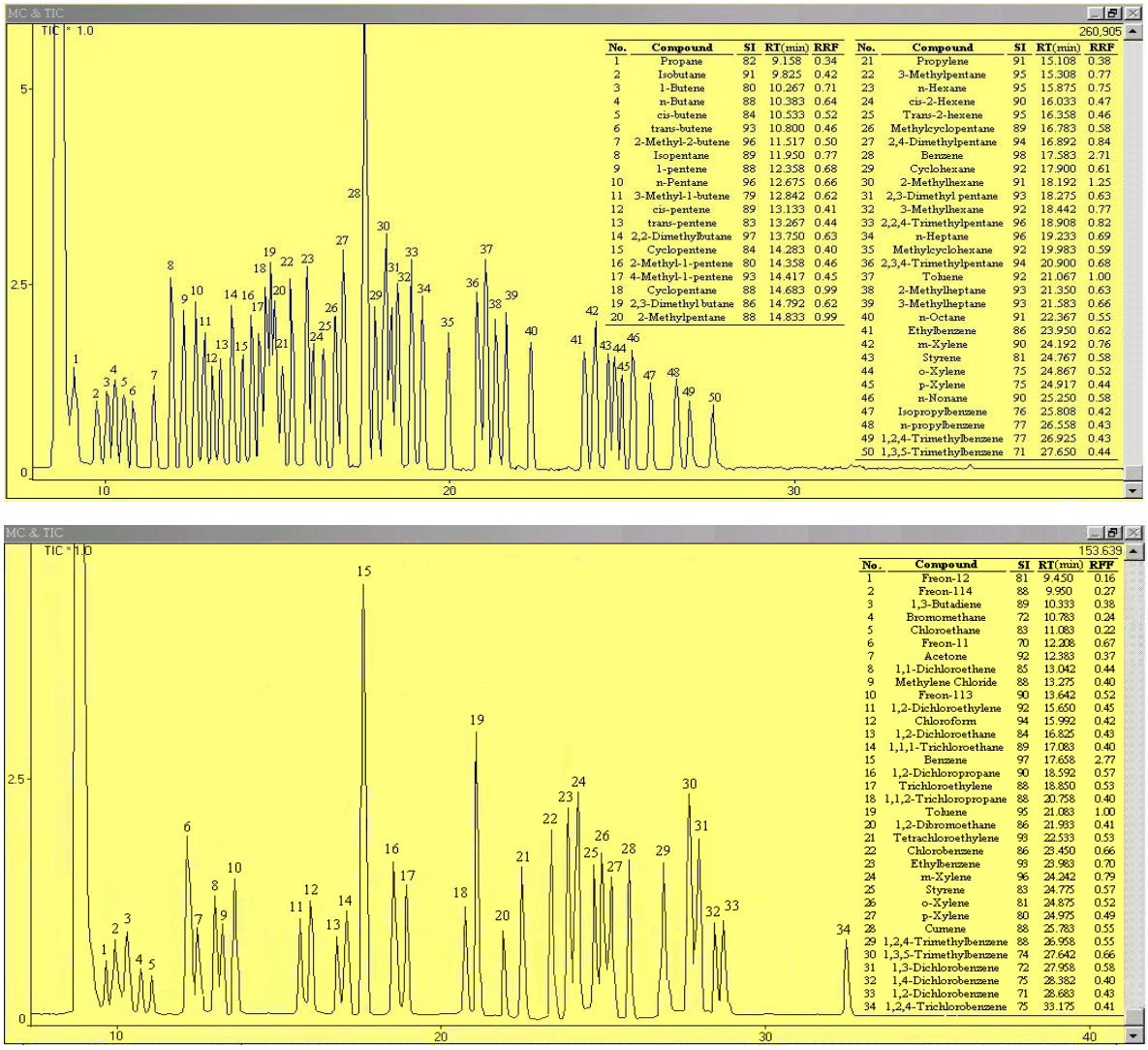

Fig. 14. Chromatogram and RRF of the standard gases separation obtained after collecting HCs in a concentrator with Tenax-TA . (a) TO-15 Ozone Precursor Mixtures (RESTEK, cat.#34420) and (b) TO-14A Calibration Mixtures (RESTEK, cat.#34400).

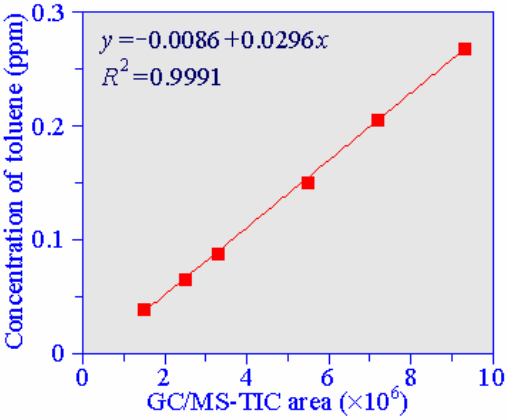

Fig. 15. Toluene standard curve.

Fig. 16-19 show that the results of HC analysis based on RRF of Fig. 14 and toluene standard curve in Fig. 15. The results reveal that: (1) alkanes and cyclo-alkanes are the richest VOC compounds in the lower atmosphere; (2) alkenes are the second, followed by organic halides, alcohols, and aromatics; (3) there is some benzene, ethyl benzene, toluene and xylene, BETX obvious; (4) other VOC compounds are fewer in ambient air; (5)

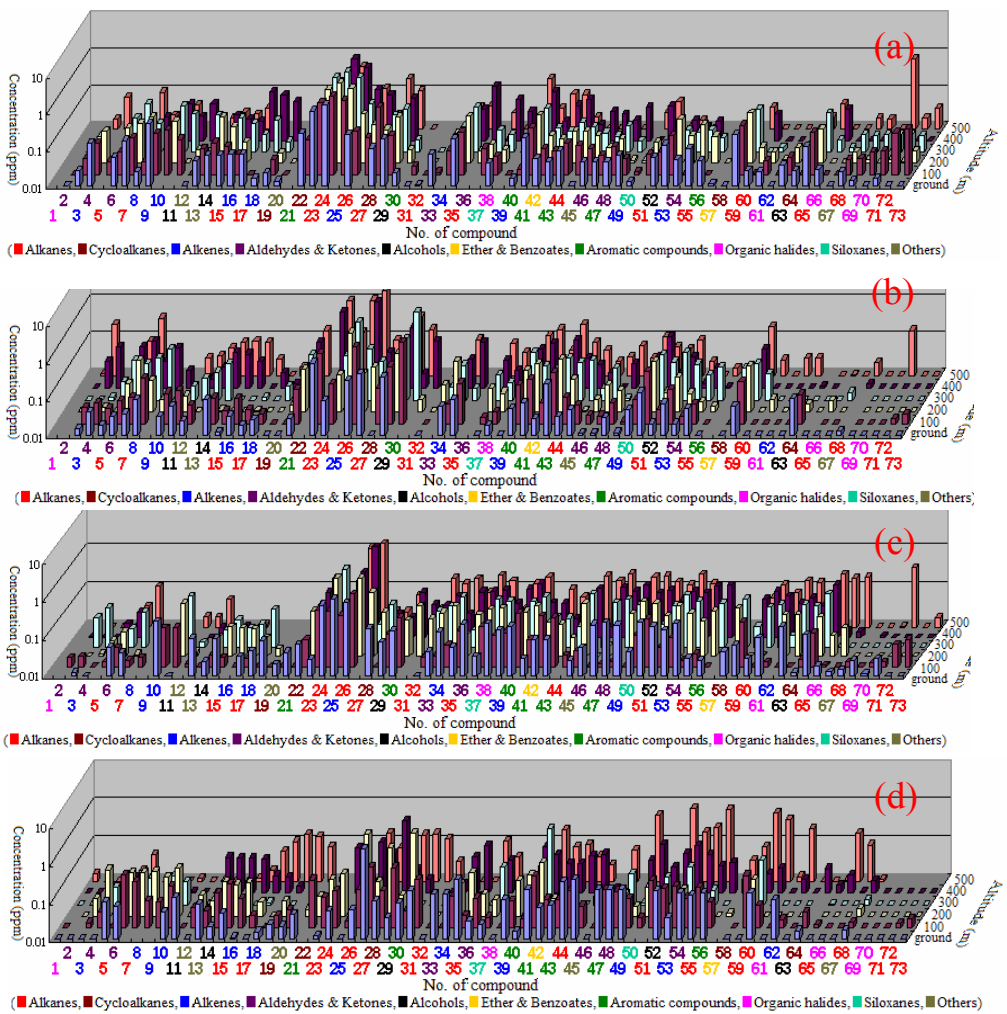

Fig. 16. Plot of concentration and compound distribution at different altitude at (a) S1, (b) S2, (c) S3, and (d) S4, in the coastal area on June 27 and 28, 2002.

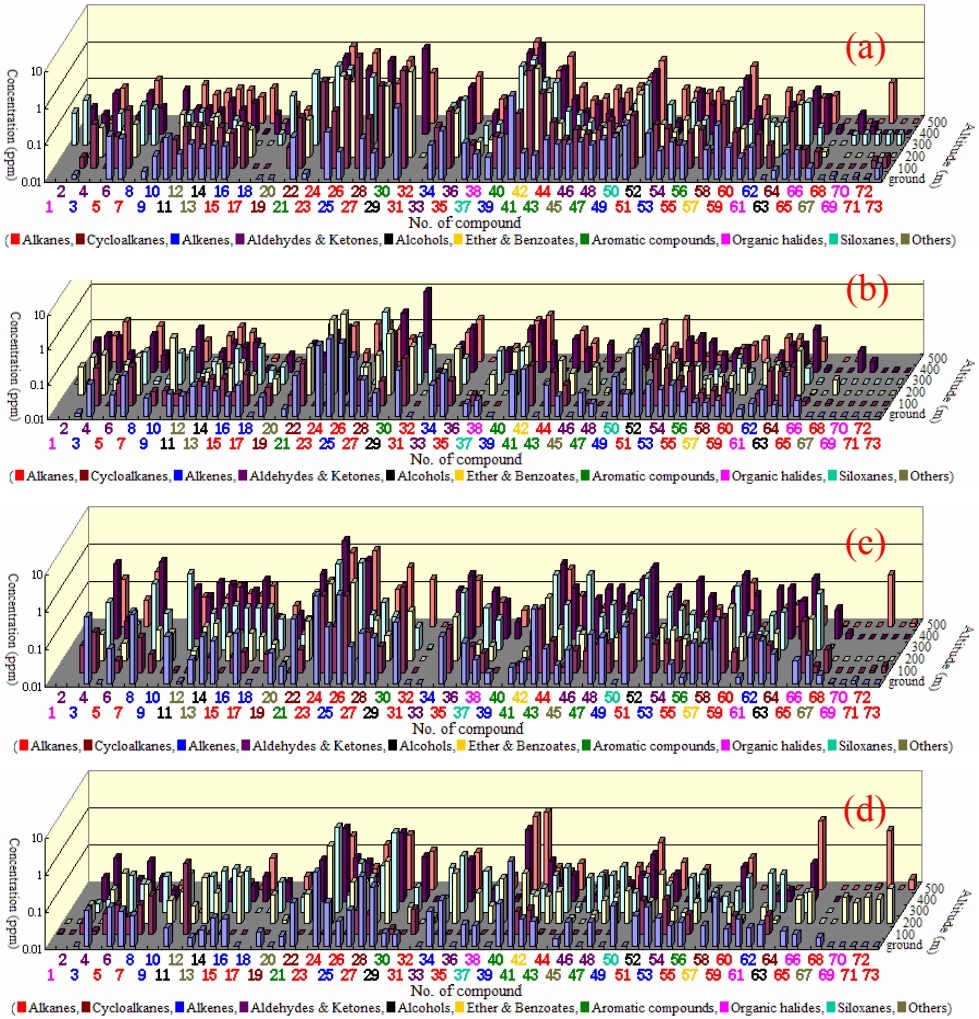

Fig. 17. Plot of concentration and compound distribution in the different altitude at (a) L1, (b) L2, (c) L3, and (d) L4, in Taichung Basin on July 1 and 2, 2002.

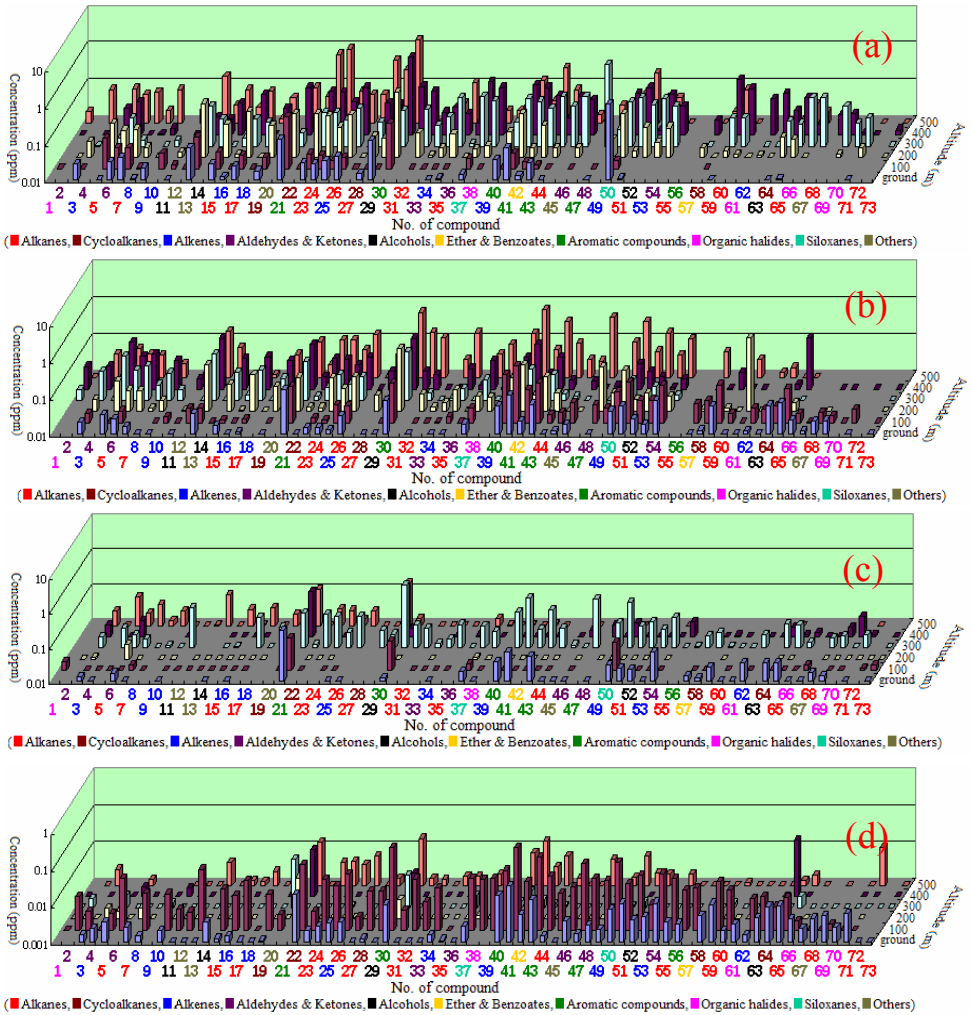

Fig. 18. Plot of concentration and compound distribution in the different altitude at (a) S1, (b) S2, (c) S3, and (d) S4, in the coastal area on August 1 and 2, 2002.

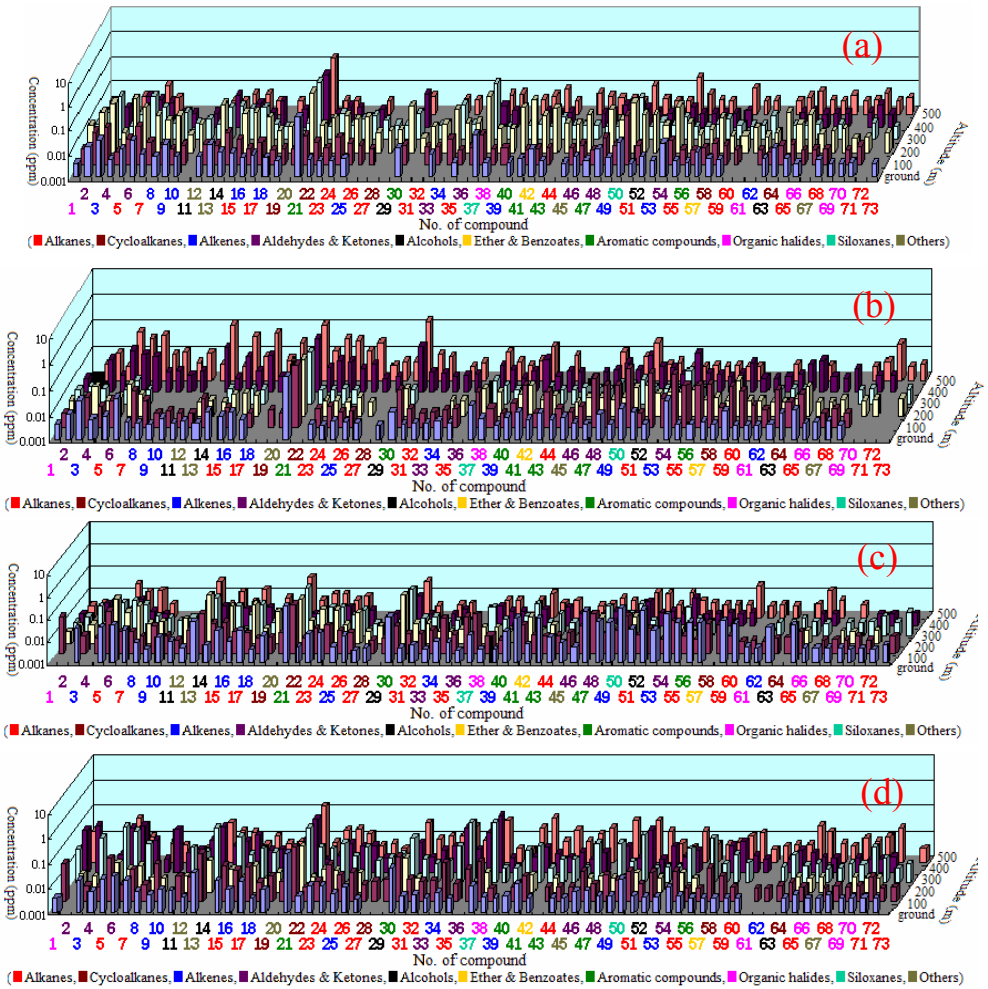

Fig. 19. Plot of concentration and compound distribution in the different altitude at (a) L1, (b) L2, (c) L3, and (d) L4, in Taichung Basin on September 14 and 15, 2002.

Fig. 20, 23, 26, and 29 show that the results of O_3, NO, NO_2, and HC in the field measurement. The ozone concentration distributions and surface wind field on same time of the sampling days are plotted in Fig 21, 22, 24, 25, 27, 28, 30, and 31. There are two types of ozone event day: (1) the wind blew out of the basin, and ozone concentration decreased with wind direction (Fig. 24, July 1, 2002) and (2) the wind blew into the basin, and ozone concentration increased with wind direction (Fig. 28, August 2, 2002).

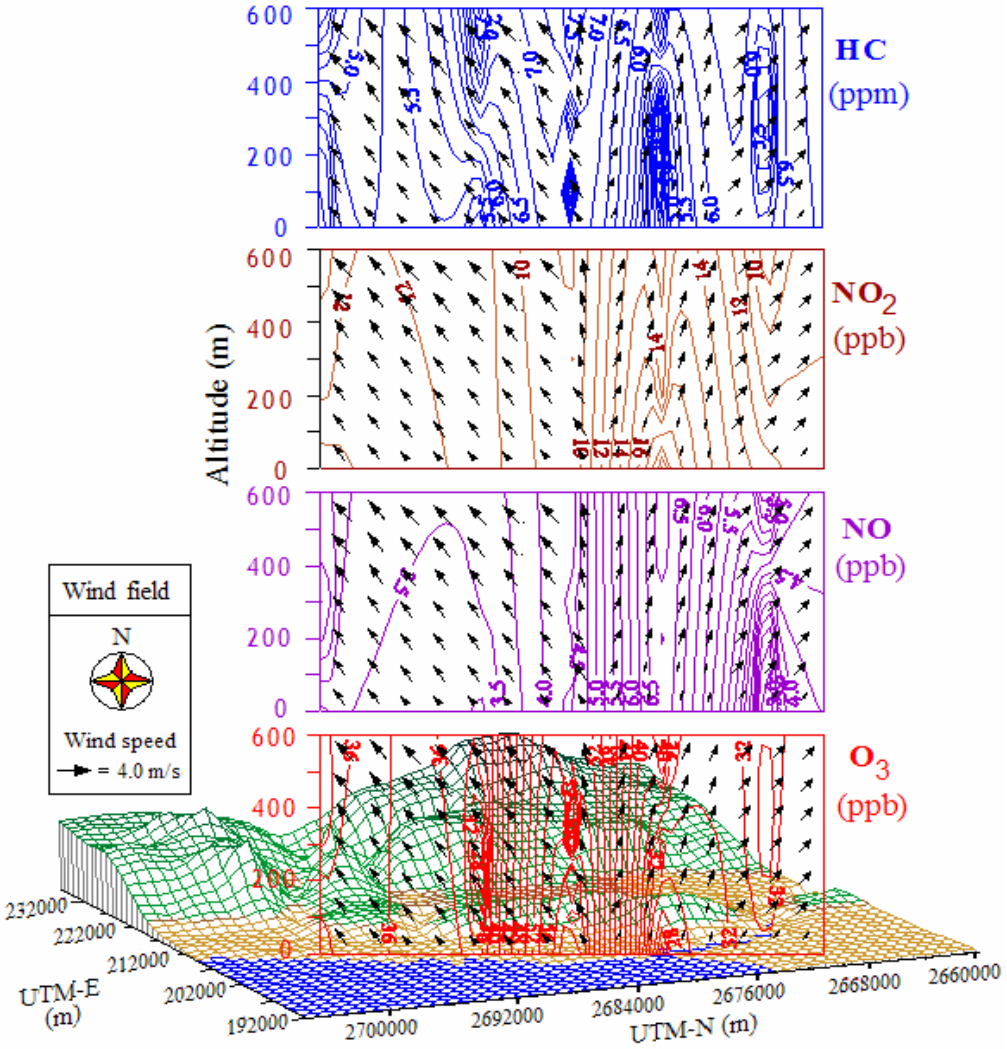

Fig. 20. Concentration distribution of O_3, NO, NO_2 and HC and wind field, in the coastal area on June 27 and 28, 2002.

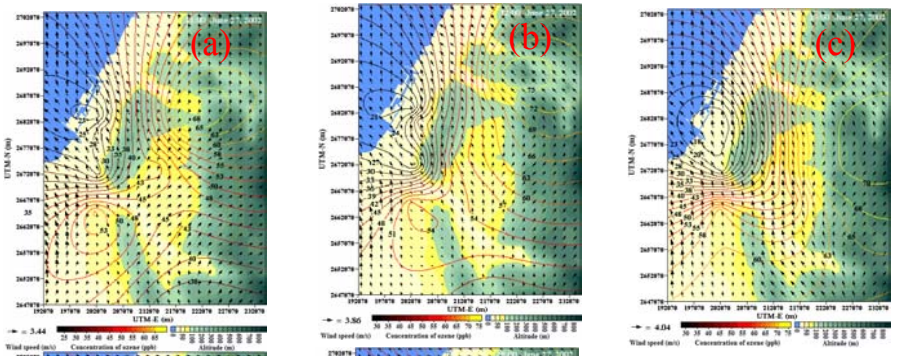

Fig. 21.
Ozone concentration distributions and wind field on June 27, 2002 at (a) 11: 00, (b) 12: 00, (c) 13: 00, (d) 14: 00, (e) 15: 00.

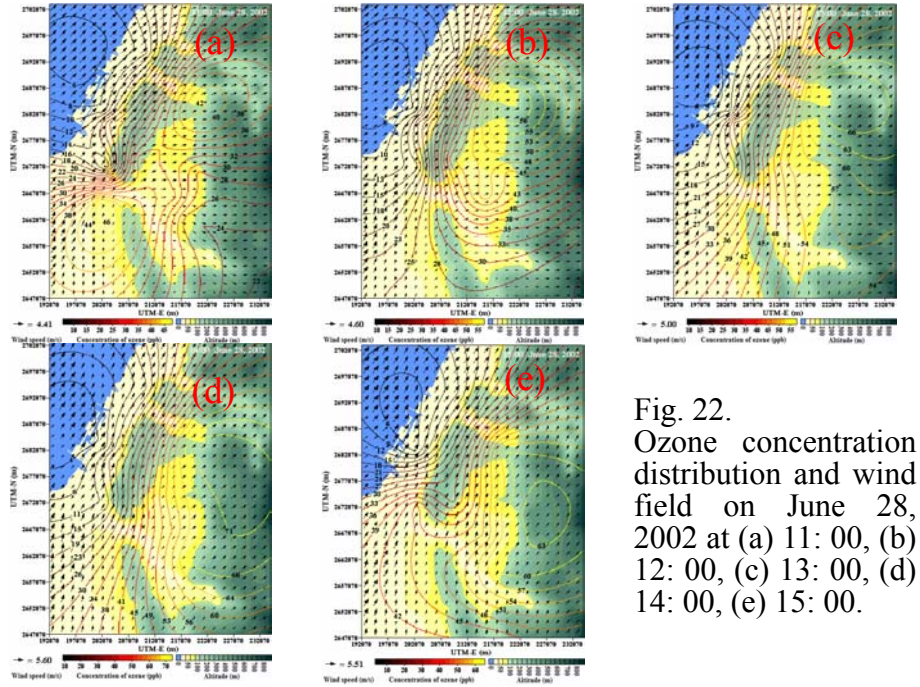

Fig. 22.
Ozone concentration distribution and wind field on June 28, 2002 at (a) 11: 00, (b) 12: 00, (c) 13: 00, (d) 14: 00, (e) 15: 00.

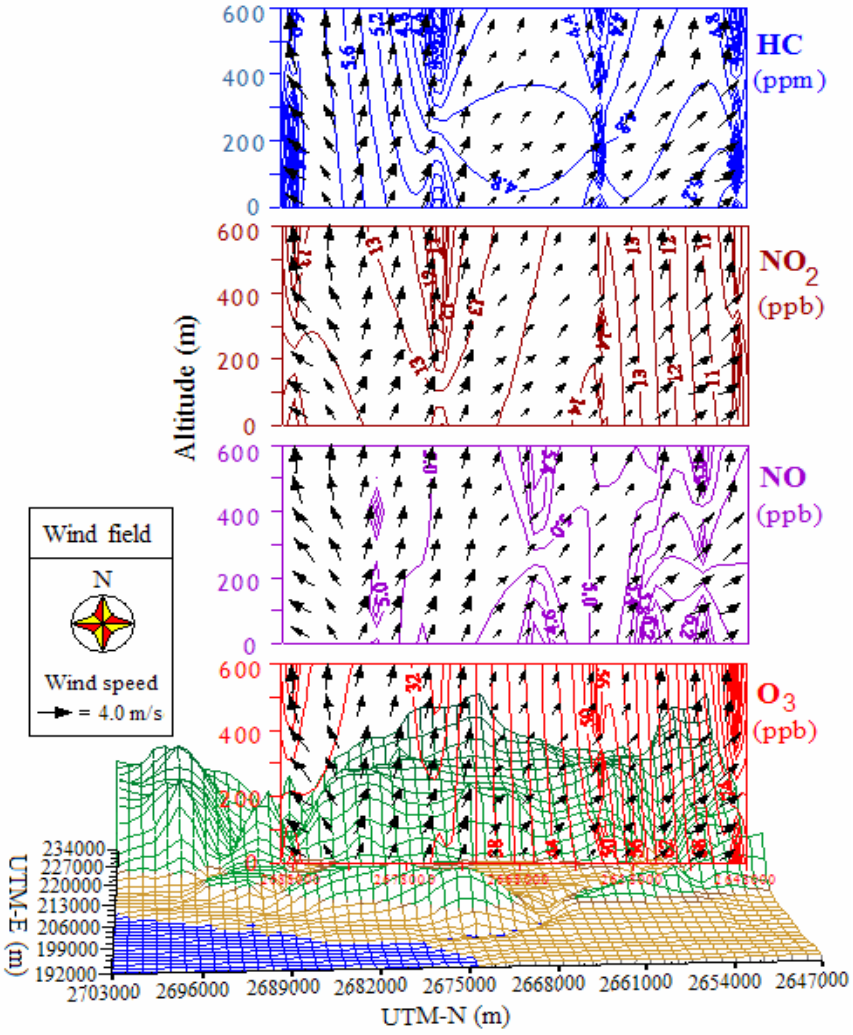

Fig. 23. Concentration distribution of O_3, NO, NO_2 and HC and wind field, in the Taichung Basin at July 1 and 2, 2002.

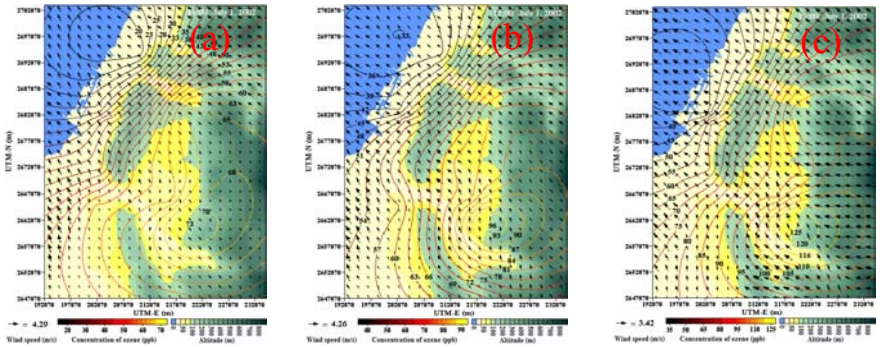

Fig. 24.
Ozone concentration distribution and wind field on July 1, 2002 at (a) 11: 00, (b) 12: 00, (c) 13: 00, (d) 14: 00, (e)

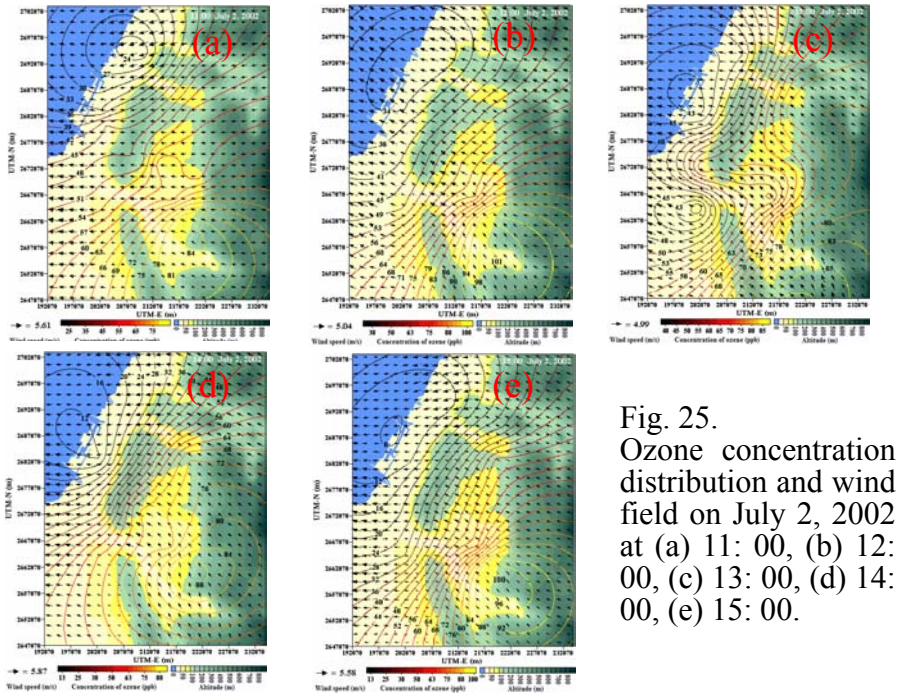

Fig. 25.
Ozone concentration distribution and wind field on July 2, 2002 at (a) 11: 00, (b) 12: 00, (c) 13: 00, (d) 14: 00, (e) 15: 00.

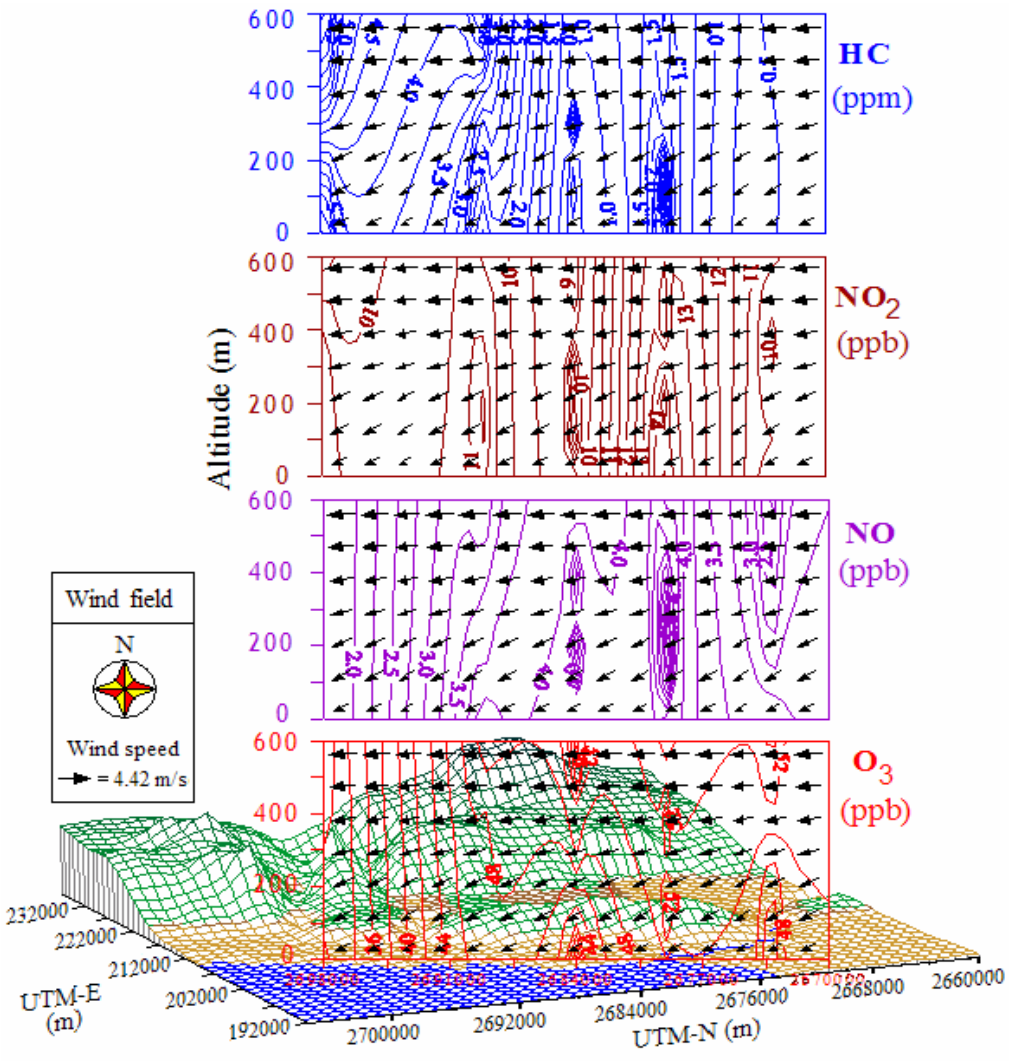

Fig. 26. Concentration distribution of O_3, NO, NO_2 and HC and wind field, in the coastal area on August 1 and 2, 2002.

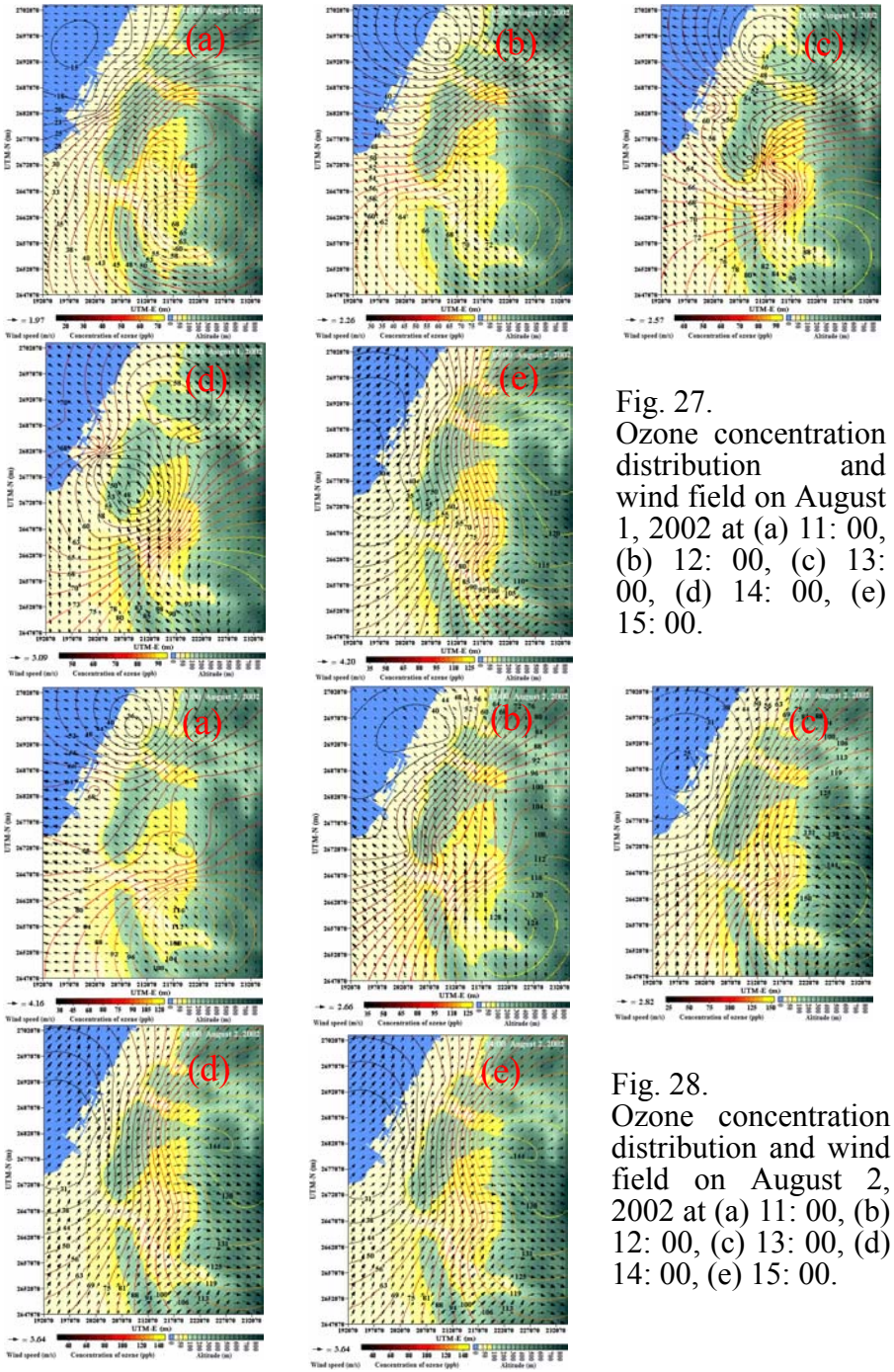

Fig. 27. Ozone concentration distribution and wind field on August 1, 2002 at (a) 11: 00, (b) 12: 00, (c) 13: 00, (d) 14: 00, (e) 15: 00.

Fig. 28. Ozone concentration distribution and wind field on August 2, 2002 at (a) 11: 00, (b) 12: 00, (c) 13: 00, (d) 14: 00, (e) 15: 00.

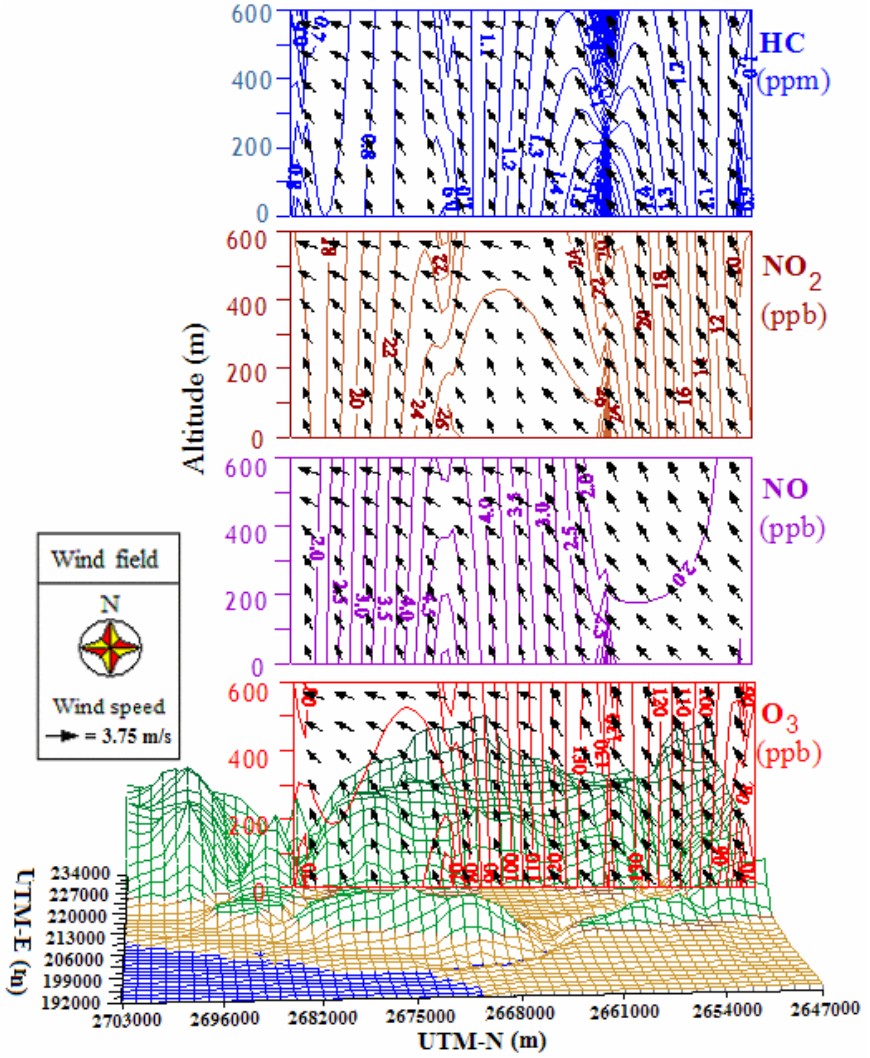

Fig. 29. Concentration distribution of O_3, NO, NO_2 and HC and wind field, in the Taichung Basin on September 14 and 15, 2002.

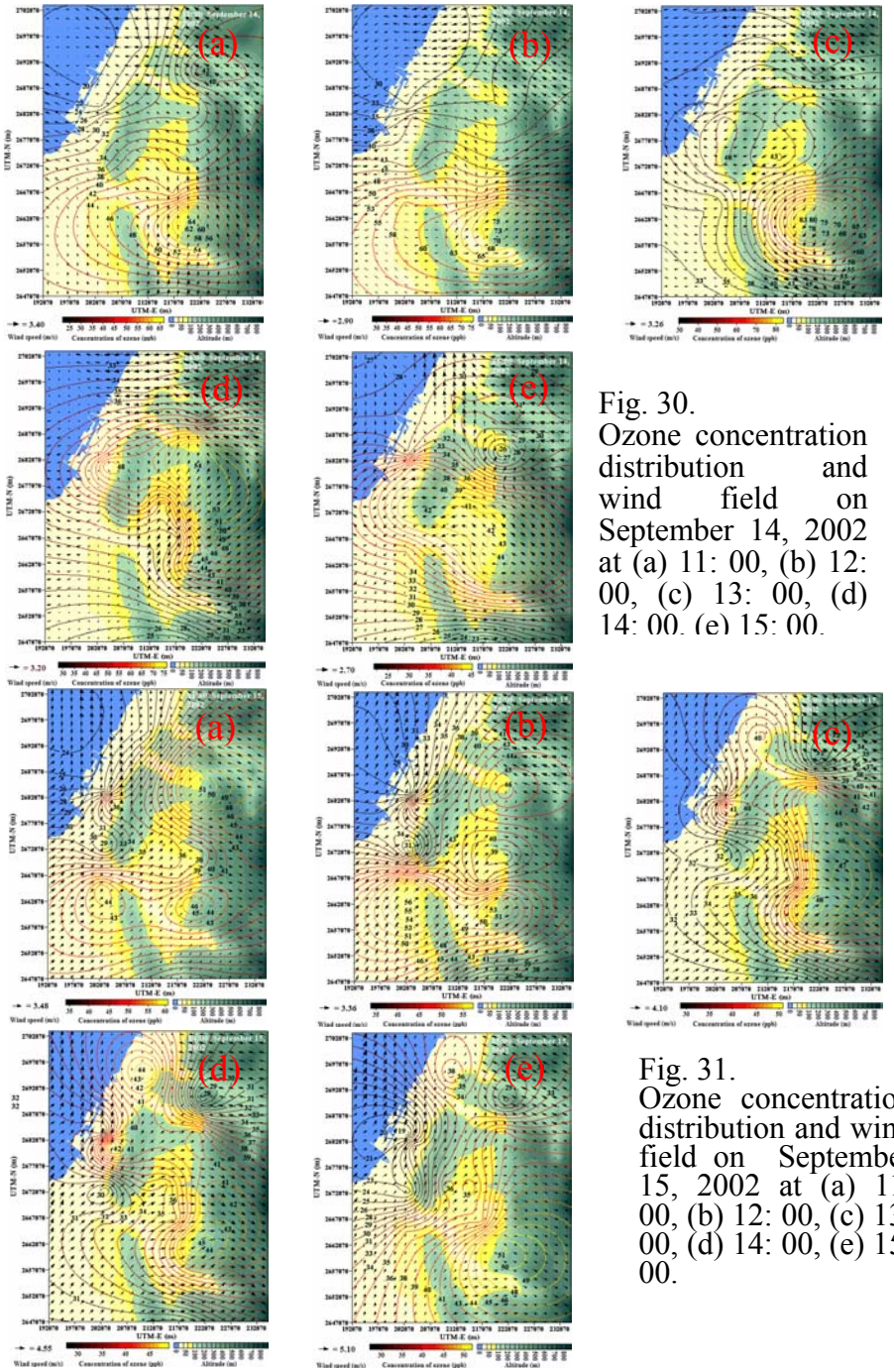

Fig. 30. Ozone concentration distribution and wind field on September 14, 2002 at (a) 11: 00, (b) 12: 00, (c) 13: 00, (d) 14: 00, (e) 15: 00.

Fig. 31. Ozone concentration distribution and wind field on September 15, 2002 at (a) 11: 00, (b) 12: 00, (c) 13: 00, (d) 14: 00, (e) 15: 00.

Fig. 23 and 24 indicate that July 1 was an ozone event day. In summary: (1) ozone forms quickly on the southeast basin, and kept high concentration for 2~3 hours; (2) high ozone concentration is due to the transformation by southeast wind; (3) a decreasing gradient of ozone concentration from mountain to sea exists, and the decreasing direction is different from surface wind direction.

August 2 was an anther ozone event day (see Fig. 26 and 28). The day the air quality are: (1) the high ozone concentration starts from 11:00; (2) the ozone concentration in the coastal is low; (3) the high ozone concentration in the east of the basin is due to the basin effect which causes changes the surface wind; and (4) in the evening, the descend rate of ozone in the coastal area is lower because ozone blows into the coastal area; (5) the decreasing direction of the ozone concentration is also different from surface wind direction.

There is no altitude gradient of the pollutant concentration in most position can be seen from Fig 20, 23, 26, and 29, but exist horizontal gradient obviously. The concentrations of HC increases with altitude exist in L3 (in the basin, see Fig. 3) and S3 (in the coastal area, see Fig. 3) from the two field measurements. The reason of L3 HC various is due to the basin effect caused by topographer and surface wind field. And the reason for S3 is the HC emission from big oil tank in Taichang Port and Taichang Power Plant. So the basin effect[11], a geological barrier tend to have stagnating air conditions, and industrial are the important contributions for altitude gradient of the pollutant concentration.

(5) Box-whisker plots of the data

In order to compare the air quality of coastal area to basin area, Fig. 32 and 33 field measurements of the variability of air pollution at different altitudes were plotted. The results reveal: (1) the average of ozone concentration in the basin is always higher than the coastal area; (2) the variability of ozone concentration in basin is more obvious than coastal area (Fig. 32 (a) and 32 (a)); (3) the variability of NO and NO_2 concentrations in basin is similar to the variability of ozone (Figure 31(b), (c) and 32(b),(c)); (4) the average of NO and NO_2 concentrations are also higher in the basin; (5) the concentration of HC increases with altitude in the coastal area (Fig. 33 (d)), but the phenomenon in basin is not the same; (6) the average of HC concentrations at all altitudes in basin are lower than the coastal area except one at the ground; (7) the concentration of ozone increases with altitude in the basin area.

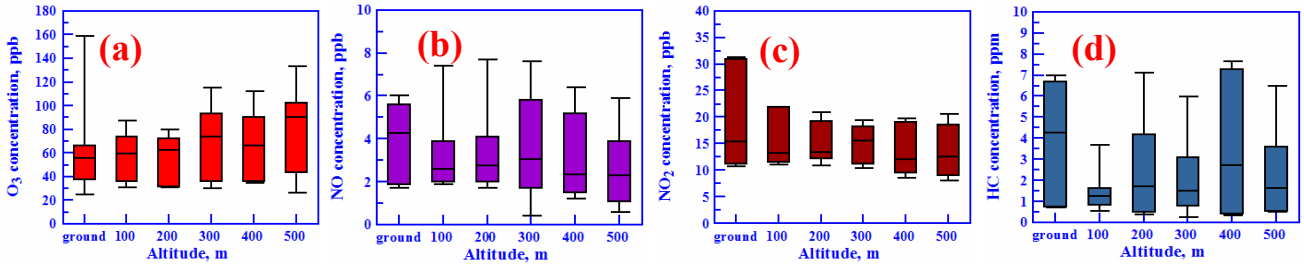

Fig. 32. Box-whisker plots of the data analysis in the basin. (a) O_3, (b) NO, (c) NO_2, (d) HC.

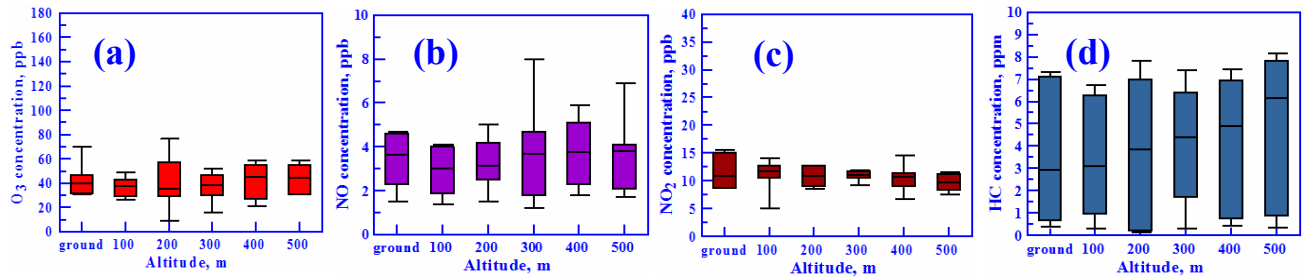

Fig. 33 Box-whisker plots of the data analysis in the coastal area. (a) O_3, (b) NO, (c) NO_2, (d) HC.

Fig. 34 and 35 based on field measurements of the variability of HC concentration at different altitudes. It helps to compare the differences of the two areas. To compare the variability of organic compounds at different altitudes of the coastal area to the basin area, the results reveal: (1) the average of paraffins and olefins concentration in the coastal area are always increasing with altitude (Fig. 35 (a), (b)), but it is quite different in the basin (Fig. 34 (a), (b)); (2) the concentrations of organic halides at all altitudes are relatively low in both areas (Fig. 34 (c) and 35(c); (3) the variability of organic halides at 300m in the coastal area is little obvious; (4) the concentration of aromatics are relatively low and stable in basin area(Fig. 34(d)); (5) the concentration of aromatics are relatively low but various with altitudes in coastal area(Fig. 35 (d)); (6) the concentration of organic oxides are all low than 250 ppb in both areas (Fig. 34 (e) and 35 (e)), but variations at 300 m is obvious; (7) the concentration of other organics are all low than 200 ppb in both areas, and it is little higher in the basin area.

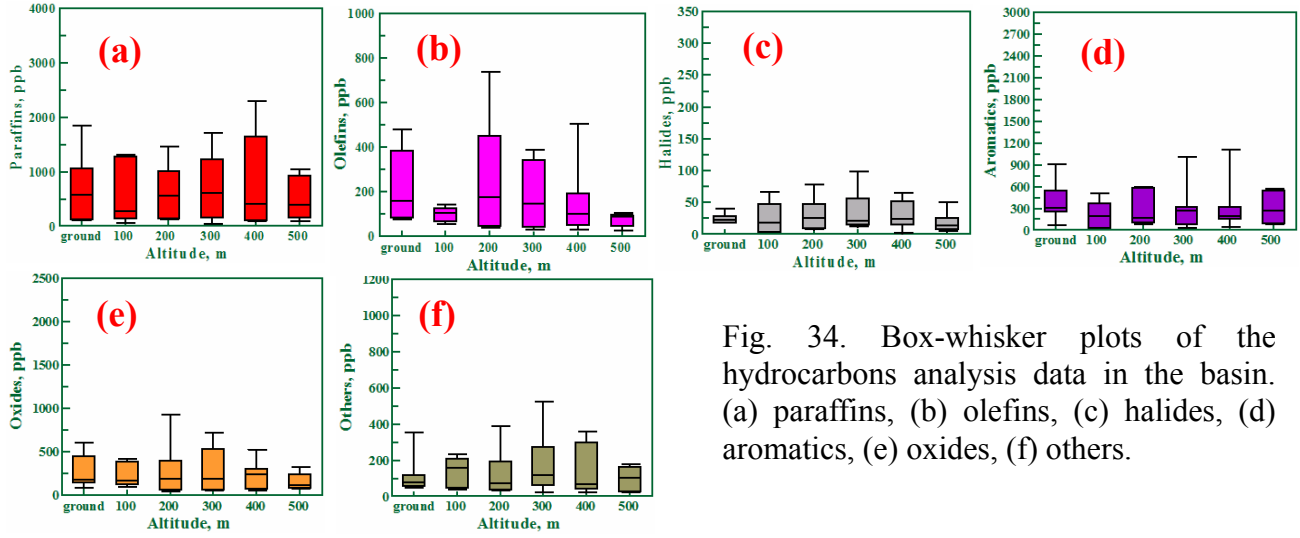

Fig. 34. Box-whisker plots of the hydrocarbons analysis data in the basin. (a) paraffins, (b) olefins, (c) halides, (d) aromatics, (e) oxides, (f) others.

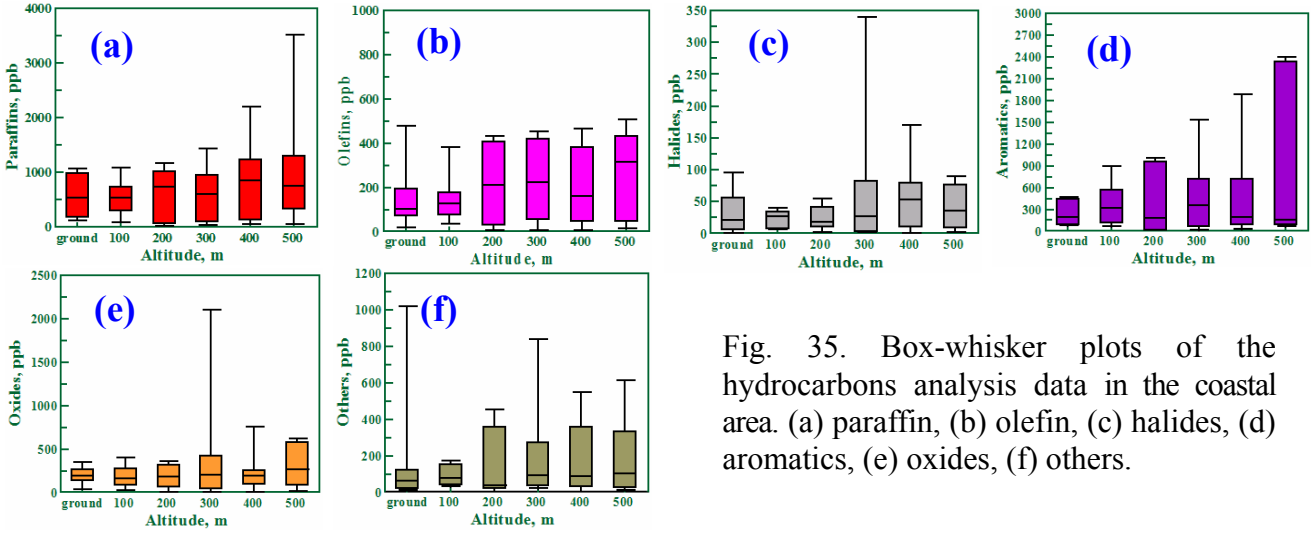

Fig. 35. Box-whisker plots of the hydrocarbons analysis data in the coastal area. (a) paraffin, (b) olefin, (c) halides, (d) aromatics, (e) oxides, (f) others.

In summary: (1) the average of O_3, NO, and NO_2 concentration in the basin is always higher than coastal area, and the variability with altitudes are obvious; (2) the concentration of HC increases with altitude in the coastal area, but the phenomenon in basin is different, and the of HC concentrations at all altitudes in the coastal area are higher except at the ground; (3) the average of paraffin and olefins concentration in the coastal area are always minimally increasing with altitude, but it is different in the basin; (4) the concentration of organic halides, aromatics, organic oxides and others organics are all low in both areas, and variability is obvious in the coastal area.

(6) Case study

Consider a steady state and one dimensional atmospheric transport equation for ozone, the equation (2) be changed to

$$\frac{u_i[\mathrm{O_3}]_i - u_{i-1}[\mathrm{O_3}]_{i-1}}{\Delta x_{i\leftrightarrow i-1}} = R - L[O_3]_i \qquad (4)$$

There are two types of ozone transformation (see Fig. 21-31): (1) when the wind blew into the basin, and ozone concentration increased with wind direction; (2) when the wind blew out of the basin, and ozone concentration decreased with wind direction. Using the data of wind field and ozone concentration on Jun 28 and July 1 at 12:00-14:00 to set up 4 lines parallel with wind direction (be seen in Fig. 36 (a)-(d)). Plotting $\left(\frac{u_i[\mathrm{O_3}]_i - u_{i-1}[\mathrm{O_3}]_{i-1}}{\Delta x_{i\leftrightarrow i-1}}\right)$ against $[\mathrm{O_3}]_i$ the slop of such a plot is $-L$ and the intercept R. The data and results all be listed in Table 4. Table 4 reveals that: (1) when the wind blew out of basin, the values of R and L change from positive (12:00) to negative (14:00). The result just the same to Table 2, which is ozone concentration decreased with wind direction after 14:00; (2) when the wind blew into the basin, the value of R and L are negative values at 12:00, but at 14:00 R changed to more large value (because of ozone descend) and L to positive value ($-L[\mathrm{O_3}]$ changed to descend item). (3) In summary the ozone concentration does not dependent on just wind direction, topography and surrounding conditions are more important.

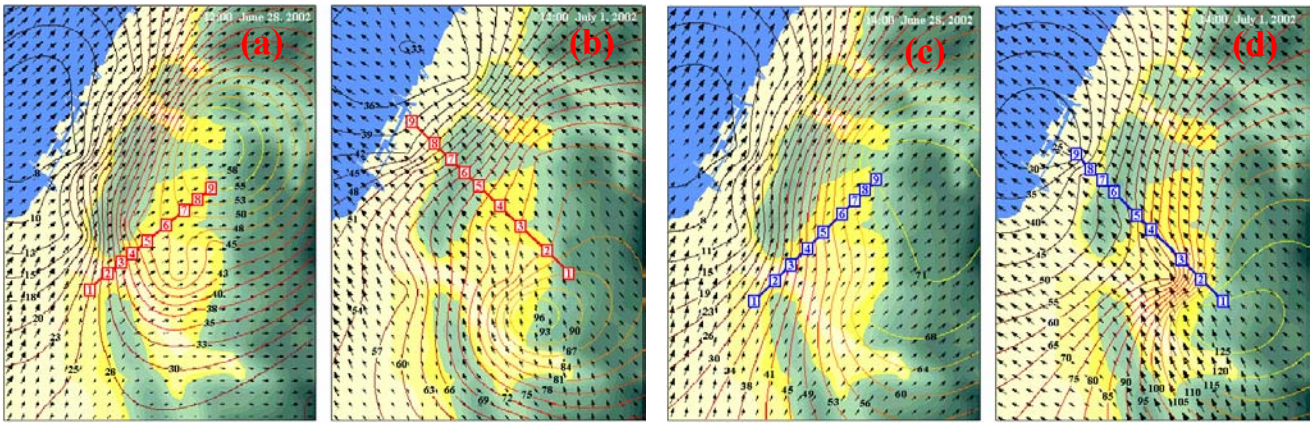

Fig. 36. Wind trajectory and ozone contour in the Taichung area. (a) 12:00, June 28, 2002, (b) 12:00, July 1, 2002, (c) 14:00, June 28, 2002, (d) 14:00, July 1, 2002.

Table 4 The data of two lines of Fig. 36 to calculate R and L values

Point-1		Point-2		Point-3		Point-4		Point-5		Point-6		Point-7		Point-8		Point-9		**R**	L
$[O_3]$	u	$[O_3]$	u	$[O_3]$	u	$[O_3]$	u	$[O_3]$	u	$[O_3]$	u	$[O_3]$	u	$[O_3]$	u	$[O_3]$	u		
Surface wind blew into the basin at 12:00, June 28, 2002																			
48	6120	58	6840	67	9180	77	9360	86	9180	91	8820	92	7200	101	8280	106	8280	**109.622**	**0.913**
$\Delta x_{1\leftrightarrow2}$=3284 m, $\Delta x_{2\leftrightarrow3}$=2512 m, $\Delta x_{3\leftrightarrow4}$=1932 m. $\Delta x_{4\leftrightarrow5}$=2512 m, $\Delta x_{5\leftrightarrow6}$=3478 m, $\Delta x_{6\leftrightarrow7}$=3284 m. $\Delta x_{7\leftrightarrow8}$=2125 m, $\Delta x_{8\leftrightarrow9}$=2318 m																			
Surface wind blew out of the basin at 12:00, July 1, 2002																			
167	7380	156	8280	150	10080	144	11520	132	12960	121	13140	109	12960	92	12240	75	11520	**–202.561**	**–1.621**
$\Delta x_{1\leftrightarrow2}$=4250 m, $\Delta x_{2\leftrightarrow3}$=3090 m, $\Delta x_{3\leftrightarrow4}$=2473 m. $\Delta x_{4\leftrightarrow5}$=2705 m, $\Delta x_{5\leftrightarrow6}$=3864 m, $\Delta x_{6\leftrightarrow7}$=3980 m. $\Delta x_{7\leftrightarrow8}$=4753 m, $\Delta x_{8\leftrightarrow9}$=4250 m																			
Surface wind blew into the basin at 14:00, June 28, 2002																			
58	6900	65	6650	73	6480	86	7410	102	7410	115	7880	123	7880	131	9500	136	9970	**–52.083**	**–0.968**
$\Delta x_{1\leftrightarrow2}$=3719 m, $\Delta x_{2\leftrightarrow3}$=2819 m, $\Delta x_{3\leftrightarrow4}$=3054 m. $\Delta x_{4\leftrightarrow5}$=2936 m, $\Delta x_{5\leftrightarrow6}$=3602 m, $\Delta x_{6\leftrightarrow7}$=2036 m. $\Delta x_{7\leftrightarrow8}$=1957 m, $\Delta x_{8\leftrightarrow9}$=1957 m																			
Surface wind blew out of the basin at 14:00, July 1, 2002																			
240	15120	211	14760	163	14500	144	14400	125	14050	106	13680	96	13500	86	12960	58	12600	**–76.411**	**0.244**
$\Delta x_{1\leftrightarrow2}$=4064 m, $\Delta x_{2\leftrightarrow3}$=3861 m, $\Delta x_{3\leftrightarrow4}$=5690 m. $\Delta x_{4\leftrightarrow5}$=2845 m, $\Delta x_{5\leftrightarrow6}$=4268 m, $\Delta x_{6\leftrightarrow7}$=2439 m. $\Delta x_{7\leftrightarrow8}$=2032 m, $\Delta x_{8\leftrightarrow9}$=2642 m																			

The unit of $[O_3]$, u, R, and L are μg/m^3, m/hr, μg/m^3-hr, and 1/hr.

6 A statistical model

A purely statistical model, multiple regression equation, was developed. This equation depends on *m* number of $x_1, x_2, x_3 \ldots x_m$ as follows:

$$y = a_o + a_1 x_1 + a_2 x_2 + \cdots + a_m x_m \tag{5}$$

If given *n* sets of data, then Eq.(5) trans to: If given *n* sets of data, then Eq.(5) trans to:

$$y_i = a_o + a_1 x_{1i} + a_2 x_{2i} + \cdots + a_m x_{mi} \tag{6}$$

It written in the matrix form, Eq.(6) is

$$\mathbf{Y} = \mathbf{X}\vec{\alpha} \tag{7}$$

where $\mathbf{Y} = \begin{bmatrix} y_1 \\ y_2 \\ y_3 \\ \vdots \\ y_n \end{bmatrix}$, $\mathbf{X} = \begin{bmatrix} 1 & x_{11} & x_{21} & \cdots & x_{m1} \\ 1 & x_{12} & x_{22} & \cdots & x_{m2} \\ 1 & x_{13} & x_{23} & \cdots & x_{m3} \\ \vdots & \vdots & \vdots & & \\ 1 & x_{1n} & x_{2n} & \cdots & x_{mn} \end{bmatrix}$, $\vec{\alpha} = \begin{bmatrix} \alpha_o \\ \alpha_1 \\ \alpha_2 \\ \vdots \\ \alpha_m \end{bmatrix}$ therefore

$$\vec{\alpha} = (\mathbf{X}^\mathbf{T}\mathbf{X})^{-1}(\mathbf{X}^\mathbf{T}\mathbf{Y}) \tag{8}$$

And find *m*+1 coefficients, α_o, α_1, α_2, $\alpha_3 \ldots \alpha_m$, by using Eq.(7). Finally, an equation (Eq.(9)) was developed, this equation depends on radiation, humidity, concentration of NO, NO_2, paraffin, olefins, aromatics, organics organic halides, and others.

$$\begin{aligned}[O_3] = {} & 77.6 + 17.994[\text{Radiation}] - 6.408[\text{Humidity}] - 2.703[NO] + 1.752[NO_2] \\ & - 4.22\times10^{-3}[\text{Paraffins}] - 1.01\times10^{-2}[\text{Olefins}] - 9.45\times10^{-3}[\text{Aromatics}] \\ & - 8.147\times10^{-3}[\text{Organicoxides}] - 1.56\times10^{-2}[\text{Organichalides}] - 9.96\times10^{-3}[\text{Others}]\end{aligned} \tag{9}$$

The unit of radiation, humidity, and concentration of each pollutant are MJ/m^2, g/m^3, and ppb. The importance of radiation and humidity is the highest of the variables. A similar result had been discussed by Jeffries and Crouse[21, 23].

7 Laboratory experiments

To investigate the basic formation and descend of ozone with the diagnostic relative humidity, solar radiation and HC, an experimental arrangement for photochemical reaction was applied (as shown in Fig. 37). The photochemical reactor is a 150 L square ($60\times60\times50$ cm^3) 5 mm-glass chamber, surroundings were covered by mirror-like thin slice of stainless steel to enhance lights reflection, the bottom was on a black rubber pad and the top side is the source of solar energy. The solar source were six independent 300~400 nm (365 respected) 90 μW\cm^2 UV-lights (EAST ASIA, FL 20BL/18W). The experiment conditions were (1) the glass chamber was full of pure air gas from container; (2) all monitors were warmed up for at least two hours, then spanned and calibrated using standard gas;(3) NO_X and O_3 were mixing in quantity in the chamber; (4) injected selected HC and moisture via the injection pore; moisture needed to evaporate completely; (5) all the equipment was connected via Teflon tubes and three way valves in a cycle, so the experiment run and data collection were continuous, all data was treated by Data Acquisition System.

(1) Effect of HC variables

The effects of toluene, iso-octane, and pentene on the formation and descend of ozone were approached. Fig. 38 (a)~(c) shows that pentene is more active than toluene and isooctane in the photochemical reaction. The concentration of ozone decreases with decreasing toluene obviously, but a decrease with decreasing octane is not obvious. Even NO turns to NO_2 rapidly in the reaction

and the concentration of NO_2 also decreases in the reaction. It is summarized that different kinds of HC make different descend coefficients.

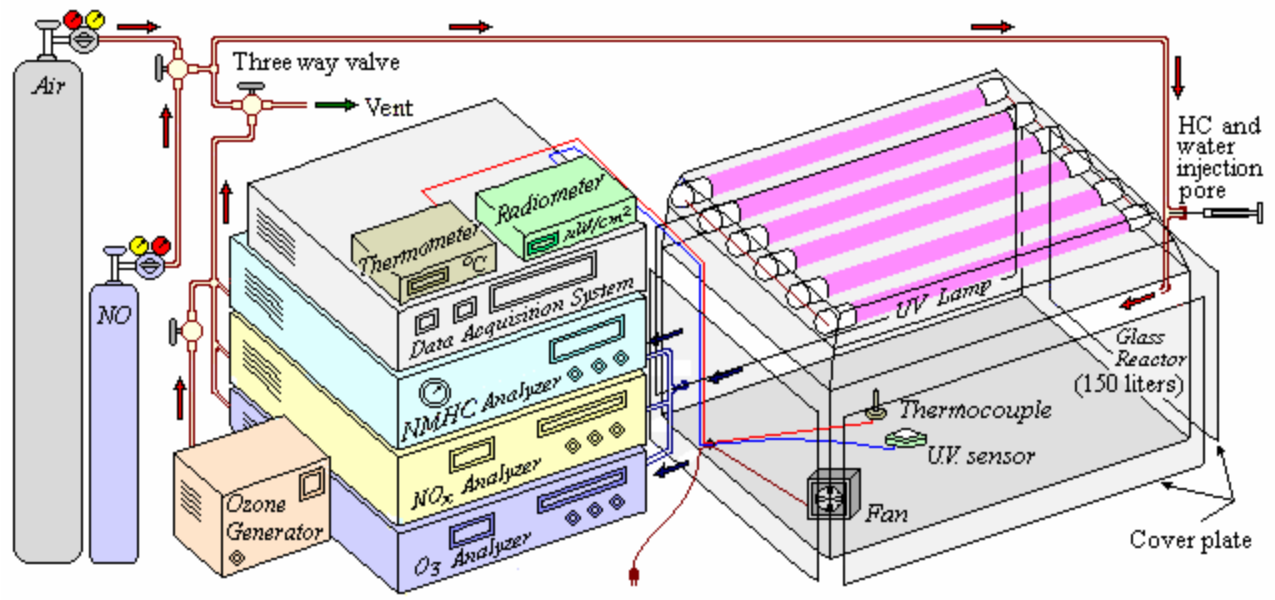

Fig. 37. Experimental apparatus for examining ozone reaction to various parameter (in neighbor university.)

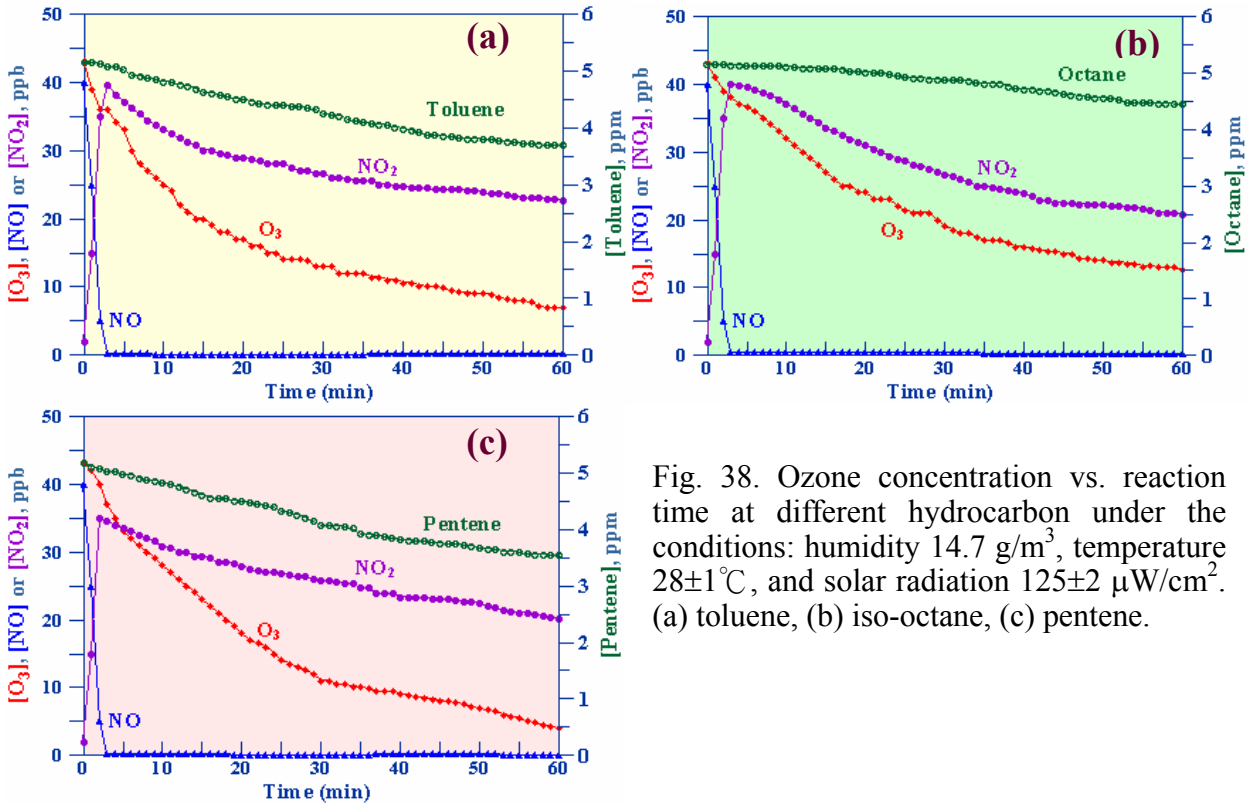

Fig. 38. Ozone concentration vs. reaction time at different hydrocarbon under the conditions: humidity 14.7 g/m^3, temperature 28±1℃, and solar radiation 125±2 μW/cm^2. (a) toluene, (b) iso-octane, (c) pentene.

(2). Effect of NO initial concentration

The concentration of ozone decreases with differential NO initial concentrations ($[NO]_o$) is not obvious (see Fig. 39), the decreasing trends are similar. But it is generally known that NO is a precursor for ozone, therefore, higher ($[NO]_o$) makes the decreasing trend slower.

(3). Effect of humidity

The most effective ozone descent is humidity, with reference to the following reaction: $O_3 + H_2O \rightarrow H_2O_2 + O_2$. Figure 39(a) shows that injecting a little moisture makes ozone descend obvious

at lower ozone initial concentration ($[O_3]_o$<47±2 ppb), but at higher ozone initial concentration the descend trend with increasing moisture become steeper (see Figure 39(b), (c)). And the ozone descent rate increases with increasing moisture amount.

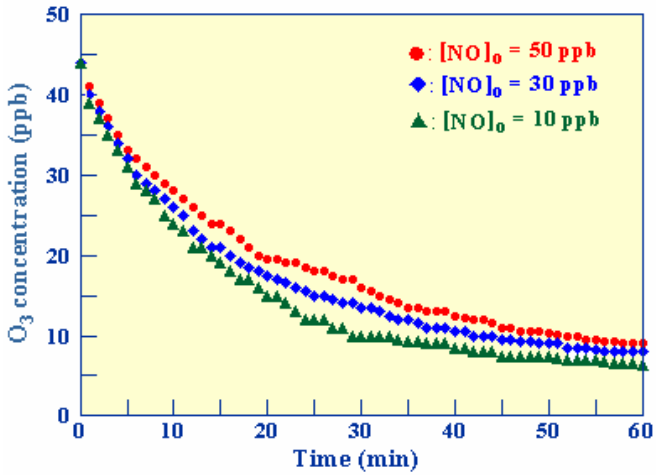

Fig. 39. Ozone concentration vs. reaction time at different nitric oxide initial concentration under the conditions: humidity 14.7 g/m^3, temperature 28±1℃, and solar radiation 125±2 μW/cm^2.

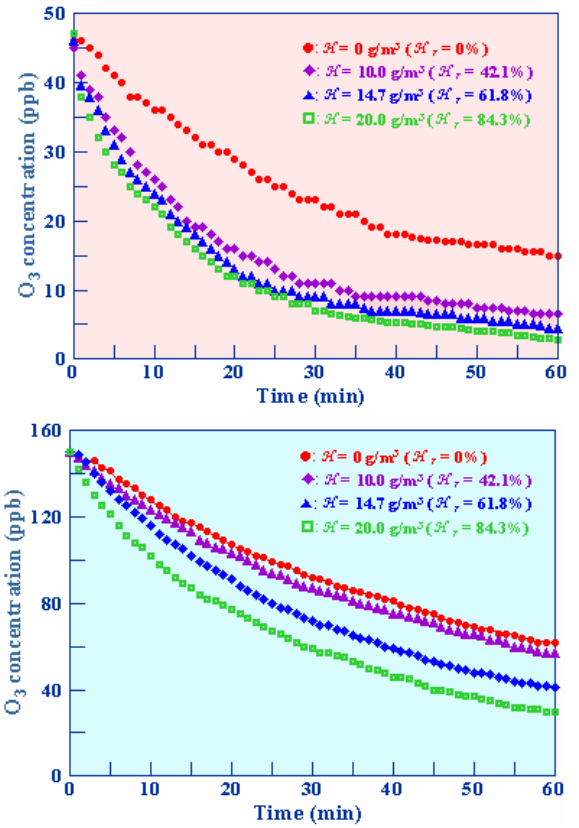

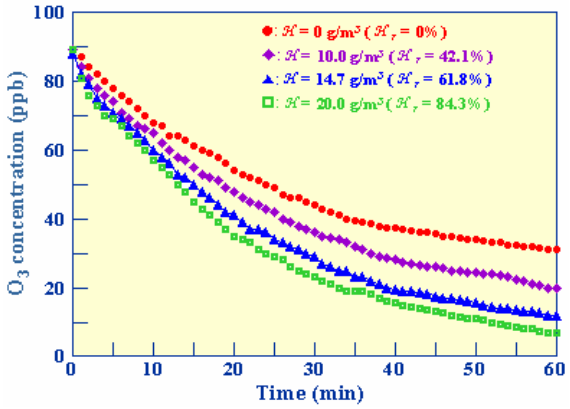

Fig. 40. Ozone concentration vs. reaction time at different humidity under the conditions: toluene initial concentration 5±0.2 ppm, temperature 28±1℃, and solar radiation 125±2 μW/cm^2. (a) toluene, (b) isooctane, (c) pentene.

Fig. 41 shows that the variation with time of differential ozone concentration ratio ($[O_3]/[O_3]_o$) on absolutely humidity $\mathcal{H}$=14.7 g/m^3 .The red circle line indicates that ozone descend is the worst at the highest ozone initial concentration $[O_3]_o$=185 ppb or the highest ratio $[O_3]/[O_3]_o$. Ozone descend decreases with increasing ozone initial concentration at the same absolutely humidity, because of the volume effect on normal atmosphere, high ozone initial concentration needs more time to react with moisture and other compounds.

It is summarized that ozone concentration decreases with decreasing [HC] and [NO_X], but decreases with increasing moisture more obviously. Ozone descent rate decreases with increasing ozone initial concentration.

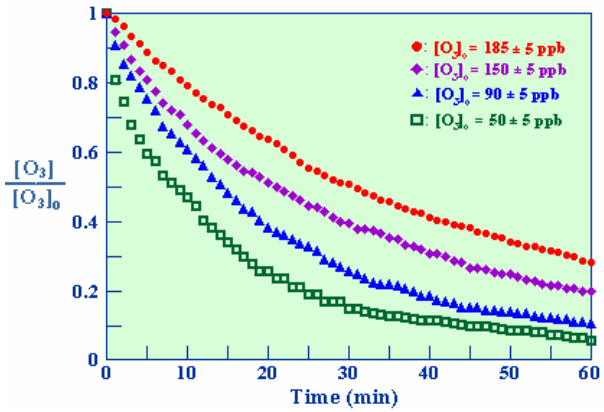

Fig. 41. $[O_3]/[O_3]_o$ vs. reaction time with different ozone initial concentration under conditions: humidity 14.7 g/m^3, temperature 28±1℃, solar radiation 125±2 μW/cm^2, and toluene initial concentration 5±0.2 ppm.

(4) Kinetic investigation

The photochemical reaction kinetics and reaction rate based on above experimental data were developed. Assuming the concentration of all precursors remains unchanged, the rate equation is[12]

$$\frac{d[O_3]}{dt} = -k_{observed}[O_3] \tag{10}$$

which on integration gives

$$\ln\frac{[O_3]_o}{[O_3]} = k_{observed} \cdot t \tag{11}$$

where $k_{observed}$ is observed rate constant, which is done by plotting the time against the ozone concentration as shown in Fig. 42. The slope of such a plot is $k_{observed}$. If all reactants reacted with ozone, $k_{observed}$ can write to

$$k_{observed} = \sum_{i=1}^{N} k_i[\text{Parameter}]_i = k^* + k_H\mathcal{H} \tag{12}$$

where $k^* = \sum_{j=1}^{N-1} k_j[\text{Parameter}]_j$ k_H is the rate constant of ozone reaction with moisture. It is done by plotting $\mathcal{H}$ against $k_{observed}$ as shown in Fig. 43. The slope of such a plot is k_H=1.08×10^{-3} and the intercept k^*=2.07×10^{-2}. However, $k_{observed}$ was obtained from this experiment and k^* varies with reaction conditions. Thus the rate equation becomes

$$\frac{d[O_3]}{dt} = -(k^* + 1.08\times10^{-3}\mathcal{H})[O_3] \tag{13}$$

$$[O_3] = [O_3]_o \exp[-(k^* + 1.08\times10^{-3}\mathcal{H})t] \tag{14}$$

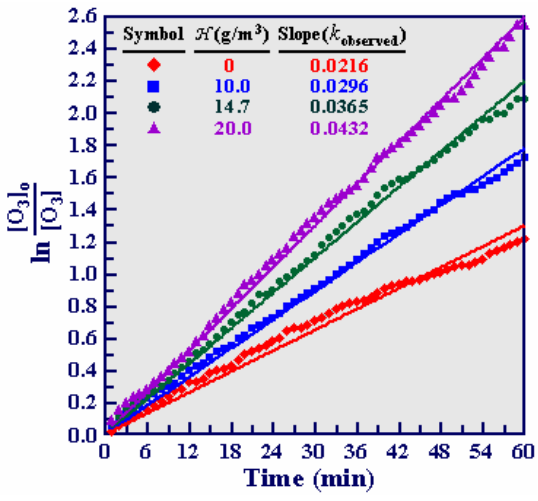

Fig. 42. Determination of observed rate constant ($k_{observed}$) for ozone at different humidity.

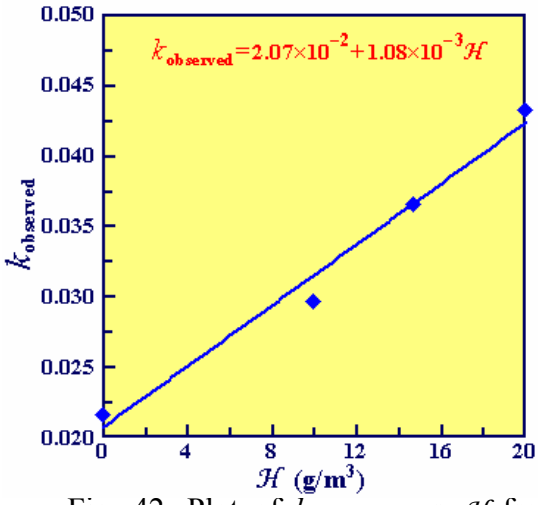

Fig. 42. Plot of $k_{observed}$ vs. $\mathcal{H}$ from which k^* and k_H were calculated.

The unit of ozone concentration, $\mathcal{H}$ and t are ppb, g/m^3 and minute. It is profiled from Eq.(13-14) that the ozone concentration decreases with moisture. Otherwise the $\mathcal{H}$ is always bigger than 14.5 g/m^3 (the relative humidity at about 60%) in Taiwan weather type, so the value of k^* almost the same to $1.08\times10^{-3}\mathcal{H}$. The effect of moisture can be certified. The ways to rich moisture are planting, making wetlands, and keeping forest, etc.

8 Conclusion

1. The relative importance coefficients r_{xy} of relatively humidity is the highest base on air quality monitoring station monthly and annual data analysis during daytime, and solar energy is the second. Increasing humidity of atmosphere makes ozone concentration decrease efficiently. During nighttime, ozone still reacts with moisture, HC, NO, and NO_2 with the relative importance coefficients r_{xy} of NO the highest, and relative humidity is the second.
2. Research over the past two years on ozone event days; (1) high ozone concentration appeared from 11:00; (2) wind field changed with basin effect, so ozone concentration stayed high in the east of the basin; (3) although on the ozone event days, ozone concentration is relatively lower in the coastal area because of high relative humidity; (4) ozone descend rate slows down in the evening in the lower-wind of the coastal area because of continuous ozone transport; (5) the concentration of ozone and other air pollutants increases with altitude, normally the highest at 300~500m.
3. The formation rate (R) and descend rate constant (L) of the ozone event day were obtained. The values of R and L change from positive to negative before 14:00. The values of R and L are lower at 14:00~15:00 due to the photochemical smog formation. And another lower R and L value after 16:00 may be due to ozone reaction with particle or moisture.
4. The results of field measurements reveal that 73 HC compounds exist at altitudes in the lower atmosphere, there are 26 compounds of alkanes, 12 compounds of alkenes, 6 compounds of aromatics, 6 compounds of organic halides, 8 compounds of aldehydes and ketones, 5 compounds of alcohols, 2 compounds of ether and benzoates, and 7 compounds of others. The low molecular weight HC always exist at lower altitudes, and the high molecular weight HC exist at higher altitudes.
5. The results also show that: (1) [O_3], [NO], and [NO_2] in the basin are not only higher than in the coastal area, but also their variability of concentration are large, (2) THC, paraffins, and olefins in the coastal area are higher than in the basin, and the concentrations increase with increasing altitude in the coastal area, but in the basin is decreasing, (3) the average concentration of halides, aromatics, oxides, and others are similar in both area, but concentration variability in the coastal area is obvious.
6. Two types of O_3 transformation was investigated, the phenomenon indicts that: (1) when wind blew into the basin, [O_3] increased with wind direction. The value of R and L change from positive (12:00) to negative (14:00); (2) when wind blew out of the basin, [O_3] decreased with wind direction. The more small value of R (–202.561) and L (–1.621) appeared at 12:00 earlier. But the value of R and L will become bigger to –76.411 and 0.244; (3) ozone concentration does not dependent on just wind direction., topography and surrounding conditions are more important effect.
7. The experiment results indicate that the formation and descend of ozone were effected by different kinds of HC. The concentration of ozone decreases with different initial NO concentration ($[NO]_o$) is not obvious, but higher ($[NO]_o$) makes the decreasing trend slow down.

8.Ozone concentration decreases with decreasing [HC] and [NO_X], but decreases with increasing moisture more obviously. And the ozone descend rate decreases with increasing ozone initial concentration.

9. Eq. (9) and (14) can help us to understand the mechanism of ozone formation and transformation.

Reference

1.Sillman, S. (1999), "The Relation Between Ozone, NO_x and Hydrocarbons in Urban and Polluted Rural Environments", *Atmospheric Environment*, **33**, 1821- 1845.

2.Wakamatsu, S., Uno, I., Ohara, T., and Schere, K. L. (1999), "A Study of the Relationship Between Photochemical Ozone and Its Precursor Emissions of Nitrogen Oxides and Hydrocarbons in Tokyo and Surrounding Areas", *Atmospheric Environment*, **33**, 3097-3108.

3.Uno, I., Ohara, T., and Wakamatsu, S. (1996), "Analysis of Wintertime NO_2 Pollution in the Tokyo Metropolitan Area", *Atmospheric Environment*, **30**(5), 703-713.

4.Skov, H., Egeløv, A. H., Granby K., and Nielsen, T. (1997), "Relationships Between Ozone and Other Photochemical Products at Li Valby, Denmark", *Atmospheric Environment*, **31**(5), 685-691.

5.Trainer, M., Parrish, D. D., Goldan, P. D., Roberts, J., and Fehsenfeld, F. C. (2000), "Review of Observation-based Analysis of the Regional Factors Influencing Ozone Concentrations", *Atmospheric Environment*, **34**, 2045-2061.

6.Lal, S., Naja, M., and Subbaraya, B. H. (2000), "Seasonal Variations in Surface Ozone and its Precursors over an Urban Site in India", *Atmospheric Environment*, **34**, 2713-2724.

7.Chu, S. H. (1995), "Meteorological Considerations in Sitting Photochemical Pollutant Monitors", *Atmospheric Environment,* **29**(21), 2905-2913.

8.Pryor, S. C. (1998), "A case Study of Emission Changes and Ozone Responses", *Atmospheric Environment,* **32**(2), 123-131.

9.Chang, T. Y., Chock, D. P., Nance, B. I., and Winkler, S. L. (1997), "A Photochemical Extent Parameter to Aid Ozone Air Quality Management", *Atmospheric Environment*, **31**(17), 2787-2794.

10.Seinfeld, J. H. and Pandis, S. N. (1998), *Atmospheric Chemistry and Physics*, JOHN WILEY & SONS, INC. pp. 1217-1230.

11.Botkin, D. B. and Keller, E. A. (2000), *Environmental Science*, 3rd Edition, JOHN WILEY & SONS, INC. pp. 474-477.

12.Levenspiel, O. (1972), *Chemical Reaction Engineering*, JOHN WILEY & SONS, INC. pp. 45-57.